ความเกี่ยวข้องของสัญญาณ Notch ในแมโครฝาจจากคนที่ถูกกระตุ้นด้วยอินเตอร์ลิวคิน-4

นางสาวนวลพรรณ แสงเพชร



วิทยานิพนธ์นี้เป็นส่วนหนึ่งของการศึกษาตามหลักสูตรปริญญาวิทยาศาสตรดุษฎีบัณฑิต
สาขาวิชาจุลชีววิทยาทางการแพทย์ (สหสาขาวิชา)
บัณฑิตวิทยาลัย จุฬาลงกรณ์มหาวิทยาลัย
ปีการศึกษา 2560

# INVOLVEMENT OF NOTCH SIGNALING IN INTERLEUKIN-4-STIMULATED HUMAN MACROPHAGES

Miss Naunpun Sangphech



A Dissertation Submitted in Partial Fulfillment of the Requirements
for the Degree of Doctor of Philosophy Program in Medical Microbiology
(Interdisciplinary Program)
Graduate School
Chulalongkorn University
Academic Year 2017

| | |
|---|---|
| Thesis Title | INVOLVEMENT OF NOTCH SIGNALING IN INTERLEUKIN-4-STIMULATED HUMAN MACROPHAGES |
| By | Miss Naunpun Sangphech |
| Field of Study | Medical Microbiology |
| Thesis Advisor | Associate Professor Tanapat Palaga, Ph.D. |

Accepted by the Graduate School, Chulalongkorn University in Partial Fulfillment of the Requirements for the Doctoral Degree

.....Dean of the Graduate School
(Associate Professor Thumnoon Nhujak, Ph.D.)

THESIS COMMITTEE

.....Chairman
(Associate Professor Ariya Chindamporn, Ph.D.)

.....Thesis Advisor
(Associate Professor Tanapat Palaga, Ph.D.)

.....Examiner
(Assistant Professor Asada Leelahavanichkul, M.D.,Ph.D.)

.....Examiner
(Assistant Professor Viroj Boonyaratanakornkit, Ph.D.)

.....Examiner
(Assistant Professor Patcharee Ritprajak, D.D.S., Ph.D.)

.....External Examiner
(Professor Pongsak Utaisincharoen, Ph.D.)

นวลพรรณ แสงเพชร : ความเกี่ยวข้องของสัญญาณ Notch ในแมโครฝาจจากคนที่ถูกกระตุ้นด้วยอินเตอร์ลิวคิน-4 (INVOLVEMENT OF NOTCH SIGNALING IN INTERLEUKIN-4-STIMULATED HUMAN MACROPHAGES) อ.ที่ปรึกษาวิทยานิพนธ์หลัก: รศ. ดร. ธนาภัทร ปาลกะ, หน้า.

แมโครฝาจตอบสนองต่อสิ่งเร้าต่างๆ หลากหลาย ซึ่งส่งผลให้มีฟีโนไทปด์ที่แตกต่างกันอย่างหลากหลายตั้งแต่แมโครฝาจที่เอื้อต่อการอักเสบที่ถูกกระตุ้นโดยลิโปโพลีแซ็กคาไรด์ ไปจนถึงแมโครฝาจที่เอื้อต่อการสมานรักษาที่กระตุ้นโดยอินเตอร์ลิวคิน 4 กลไกการควบคุมฟีโนไทปด์เหล่านี้ยังไม่เป็นที่ทราบแน่ชัด วิถีสัญญาณ Notch เป็นวิถีสัญญาณที่มีการอนุรักษ์ไว้ในสายวิวัฒนาการและมีการรายงานว่า เกี่ยวข้องกับการตอบสนองของแมโครฝาจ โดยเฉพาะอย่างยิ่งแมโครฝาจที่เอื้อต่อการอักเสบ บทบาทของวิถีสัญญาณ Notch ในแมโครฝาจที่กระตุ้นด้วย IL-4 (M(IL-4)) นั้น ยังไม่เป็นที่ทราบกันแน่ชัด PPARgamma เป็นหนึ่งในเอกลักษณ์โปรตีนชนิดนิวเคลียร์รีเซพเตอร์ ทำหน้าที่หลักในการควบคุมการสร้างและสลายไขมันของ M(IL-4) มีหลายรายงานที่ได้กล่าวถึงปฏิสัมพันธ์กันระหว่างวิถีสัญญาณ Notch และ PPARgamma ในเซลล์หลายชนิดแต่ไม่พบรายงานในแมโครฝาจ งานวิจัยนี้จึงศึกษาการอันตรกิริยาของสัญญาณระหว่าง Notch และ PPARgamma ใน M(IL-4) โดยใช้เซลล์ไลน์ THP-1 และเซลล์แมโครฝาจปฐมภูมิ พบว่า M(IL-4) มีการกระตุ้นวิถีสัญญาณ Notch ซึ่งต้องอาศัยแอคทิวิตีของเอนไซม์ g-secretase ในการตัด Notch1 รีเซพเตอร์ ในภาะที่มีการแสดงออกเกินของ Notch1 intracellular domain (NIC1) พบว่า มี PPARgamma มากขึ้นทั้งที่มีและไม่มี IL-4 นอกจากนี้การใช้ตัวยับยั้งเอนไซม์ gamma-secretase ก่อนกระตุ้นด้วย IL-4 ลดการแสดงออกของ PPARgamma ในทางกลับกันเมื่อมีการแสดงออกเกินของโปรตีนที่ทำงานเชิงลบต่อวิถีสัญญาณ Notch ซึ่งคือ dominant negative mastermind-like (DNMAML) ใน M(IL-4) กลับไม่มีผลต่อระดับ PPARgamma การที่เซลล์มีการแสดงออกเกินของ NIC1 เพิ่มความเสถียรของ PPARgamma โดยลดการถูกทำลายจากโปรตีเอโซม แต่ไม่เกี่ยวข้องกับการถอดรหัสหรือความเสถียรของ mRNA การศึกษารูปแบบการเปลี่ยนแปลง RNA โดยวิธี RNAseq ถูกนำมาใช้เพื่อให้เข้าใจผลโดยรวมของวิถีสัญญาณ Notch ใน M(IL-4) พบว่า เมื่อมีการแสดงออกเกินของ NIC1 ใน M(IL-4) พบการเพิ่มชุดยีนที่เกี่ยวข้องกับการอักเสบที่ได้มีรายงานมาก่อนหน้านี้ ที่สำคัญกว่านั้นพบว่ามีการเพิ่มขึ้นของยีนในกลุ่มการสมานรักษาด้วยเช่นกัน จากการวิเคราะห์เครือข่ายความเชื่อมโยง (network analysis) เปิดเผยให้เห็นถึงความเชื่อมโยงกันระหว่าง Notch และ PPARgamma ผ่าน NEDD4L ซึ่งเป็น E3 ubiquitin ligase ชนิดหนึ่ง และ SGK1 ที่มีส่วนที่ทำงาน (catalytic domain) คล้ายคลึงกับ AKT ถึง 45-55% เมื่อตัดยีน NEDD4L ออก ภายใต้ภาวะที่มีการแสดงออกเกินของ NIC1 ใน M(IL-4) พบว่ามีการลดการแสดงออกของ *PPARG* mRNA ร่วมกันนี้ยังลด AKT phosphorylation ผลการศึกษานี้บ่งชี้ว่า วิถีสัญญาณ Notch จำเป็นต้องมี NEDD4L เพื่อการการถอดรหัสที่เหมาะสมของ PPARgamma การกระตุ้นวิถีสัญญาณ Notch ยังส่งผลถึงกระบวนการเมตาบอลิซึมของไขมันใน M(IL-4) โดยเพิ่มการสะสมของไขมันผ่านกลไลการนำเข้าเซลล์ของ CD36 โดยรวมแล้วการศึกษานี้แสดงหลักฐานให้เห็นความเชื่อมโยงของ Notch และ PPARgamma ด้วยการทำให้โปรตีนเสถียรขึ้นและใช้ NEDD4L เป็นตัวกลางการควบคุมยีน PPARgamma และผลต่อกระบวนการนำไขมันเข้าสู่เซลล์ ผลที่ได้จากการศึกษานี้บ่งชี้ว่า วิถีสัญญาณ Notch ทำงานในแมโครฝาจทั้งภาวะเอื้อต่อการอักเสบและภาวะเอื้อต่อการสมานรักษา

สาขาวิชา จุลชีววิทยาทางการแพทย์ ลายมือชื่อนิสิต .....

ปีการศึกษา 2560 ลายมือชื่อ อ.ที่ปรึกษาหลัก .....

# # 5587779520 : MAJOR MEDICAL MICROBIOLOGY
KEYWORDS: NOTCH SIGNALING / IL-4 / MACROPHAGES POLARIZATION / NEDD4L / PPARG

NAUNPUN SANGPHECH: INVOLVEMENT OF NOTCH SIGNALING IN INTERLEUKIN-4-STIMULATED HUMAN MACROPHAGES. ADVISOR: ASSOC. PROF. TANAPAT PALAGA, Ph.D., pp.

Macrophages respond to various stimuli, resulting in distinct effector phenotypes that range from LPS-stimulated proinflammatory to IL-4-activated pro-healing phenotype. The regulatory mechanism of this polarization is not fully understood. Notch signaling pathway is a conserved signaling pathway involved in polarization of macrophages, especially proinflammatory macrophages. However, the role of Notch signaling in IL-4 stimulated macrophages (M(IL-4)) is not well defined. PPARgamma is a signature nuclear receptor in M(IL-4) that function mainly in regulating lipid metabolism. There are many reports that revealed the interaction of Notch signaling and PPARgamma in various cells but not in macrophages. In this study, the interaction between Notch signaling and PPARgamma in M(IL-4) using THP-1 cell line and primary human monocytes derived macrophages was investigated. M(IL-4) activated Notch signaling that required the activity of g-secretase to cleave Notch1 receptor. Notch1 intracellular domain (NIC1) overexpressing THP-1 increased PPARgamma expression in the presence or absence of IL-4. Furthermore, g-secretase inhibitor pretreated M(IL-4) decreased PPARgamma level. In contrast, overexpression of dominant negative mastermind-like (DNMAML), a dominant negative for Notch signaling, in M(IL-4) had no effect on PPARgamma level. NIC1 overexpression increased PPARgamma stability by delayed proteasome degradation but not the mRNA transcription or stability. RNAseq was performed to obtain global insight of Notch signaling in M(IL-4). NIC1 overexpressing M(IL-4) showed enrichment of proinflammatory gene sets consistent with previous reports. More importantly, some gene sets of pro-healing macrophages were enriched as well. Network analysis revealed the links between Notch and PPARgamma through NEDD4L, an E3 ubiquitin ligase and SGK1, which has 45-55% of catalytic domain similar to AKT. Deletion of *NEDD4L* in the presence of NIC1 overexpression in M(IL-4) reduced *PPARG* mRNA expression. This reduction of *PPARG* mRNA was accompanied by decreasing AKT phosphorylation. These results indicated that Notch signaling required NEDD4L for optimal expression of *PPARG* mRNA. Activation of Notch signaling increased lipid metabolism in M(IL-4) by increasing lipid accumulation via CD36 uptake mechanism. Collectively, this study provides evidences linking Notch signaling and PPARgamma via protein stabilization and NEDD4L mediated *PPARG* regulation and its effect on lipid uptake. The results obtained in this study indicated that Notch signaling operates in both proinflammatory and pro-healing macrophages.



Field of Study: Medical Microbiology Student's Signature .....

Academic Year: 2017 Advisor's Signature .....

# ACKNOWLEDGEMENTS

This project was supported from many people that kindly gave useful suggestion especially, my advisor, Associate Prof. Tanapat Palaga, for valuable counsel. In addition, I appreciated Dr. Sira Srisawasdi at Research Division, Faculty of Medicine, Dr. Pinidphon Prombutara at Chulalongkorn University Omics Sciences and Bioinformatics Center and Dr. Pattarin Tangtanatakul for helping with the transcriptomic analysis and suggesting for data visualization.

I am grateful to Professor. Subbra Kumar Biswas for advice and good support when I worked in his lab in A*STAR, Singapore.

I am thankful to Dr. Dilip Kumar at A*STAR, Singapore for overexpression Notch1 lentivector and control plasmid.

This study was supported by the Thailand Research Fund through the Royal Golden Jubilee Ph.D. Program PHD268/2553. This work was also supported by The 90th anniversary of Chulalongkorn University fund (Ratchadaphiseksomphot Endowment Fund), GCUGR11255725013D no. 12.

Finally, I appreciated for all helping and supporting from friends and co-workers at Tanapat Palaga lab and Inter-disciplinary Graduate Program in Medical Microbiology, Graduate School, Chulalongkorn University.

**CONTENTS**

Page

Page

Page

# FIGURE CONTENTS

# TABLE CONTENTS

## LIST OF ABBREVIATIONS

| | | |
|---|---|---|
| 1 | 13-HODE | 13-hydroxyeicosattraenoic |
| 2 | 15-HETE | 15-hydroxyeicosatetraenoic |
| 3 | ACAT | Acetyl coenzyme A acetyltransferase |
| 4 | ACP5 | Acid Phosphatase 5, Tartrate Resistant |
| 5 | ADAMs | A disintegrin and metalloprotease |
| 6 | AKT | Protein kinase B |
| 7 | ALOX15 | 12/15-Lipoxygenase |
| 8 | APH-1 | Anterior Pharynx-defective-1 |
| 9 | ApoE | Apolipoprotein E |
| 10 | Arg1 | Arginase 1 |
| 11 | ARNT2 | Aryl hydrocarbon receptor nuclear translocator 2 |
| 12 | ATMs | Adipose tissue macrophages |
| 13 | BADGE | Bisphenol A diglycidyl ether |
| 14 | BCA | Bicinchoninic acid |
| 15 | BSA | Bovine serum albumin |
| 16 | C/EBPβ | CCAAT/Enhancer Binding Protein Beta |
| 17 | CBP | CREB Binding Protein |
| 18 | CCL2 | C-C Motif Chemokine Ligand 2 (also known as MCP1) |

| | | |
|---|---|---|
| 19 | CD36 | Cluster of differentiation |
| 20 | CD98 | Cluster of differentiation 98 |
| 21 | CDK4/6 | Cyclin-dependent kinase 4/6 |
| 22 | CDK8 | Cyclin-dependent kinase 8 |
| 23 | cDNA | complementary DNA |
| 24 | CISH | Cytokine Inducible SH2 Containing Protein |
| 25 | CITED2 | Cbp/P300 Interacting Transactivator With Glu/Asp Rich Carboxy-Terminal Domain 2 |
| 26 | CSF1 | Monocytes-Colony Stimulating Factor |
| 27 | CSF1R | Monocytes-Colony Stimulating Factor Receptor |
| 28 | CSL | CBF1/RBPJκ in vertebrates/Suppressor of Hairless in *Drosophila*, Lag-1 in *C.elegans*) |
| 29 | DEPC | Diethylpyrocarbonate |
| 30 | Dim | Dimension |
| 31 | DLL1 | DELTA-LIKE 1 |
| 32 | DLL3 | DELTA-LIKE 3 |
| 33 | DLL4 | DELTA-LIKE 4 |
| 34 | DMEM | Dulbecco's Modified Eagle Medium |
| 35 | DNMAML | Dominant negative MAML |
| 36 | DNMT | DNA methyltransferase |

| | | |
|---|---|---|
| 37 | dNTP | deoxyribonucleotide triphosphates |
| 38 | DTX1 | Deltex1 |
| 39 | ERK1/2 | Extracellular signal-Related Kinases 1/2 |
| 40 | FDR | False Discovery Rate |
| 41 | Fizz1 | Resistin like beta (RETNLB, synonym) |
| 42 | g (Centrifugation speed) | Gravity |
| 43 | GBR10 | Growth Factor Receptor Bound Protein 10 |
| 44 | GO | Gene Ontology |
| 45 | GPR132 | G-protein coupled receptor receptor G2A |
| 46 | GSEA | Gene Set Enrichment Analysis |
| 47 | GSI | gamma-secretase inhibitor |
| 48 | GSK3b | Glycogen kinase 3b |
| 49 | HERP1 | Hairy and Enhancer of Split Related Repressor Protein1 |
| 50 | HES | Hairy and Enhancer of Split |
| 51 | HEY | Hairy and Enhancer of Split Related With YRPW Motif |
| 52 | HMDMs | Primary human monocytes derived macrophages |
| 53 | HRE | Hormone Responsive Element |
| 54 | IFNα | Interferon alpha |
| 55 | IGF-1 | Insulin-Like Growth Factor 1 |
| 56 | IκB | I-kappa-B |

| | | |
|---|---|---|
| 57 | IKKα | I kappa B kinase alpha |
| 58 | IKKβ | I kappa B kinase beta |
| 59 | IL-10 | Interleukin-10 |
| 60 | IL-13 | Interleukin-13 |
| 61 | IL-13Rα1 | Interleukin-13 Receptor alpha 1 |
| 62 | IL-1β | Interleukin-1 beta |
| 63 | IL-2Rγc | Interleukin-2 Receptor common gamma chain |
| 64 | IL-4 | Interleukin-4 |
| 65 | IL-4R | Interleukin-4 Receptor |
| 66 | iMDM | Iscove's Modified Dulbecco's Medium |
| 67 | iNOS | Inducible Nitric Oxide Synthase |
| 68 | IRF4 | Insulin Like Growth Factor 4 |
| 69 | IRS | Insulin Receptor Substrate |
| 70 | ITCH | Itchy E3 Ubiquitin Protein Ligase |
| 71 | J1 | JAGGED1 |
| 72 | J2 | JAGGED2 |
| 73 | JAK1 | Janus Kinase1 |
| 74 | JAK2 | Janus Kinase 2 |
| 75 | JAK3 | Janus Kinase3 |
| 76 | KLF4 | Krüppel-like factor4 |

| | | |
|---|---|---|
| 77 | KO | Knockout |
| 78 | KRAS | GTPase KRas |
| 79 | log2 | Logarithm base 2 |
| 80 | LPL | Lipoprotein lipase |
| 81 | LPS | Lipopolysaccharides |
| 82 | LXR | Liver-X-Receptor |
| 83 | MAML | Mastermind-like protein |
| 84 | MAO-A | Monoamine Oxidase-A |
| 85 | MAPK | Mitogen-Activated Protein Kinase |
| 86 | MCP1 | Monocyte Chemoattractant Protein-1 (also known as CCL2) |
| 87 | MCPIP | Monocyte chemotactic protein-1-induced protein-1 |
| 88 | MEK | Mitogen-activated protein kinase kinase |
| 89 | MHCII | Major Histocompatibility Complex, Class II |
| 90 | miR-155 | microRNA-155 |
| 91 | MR | Mannose Receptor |
| 92 | mRNA | messenger RNA |
| 93 | MSigDB | Molecular Signatures Database |
| 94 | mTORC1 | Mechanistic Target Of Rapamycin Kinase Complex2 |
| 95 | mTORC2 | Mechanistic Target Of Rapamycin Kinase Complex2 |
| 96 | N4L | NEDD4L |

| | | |
|---|---|---|
| 97 | NCT | Nicastin |
| 98 | NEDD4L | Neural Precursor Cell Expressed, Developmentally Down-Regulated 4-Like, E3 Ubiquitin Protein Ligase |
| 99 | NEDD8 | Neural Precursor Cell Expressed, Developmentally Down-Regulated 8 |
| 100 | NES | Normalized enrichment score |
| 101 | NF-κB | Nuclear Factor Kappa B |
| 102 | NIC | Notch Intracellular domain |
| 103 | NK T cell | Natural Killer T lymphocyte |
| 104 | NR | Nuclear receptor |
| 105 | NR1C1,2,3 | Nuclear Receptor Subfamily 1 Group C Member 1,2,3 |
| 106 | ℃ | Degree Celsius |
| 107 | PBMCs | Peripheral Blood mononuclear cells |
| 108 | PBST | Phosphate Buffer Saline Tween 20 |
| 109 | PCA | Principle component analysis |
| 110 | PCCM | Pearson Correlation Coefficient Matrix |
| 111 | Pdgfb | Platelet-derived growth factor receptor |
| 112 | PEN2 | Presenillin Enhancer Protein2 |
| 113 | PGE2 | Prostaglandin E2 |
| 114 | PI3K | Phosphoinositide 3-kinase |

| | | |
|---|---|---|
| 115 | PI3KCA | p100 subunit of PI3K |
| 116 | PKBα | Protein kinase B alpha |
| 117 | PKBβ | Protein kinase B beta |
| 118 | PMA | Phorbol 12-myristate 13-acetate |
| 119 | PPARγ | Peroxisome Proliferator Activated Receptor gamma |
| 120 | PPRE | Peroxisome Proliferator Response Element |
| 121 | PS | Presenillin |
| 122 | PTP1B | Protein-Tyrosine Phosphatase 1B |
| 123 | PVDF | Polyvinylidene fluoride |
| 124 | qPCR | quantitative polymerase chain reaction |
| 125 | RPMI | Roswell Park Memorial Institute |
| 126 | RXR | Retinoic-X-Receptor |
| 127 | SDS-PAGE | Sodium dodecyl sulphate-polyacrylamide gel electrophoresis |
| 128 | Sel10/Fbox7 | Suppressor/enhancer of lin-12 protein 10/F-box only protein 7 |
| 129 | SEM | Standard Error Mean |
| 130 | SGK1 | Serum glucocorticoid kinase1 |
| 131 | SHIP | SH2 Domain-Containing Inositol 5-Phosphatase 1 |
| 132 | SOSC1 | Suppressor Of Cytokine Signaling 1 |

| | | |
|---|---|---|
| 133 | STAT6 | Signal Transducer And Activator Of Transcription 6 |
| 134 | TAM | Tumor associated macrophages |
| 135 | TAP/TAZ | Yes-associated protein (YAP)/ transcriptional coactivator with PDZ-binding motif (TAZ) |
| 136 | TGFβ | Transforming Growth Factor beta |
| 137 | TNFα | Tumor necrosis factor alpha |
| 138 | TSS | Transcription Start Site |
| 139 | w/v | Weight by volume |
| 140 | Ym1 | Chitinase-like protein 3 (synonym) |

# CHAPTER I

## BACKGROUND

Macrophages originate from yolk sac at the early embryonic and persists within tissue. Later that, the major source of cells is replenished from hematopoietic stem cell. Disease or tissue injury highly replenish macrophages from monocytes in blood circulation. Underlying significant of this process, due to macrophages are required for immunological response to control the abnormal status. Presenting of macrophages in diseases lesion are deviated from normal. Moreover, it implies to the diseases severity. The simplify method categorized macrophages to two phenotypes, one that is proinflammatory and the other that is pro-healing phenotypes. Proinflammatory macrophages are activated by bacterial infection (such as LPS) and danger associated molecular pattern (such as oxLDL), leading to proinflammatory cytokines production, enhancing bactericidal activity and tumors suppression. Pro-healing macrophages are activated by Th2 cytokines, especially IL-4 is well known. IL-4-stimulated macrophages M(IL-4) function in tissue repairing and tumors promotion. For example, predominantly macrophages phenotypes in atherosclerosis is proinflammatory macrophages. Reversing phenotype from proinflammatory to pro-healing phenotypes lead to good disease prognosis. In contrast, predominant macrophages in cancer are pro-healing phenotypes. Switching macrophages phenotypes can be the alternative treatment target for some diseases. Notch signaling pathway, is a conserve signaling pathway, plays a role on regulating many biological processes, including macrophages phenotypes. Modification of Notch signaling in macrophages has been patented as a novel treatment for atherosclerosis and diabetics and the mode of action was characterized. However, the role of Notch signaling in pro-healing macrophages is not well defined and still controversial. Previous study revealed that transcriptional activity of Notch signaling regulates specific gene subsets in IL-4 activated mouse macrophages. In contrast, IL-4 co-stimulation with Notch signaling in human macrophages induced macrophages apoptosis and impaired pro-healing macrophages

markers expression. Therefore, this study would examine the role of Notch signaling in pro-healing macrophages, specifically in M(IL-4) as a model.

M(IL-4) increase anti-inflammatory genes expression, change cellular glucose metabolism and lipid homeostasis. PPARγ is a transcription factor that activated by IL-4 stimulation and has a crucial role in the regulation of M(IL-4) biological functions. Previous reports indicated that ligand induced PPARγ activation alone is sufficient to induce pro-healing macrophages phenotypes. Epigenetic mediated suppression of PPARγ gene expression increased inflammation in atherosclerosis which rescued by PPARγ ligand (rosiglitazone) administration.

Evidence indicating interaction between Notch signaling and PPARγ was reported in many cell types such as adipocytes and keratinocytes, but not in macrophages. Both proteins were found in macrophages in the lesion of some diseases. For instance, oxLDL has another role to activate PPARγ to increase CD36 expression results in lipid accumulation in foam cell macrophages. On the other hand, Notch activation was found in these macrophages and involved in attenuate proinflammatory cytokine production cause enhanced disease severity. Neutralizing antibody mediated Notch inhibition has been used for treatment of atherosclerosis, due to its ability to decrease lipid accumulation and plaque size. Interestingly, hyperactivation of Notch signaling in mouse tumor associated macrophages, exhibited pro-healing phenotypes, caused macrophages phenotype switching to pro-inflammatory phenotypes. Therefore, the method to manipulate Notch signaling for alternative therapeutic requires further study to apply in novel therapeutic purpose. We hypothesize that Notch signaling may contribute to IL-4 stimulated macrophages via PPARγ and possibly controls its biological functions. This study provides the involvement of Notch signaling in IL-4 stimulated human macrophages and achieves the knowledge gap how Notch signaling affects lipid accumulation in human macrophages.

**Objective**

1. To investigate whether the interaction of Notch signaling and PPARγ in IL-4 stimulated human macrophages

2. To explore the role of Notch signaling in IL-4 stimulated human macrophages.

# CHAPTER II

# LITERATURE REVIEWS

## 2.1. Macrophages: Diverse phenotypes

Macrophages originate from yolk sac during mouse embryonic development (E7.25) [1]. Primitive macrophage progenitor persist and differentiate in tissue as tissue resident macrophages [1]. The major source of macrophages after this stage are hematopoietic stem cells [1]. Deletion of PU.1, a macrophages lineage determining transcription factor, colony stimulating factor 1 (CSF1) or CSF1 receptor (CSF1R) in macrophages increased perinatal mortality and organ development defects (such as brain [2], heart [3], bone [4] etc.), suggesting that macrophages are important for normal development organism before birth [5]. These findings extend the roles of macrophages from the first line defense against pathogens, homeostasis, inflammation tissue remodeling to regulation of organogenesis [5-7].

The involvement of macrophages in many diseases become increasingly clear in inflammatory related diseases such as atherosclerosis, diabetic, cancer, asthma, infection etc [8]. However, macrophages in these diseases do not exhibit similar phenotype due to different microenvironmental and stimuli. Definition for macrophage polarization, was purposed for the characteristics of macrophages that encounter different stimuli and exhibit distinct phenotypes. Macrophages polarization is described as spectrum of activation and phenotype because some properties are shared [9]. Simplified classification of activated human macrophages was categorized into 2 phenotypes of the opposite end of spectrum, that are proinflammatory (M1) and pro-healing (M2) [7]. Proinflammatory macrophages are mainly stimulated by lipopolysaccharides (LPS) or bacterial pathogen. Pro-healing macrophages are driven mainly by interleukin-4 (IL-4), IL-13, IL-10, and transforming growth factor β (TGFβ).

Both types of macrophages could be found in normal and diseases tissues [10]. Microenvironment in the disease stage disturb the phenotypic balance, leading to

changing of tissue homeostasis and disease pathogenesis [10]. For example, in atherosclerosis, tunica adventitia layer of blood vessel contained more pro-healing macrophages and they function as artheroprotective [11]. The plaque shoulder contains more proinflammatory macrophages which produce tissue degradation enzymes, resulting in unstable of plaque [11]. Although other plaque area (fibrous cap, vascular intima and foam cell macrophages) similarly detected both type of macrophages, the reversion phenotype from proinflammatory to pro-healing phenotype reduce plaque size and often correlate with good disease prognosis [12]. However, in tumor, tumor-associated macrophages (TAM) show pro-healing-like phenotype because of cytokine milieu such as TGFβ , IL-4, IL-10, prostaglandin E2 (PGE2) but not all are the same phenotype [13]. In non-small cell lung cancer, approximately 70% of macrophages display TAM phenotype [13]. As TAM support tumor progression and metastasis, repolarization of TAM toward proinflammatory phenotype was recently reported as novel a potential therapeutic target for cancer therapy [13, 14]. Therefore, macrophages activation can be both beneficial or harmful and controlling its activation can be an attractive alternative therapeutic choice [12, 15].

2.2 IL-4 signaling in macrophages

IL-4 is produced by various cell types, including Th2, basophil, eosinophil, which activates and induces pro-healing phenotypes of macrophages which is termed M(IL-4) [16]. IL-4 interacts with IL-4α receptor (a transmembrane protein [17]) with high affinity [18, 19]. IL-4/IL-4R form heterodimer with IL-2Rγc or IL-13Rα1 to activate downstream signaling cascade [20]. Due to low affinity binding of IL-4α and IL-2Rγc, the complex are endocytose before IL-4 and IL-4R dissociation (within 6-9 min) to a subpopulation of regular early sorting and recycling endosomes (cortex endosome) to increase the efficiency of IL-4R dimerization [18].

IL-4/IL-4R complex activates JAK1 and JAK3 by phosphorylation. Activated JAK1 in turn phosphorylates IL-4. IL-4α contains $^{488}$PL-(X4)-NPXYXSXSD$^{502}$ motif, which is also found in the cytoplasmic domain of insulin like growth factor (IGF-1) receptor [17]. This domain is necessary for insulin receptor substrate (IRS) binding. IRS-1/IRS-2 are recruited to IL-4α at phosphorylated Y497 [17]. IL-4/IL-4R complex

triggers tyrosine kinase Fes to phosphorylate IRS-1/IRS-2 [17]. Activated IRS-1 stimulates PI3K/AKT to control cell proliferation and protects cell from apoptosis in IL-3 dependent myeloid progenitor cell line (32D cells) [17]. Activated JAK1 and JAK3 also phosphorylates Signal Transducer and Activator of Transcription 6 (STAT6), which subsequently form homodimer and enters the nucleus [20].

The IL-4 signaling cascade is depicted in Figure 1. M(IL-4) upregulates a set of genes involved in anti-inflammation, lipid metabolism, apoptotic cell clearance and cellular metabolism [21-24]. Potential anti-inflammatory proteins from M(IL-4) includes 12/15-lipooxygenase (ALOX15), CD36, monoamine oxidase A (MAO-A) [25, 26].

2.3 Phenotypes and biological functions of M(IL-4)

Metabolic reprogramming is essential process to control M(IL-4) polarization. The pro-healing macrophages have metabolic shift to fatty acid oxidation and oxidative phosphorylation [27]. The initial step before this metabolic shift, M(IL-4) activates mTORC2 in synergistic with M-CSF to increase AKT(Ser473) phosphorylation [27]. This process occurs in parallel with STAT6/IRF4 activation to regulate glucose metabolism [27]. Sufficient glucose utilization in early step allows M(IL-4) to further polarize [27].



Cellular events after IL-4-stimulated macrophages are controlled by STAT6, AKT and some other factors as described above. The STAT6 effector functions have been reported. For example, STAT6 regulates IRF4 and C/EBPβ transcription factor which is important for IL-10 and Arg1 expression in murine M(IL-4) [28, 29]. STAT6 increases PPARγ expression upon IL-4 stimulation, later interacts with PPARγ and enhances magnitude of PPARγ response by facilitating the transcriptional activity [30]. Additionally, STAT6 regulates krüppel-like factor4 (KLF4) in murine macrophages.

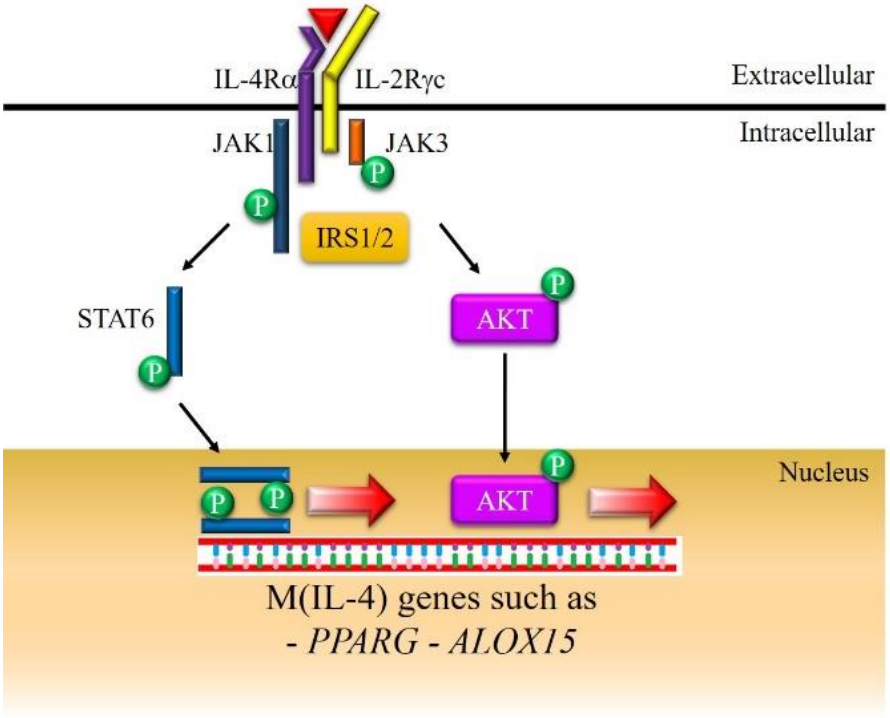


Figure 1 IL-4 signaling cascade.

(Modied from Odegaard J.I. and Chawla A., Annual Review Pathology Mechanism Diseases, 2011).

IL-4 bind to IL-4Rα recruits IL-2γc or IL-13Rα to form heterodimer. IL-4/IL-4R complex activates JAK1 and JAK3 phosphorylation. Activated JAK1/JAK3 phosphorylates STAT6 phosphorylation which subsequently form homodimer before entering to the nucleus to regulate IL-4 dependent STAT6 transcription genes such as *PPARG* and *ALOX15*. In the meantime, IL-4/IL-4R complex activates AKT phosphorylation via IRS. Phosphorylated AKT translocates to the nucleus for regulating IL-4-dependent gene expression.

These two transcription factors cooperate to increase monocyte chemotactic protein-1 (MCP1)-induced protein (MCPIP) [31, 32]. A deubiquitinase activity of MCPIP removes ubiquitin from IκB, leading to inhibition of NF-κB activation in murine macrophages [32]. Meanwhile, MCPIP has RNase activity which is capable to degrade *il-1β, il-6* and *il-12p40* mRNA for feedback mechanism in LPS stimulated human monocytes derived macrophages [33]. MCPIP RNase activity is also important for mRNA stability [34] because loss of MCPIP RNase activity severely reduces PPARγ level [31].

IL-4/STAT6 activation is important for proliferation of adipose tissue macrophages (ATMs). The early stage of obesity, ATMs has pro-healing phenotype and are responsible for resident macrophage proliferation via IL-4/STAT6 not monocyte chemotactic protein-1 (MCP1 or CCL2) [35].

PI3K/AKT is another signaling pathway activated in M(IL-4). AKT has three isoforms, encoding from three different genes (AKT1/PKBα, AKT2/PKBβ and AKT3/PKBγ) [36]. The AKT isoform specific function in macrophages has been report recently [37]. $AKT2^{-/-}$ macrophages reduced, expression of miR-155, a target of C/EBPβ, which is a key regulator for Arg1 in LPS stimulated macrophages [37], while AKT1-/- showed the opposite phenotype. IL-4 simulated thioglycolate-elicited mouse peritoneal macrophages decreased bacteria burden of *Neisseria meningitidis* [38]. The impairment of bacterial uptake in this condition can be explained by decreasing of AKT phosphorylation that is necessary for phagocytic cup closure [38]. Furthermore, PI3Kp110δ/AKT activation downregulates SH2-containing inositol-5-phosphatase (SHIP), a negative regulator for M(IL-4) [39].

## 2.4 Feedback mechanisms of IL-4 signaling in macrophages

### 2.4.1 Positive feedback mechanism

IL-4 activation is rapidly induced and transient [19]. For example, STAT6 phosphorylation reached to the half-maximum within 12.5 min [18]. Therefore, if cell requires more signal to proper response, it needs to auto amplify. IL-4 induced expression of galectin-3 (a β-galactoside binding lectin) via PI3K in the bone marrow

derived macrophages [40]. Galectin-3 binds to CD98 and stimulates AKT activation to enhance pro-healing macrophages marker such as mannose receptor (MR), Ym1, Fizz1 and suppress pro-inflammatory cytokines [40].

2.4.2 Negative feedback mechanism

Negative regulators are required to prevent hyperactivation. For instance, IL-4 stimulated DLBL cell line (diffuse large B cell lymphoma) increased and stabilized protein tyrosine phosphatase1B (PTP1B) [41]. PTP1B acts as negative regulator to directly inhibit JAK1 phosphorylation, consequently restrained STAT6 phosphorylation and obstructed the initiation of target genes transcription [41]. In IL-4 stimulated U937 (human monocytic cell line), AKT activated mTORC1, and subsequently initiated Growth Factor Receptor Bound Protein 10 (GBR10) activity [42]. GBR10 directly interacts with IL-4Rα, recruits E3 ubiquitin ligase, Neural Precursor Cell Expressed, Developmentally Down-Regulated 4-Like (NEDD4L) to ubiquitinate IL-4Rα to mark for proteasome degradation [42].

2.5 Notch signaling pathway and biological functions

Notch signaling is a conserved signaling pathway operating in invertebrates to mammals [43, 44]. Its activity is important for correct cell identity, differentiation, proliferation, tumorigenesis and inflammation [44-47]. Notch signaling is a cell-cell signaling pathway which required interaction between Notch ligands and receptors on adjacent cells (*trans*) to transmit the signal [48, 49]. Five Notch ligands (Jagged1,2, Delta-like1,3-4) and four Notch receptors (Notch 1-4) are identified in mammals. The structure of Notch ligands and receptors [50] are shown in Figure 2. Currently, Notch signaling can be categorized to 2 groups, i.e. canonical and non-canonical pathway[51].

The canonical Notch signaling is well established, starting from Notch ligand and receptor interaction to allow two enzymes to access to the recognition sites [51]. A disintegrin and metalloprotease (ADAMs) which are transmembrane proteins [52], is the first enzyme to cleave between Notch receptor extracellular domain and transmembrane. domain. Four ADAMs (ADAM9, ADAM10, ADAM12 and ADAM17) were reported to be function in this step in mammals [53]. After Notch

receptor ectodomain cleavage, the site for second enzyme (γ-secretase) is exposed. γ-secretase is aspartyl protease compose of 4 components (presenilin (PS, catalytic domain), anterior pharynx-defective 1 (APH-1), nicastin (NCT, substrate recognition site) and presenilin enhancer protein 2 (PEN2)) [54]. γ-secretase cleavage allows Notch receptor intracellular domain (NIC) to translocate to nucleus. In the nucleus, RAM domain of NIC binds with DNA binding transcription factor CSL (CBF1/RBPJκ in vertebrates/Suppressor of Hairless in *Drosophila*, Lag-1 in *C.elegans*), subsequently recruit Mastermind-like protein (MAML) and other co-factors such as CBP/p300 for transcription of the Notch target genes [51]. Notch target genes are diverse depending on cell types such as Hairy And Enhancer Of Split (HES) Related Repressor Protein1 (HERP1, smooth muscle cell) [55], Jagged1 (macrophages) [56] platelet-derived growth factor receptor (Pdgfb, in myogenic cell) [57]. Some of the Notch target genes such as HES1, Hairy/Enhancer-Of-Split Related With YRPW Motif 1 (HEY1) are well studied in many cell types and used as surrogate activation marker [55-57]. The canonical Notch signaling is depicted in Figure 3.

Non-canonical Notch signaling pathway is RBPJκ independent signaling which differs from canonical pathway [58]. In MCF-7 breast cancer cell line, Notch cooperated with IKKα and IKKβ to upregulate IL-6 which is independent of CSL [59]. Recent reports showed that cytoplasmic or membrane tether of NIC interact with mTORC2 and subsequently activates AKT (S473) to regulate survival of activated T under cytokine deprivation [58]. Moreover, canonical and non-canonical Notch signaling from the same Notch receptor and cell type functions difference. For example, non-canonical Notch4 activation in *rbpjκ* knockout mice participates in mammary gland tumorigenesis, whereas canonical Notch4 was required for mammary gland development [58].

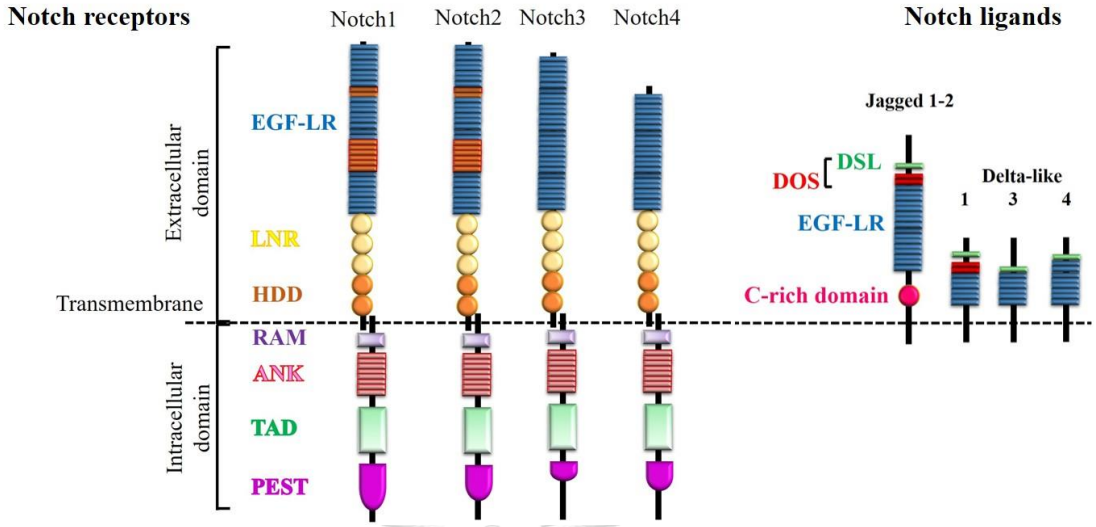


Figure 2 Mammalian Notch ligands and receptors structure.

(Modified from J. E. Johnson, *et al*, Current Topics in Developmental Biology, 2011)

Abbreviation for structural domain:

EGF-LR: epidermal growth factor (EGF)-like repeats (EGF-LR)

LNR: LIN12-NOTCH repeats

HDDs: heterodimerization domains (HDDs)

N-HDDs: N-terminal HDDs

C-HDDs: C-terminal HDDs

NRR: negative regulatory region

RAM: recombining binding protein suppressor of hairless (RBPJ) association molecule

ANK: ankyrin repeats

TAD: transactivation domain

PEST: polypeptide enriched in proline, glutamate, serine and threonine polypeptide enriched in proline, glutamate, serine and threonine

DOS: DSL domain along with the first two EGF-like repeat.

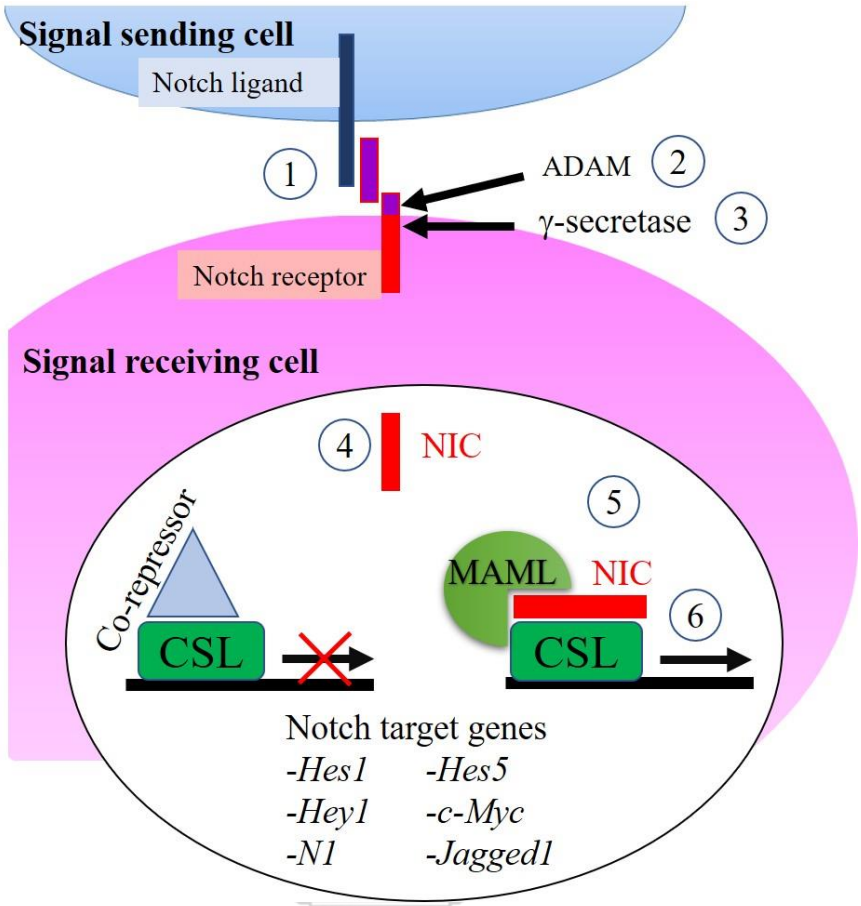




Figure 3 Canonical Notch signaling pathway

(Modified from Hamed J. N., *et al*, Glycobiology, 2012). Notch signaling begins when (1) ligand-receptor interaction trigger (2) ADAM and (3) γ-secretase cleavage at Notch receptor, this event releases (4) NIC to translocate to nucleus. In the nucleus, CSL constitutingly binds with co-repressor to suppress transcription of target genes. (5) NIC replaces co-repressor, bind to CSL and recruits MAML and other co-activator to (6) induce Notch target genes transcription.

Notch signaling is rapidly turnover for allowing new round of signaling activation [60]. Previous reports revealed that biological outcome of Notch signaling depends on dose, timing and cellular context [48, 60, 61]. Dose dependence phenomenon disappears when NIC reached a threshold level. NIC functions as on-off switch rather than graded response [48]. Abnormal activation or loss of function has been associated with various diseases [60]. The cellular mechanism to shutdown Notch signaling is mediated by proteasome degradation of NIC. As previously described, MAML is required for Notch signaling mediated transcription by promoting the recruitment of CBP/p300 in the nucleus [46, 48]. MAML also reduces Notch signaling by enhancing the modification of NIC for proteolysis degradation [46]. In some cases, CDK8 phosphorylated PEST domain of NIC and target it for proteasome degradation by E3 ubiquitin ligase that include Sel10/Fbox7 [61]. However, if cells need Notch signaling, there are mechanisms to prolong NIC half-life. For example, in *Drosophila*, glycogen kinase 3b (GSK3b) activity prolongs NIC by protecting it from proteasome degradation [62]. Therefore, balancing activation and degradation of Notch signaling is important for appropriate cellular processes.

2.6 Notch signaling in macrophages

Notch signaling activation was reported as one indicator for proinflammatory macrophages because its activation mostly found in these cells [63, 64]. Stimulation of macrophages with LPS, activated Notch signaling which play a role to regulate effector functions, cytokine productions and cell survival [65]. In an *in vitro* experiment, coculturing human macrophages with Notch ligand expressing cell (DLL4) were sufficient to activate NF-κB, MAPK and AKT pathway to increase inducible nitric oxide synthase (iNOS) (one of M1 signature protein) [66]. The result from individual silencing of Notch1-4 in phorbol 12-myristate 13-acetate (PMA) stimulated human monocytes derived macrophages isolated from atherosclerosis patients indicate that Notch1 plays more important role than Notch2-3, while no effect from Notch4 was observed [67]. Notch1 silencing strongly decreased JAGGED1, DLL4 and increased IκBα protein expression [67]. Moreover, forced activation of Notch1 in TAM induces proinflammatory phenotype and increasing tumoricidal activity [68]. These results were partly documented to show that Notch signaling plays a role in regulating

proinflammatory macrophages. More importantly, Notch signaling is proposed as therapeutic targets for many diseases including, atherosclerosis, obesity, metabolic syndrome, vein graft failure and cancer since 2006 (https://patents.google.com/patent/US20090175849#patentCitations).

Several documents demonstrated for the role of Notch signaling in pro-healing macrophages. For instance, *rbpjκ*$^{-/-}$ murine M(IL-4) selectively regulated pro-healing macrophages genes (*arg1*) without interfering well known signature genes in STAT6 and C/EBPβ independent manner [69]. Furthermore, DLL4 co-activated with IL-4 in human macrophages induced cells apoptosis and impeded CD200R and CD206 expression [70].

2.7 Nuclear hormone receptors (NR)

NR are ligand dependent transcription factors [71]. Their ligands are lipid soluble signal, which can cross plasma membrane, such as thyroid hormone, estrogen, retinoic acid, fatty acid etc [72]. NR are classified based on the mode of action into 4 groups. Type I NR are anchored receptor in the cytoplasm with chaperon protein [72]. Ligand binding to type I NR dissociates receptor from chaperone. Activated ligand induces receptor homodimerization and translocates to nucleus to bind with DNA binding site, hormone responsive element (HRE) [72]. Type II NR locates in nucleus, binds with HRE in the presence or absence of ligand. Ligand binding to type II receptor induces receptor heterodimerization with another NR, retinoic-X-receptor (RXR), subsequently replaces repressors [72]. Type III NR are similar to type I NR except for the arrangement of HRE. Type IV NR bind at HRE as monomer [72].



2.8 Peroxisome proliferator activated receptor gamma (PPARgamma)

The PPAR family are type II NR, containing three isoforms, i.e. PPARα (NR1C1), PPARβ/δ (NR1C2) and PPARγ (NR1C3). They are encoded in 3 genes locating on 22q12- q13.1, 6p21.2-p21.1, and 3p25.2 of human chromosome [73, 74]. These isoforms are differentially expressed among tissues and during development stage [73]. PPAR members are able to bind with the same DNA motif which is called peroxisome proliferator response element (PPRE) [71, 73, 75]. Seventy-three PPRE

sequences were reported untill now [71]. Conserved PPRE sequences contain 2 consensus sequences of AGGTCA separated by 1 nucleotide, AGGTCANAGGTCA [75] .

In the absence of ligand, PPARγ is rapidly degraded by proteolysis cleavage [71]. Additionally, PPARγ transcription activity is silent upon binding with co-repressor [76]. Ligand binding to PPARγ stabilizes this conformation and induces its activity, while reduce its degradation rate [71]. Activated PPARγ can heterodimerize with RXR (RXRα, RXRβ or RXRγ) [77], resulting in the release of co-repressors, while allows co-activator recruitment to the complex [76]. PPARγ/RXR binding sites are found throughout the genome but were enriched at the proximity sequence of genes, particularly at the transcription start site (TSS). PPARγ/RXR binding sites (18% that were identified) were located within 10 kb of TSS [77].

Human PPARγ has 6 isoforms (PPARγ 1-5,7) and different isoforms are expressedin different tissues [78, 79]. PPARγ binding to PPRE in different cell types showed noticeable distinct profile because of the additional transcription factors [77]. For example, some of PPARγ and PPARγ/RXR binding sites in human and mouse macrophages are co-occupied with PU.1 binding site (macrophage lineage specific transcription factor) [74, 78]. PU.1 binds to PU.1 binding site to act as an anchor for PPARγ to bind to PPRE [74]. Therefore, co-binding of PPARγ or PPARγ/RXR with PU.1 established the tissue specific binding sites for PPARγ in macrophages [74, 80].



The PPARγ ligand binding pocket is large. This allows binding of PPARγ with the broad range of ligands [81]. Many reported PPARγ ligands are categorized to endogenous such as oxLDL, polyunsaturated fatty acid, 15-deoxy-Δ, prostaglandin J2, 13-hydroxyeicosattraenoic (13-HODE) and 15-hydroxyeicosatetraenoic acid (15-HETE)) etc. [81] or chemical synthetic substances such as thiazolidinediones, rosiglitazone etc. [81]. However, PPARγ is also found to function in a ligand independent. For example, DNA damage in cortical neuron activated cyclin dependent kinase 4/6 (CDK4/6) to increase CBP/P300-interacting manner transactivator with glutamic acid/aspartic acid-rich carboxyl-terminal domain 2 (CITED2) expression.

CITED2 activated and directly bound to PPARγ to control neuron death [82]. In mouse macrophages, CITED2 deficiency had ambiguous role to regulate inflammatory response, due to its increased PPARγ activity as well as enhanced proinflammatory cytokines production [83]. Therefore, PPARγ has ability to function in both ligand dependent and ligand independent manner.

2.9 Biological functions of PPARgamma

Gain and loss of function study were utilized to study biological functions of PPARγ. Whole body knockout of PPARγ in mice resulted in embryonic lethal due to multiple defects of organ development such as epithelial cell differentiation, placenta function, myocardial development, lipotrophy [84]. Therefore, the functional study of PPARγ mostly used conditional knockout or synthetic drug. *PPARγ*$^{+/-}$ mice decreased PPARγ activity, indicating that PPARγ expression level could be used for its activity determination [77]. PPARγ biological activities are broad but generally accepted as a key transcription factor for lipid and glucose metabolism in macrophages [77, 85]. PPARγ modulates lipid metabolism via regulation of many lipid regulating protein including CD36 (scavenger receptor for oxidized low density lipoprotein (oxLDL) uptake), lipoprotein lipase (LPL, catalytic enzyme for hydrolysis triglyceride and store intracellular lipid in cholesterol ester form [86]), acetyl coenzyme A acetyltransferase (ACAT, function similar to LPL [87]) [77].



In macrophages, PPARγ has additional function besides lipid homeostasis. It contributes to anti-inflammatory properties of macrophages which are crucial part of pro-healing macrophages polarization. As described earlier, PPARγ is the secondary response mediator of IL-4 stimulated macrophages. IL-4 controls PPARγ expression via JAK3 and STAT6, which JAK2 inhibitor (TYRPhostin) or PI3K inhibitor (wortmannin) has no effect on *PPARG* level [30]. However, pan PI3K inhibitor (LY294002) decreased STAT6 transcriptional activity [39]. IL-4 also induced PPARγ ligands, not directly, but via enzyme that is 12/15-lipoxygenase (ALOX15) [30, 81, 88]. ALOX15 utilizes linoleic and arachidonic to PPARγ ligand 13-HODE and 15-HETE, respectively [81, 88].13-HODE and 15-HETE could inhibit iNOS expression in IL-4

activated macrophages in PPARγ dependent manner in RAW264.7 macrophage cell line [81, 88].

In atherosclerosis plaque, oxLDL activated and elevated PPARγ expression to control lipid uptake and accumulation via some target genes as describe above [89]. The role of PPARγ in atherosclerosis is to limit inflammation because of overexpression DNA methyltransferase (DNMT transgenic on *apoE*$^{-/-}$) in macrophages decreased PPARγ expression, which caused increasing proinflammatory cytokines (TNFα, IL-1β and IL-6) in plasma of DNMT transgenic mice. This phenotype can be rescued by rosiglitazone administration [11]. This report is consistent with previous report that PPARγ synthetic ligand stimulated macrophages polarization to pro-healing phenotypes which does not require additional stimuli [90, 91]. Therefore, foam cells are presumably pro-healing rather than proinflammatory macrophages. However, oxLDL stimulated TLR-2 and-4 in macrophages, resulting in increased proinflammatory cytokine [92]. Recent evidence contradicted with these hypothesis because foam cells expressed proinflammatory macrophages marker (HLA-DP/Q/R, iNOS) with in a comparable level as non-foamy cell in human atherosclerotic lesions [11] because fatty acid metabolism in foam cell generate desmosterol to activate liver-x-receptor (LXR, one of PPARγ binding partner [93]), resulting in reduction of proinflammatory cytokines [92, 94].



In turn, PPARγ activation in macrophages play a surprising role to regulate mammary tumor. Previous reports indicated that pro-healing macrophages promote tumor growth. However, PPARγ activation in macrophages in mammary tumor reduced tumor growth by inhibiting G-protein coupled receptor G2A receptor (GPR132) [95]. Therefore, PPARγ can be a potential therapeutic target of macrophages in diseases.

2.10 Regulating PPARgamma expression and function

Inhibition of PPARγ activity can be managed by various mechanism. First, as described previously, DNMT modulates on/off *PPARG* transcription by epigenetic mechanism [96]. Second, at the transcriptional level, for example, IL-4 activated

STAT6 phosphorylation to increase PPARγ expression in macrophages [22, 30]. Third, at the protein level, PPARγ activity is regulated by 2 mechanisms; positive and negative regulation. Positive regulation is strategized to activate PPARγ using ligand and non-ligand as described above [82, 89, 97, 98]. Negative regulation is the way to decrease or inhibit PPARγ activity using synthetic antagonist (such as bisphenol A diglycidyl ether (BADGE) [99], GW9662 [100] etc.).

PPARγ degradation can result in increasing or decreasing its transcriptional activity. Generally, PPARγ is ubiquitinated by E3 ubiquitin ligase and targeted for proteasome degradation [101]. For instance, IFNγ-induced PPARγ phosphorylation at Ser112 by ERK1/2, targeting PPARγ for ubiquitination and proteasome degradation in adipocytes [102]. However, phosphorylation of PPARγ at Ser112 by MEK/ERK in hepatocellular carcinoma increases PPARγ activity, promotes glycolysis and tumor cell proliferation [103]. A ubiquitin-like protein, NEDD8 regulates PPARγ by the post translation modification (neddylation) that tags NEDD8 to PPARγ by covalent bond [104, 105]. This NEDD8 tagged PPARγ competes with ubiquitin to reduce PPARγ degradation and increased its activity in adipocytes [105]. In addition, NEDD4 (or NEDD4L in human), a ubiquitin ligase, ubiquitinate PPARγ but prevent it from degradation [101].

2.11 Neural Precursor Cell Expressed, Developmentally Down-Regulated (NEDD4L)



NEDD4L (also known as NEDD4-2 and KIAA0439) [106] is a conserved E3 ubiquitin ligase which belongs to the Nedd4 family of ubiquitin ligases [106].Proteins in Nedd4 family contain unique specific domains that are the amino terminal Ca2+ phospholipid binding (C2 domain), WW domains and the HECT domain from N-to C-termini, respectively (Figure 4). The C2 domain functions to bind with lipid membrane. WW domains are interactive sites for protein containing PY (PPxY) and LYSP motifs. They can bind with several proteins at once, due to several WW domains (4 domains). HECT domain consist of 2 subunits, which subunit at C-termini is called C-lobe (acceptor for cysteine) and subunit at N-terminal site is called N-lobe (interacting site for ubiquitin-charged E2 protein). Human NEDD4L is encoded by gene containing 38

exons locating on chromosome 18q21.31 [106]. There are 17 predicted isoforms of NEDD4L in human [106].

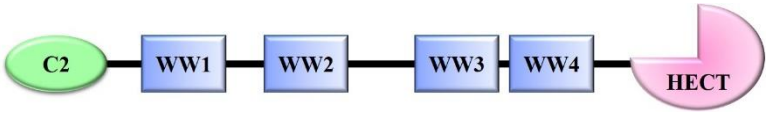


Figure 4 NEDD4L primary structure.

(modified from P. Goel, *et al*, Gene, 2015 [106]).

2.12 Biological functions of NEDD4L

NEDD4L was first reported to function in ion channel regulation, TGFβ signaling, Wnt signaling, virus budding [106]. Study in *NEDD4L* knockout mice found that there was severe abnormal lung and kidney development, hypertension and hepercalciuria when fed with high Na+ diet, neurite growth etc [106]. In human, decreased NEDD4L level has been detected in gastric cancer, malignant glioma, non-small cell lung cancer, and colorectal cancer [107]. Some cancers (melanoma and prostate cancer) show increased NEDD4L expression, indicating the complex role of NEDD4L in cancer development [107]. One clear evidence is that NEDD4L overexpression enhanced PI3KCA (p100 subunit of PI3K) turnover rate by targeting its proteasome degradation which impaired AKT phosphorylation and decreased cancer growth [107].

2.13 Notch signaling and NEDD4L

Epidermal somatic stem cells control cell fate decision though Notch signaling. In order to maintain undifferentiation stage, Yes-associated protein (TAP)/ transcriptional coactivator with PDZ-binding motif (TAZ) induced DLL1 by binding at the enhancer element [108]. DLL1 inhibited Notch activation via *cis* inhibition. Moreover, direct target of TAP/TAZ was NEDD4L which antagonized Notch signaling through ubiquitination [108]. Dynamic of Notch receptor on cell surface in the basal insisted on NEDD4L activity. In *Drosophila* S2 cell, NEDD4L homolog (Nedd4)

modulates Notch receptor ubiquitination at PPSY motif in PEST domain, led to receptor internalization and degradation [109]. Dominant negative Nedd4 blocked receptor internalization and activated Notch in a ligand independent manner [109]. These results suggested that NEDD4L is a negative regulator of Notch signaling.

2.14 Notch signaling and PPARγ

KRAS mutation in pancreatic ductal carcinoma and transformed lung epithelial cell which is inflammation-induced carcinogenesis, exhibit NF-κB activation to control proinflammatory cytokines expression [110] in which, Notch signaling was activated [111]. The synergistic effect of TNFα, Iκk2 and Notch signaling by phosphorylation at histone H3 of HES1 by Iκk, enhances HES1 expression [112] and HES1 subsequently suppresses PPARγ results in autocrine inflammation perpetuation [110, 112].

The crosstalk between Notch and PPARγ had been documented in 3T3-L1 (preadipocytic cell line) and keratinocytes. In 3T3-L1, Notch1 upregulates PPARγ and PPARγ that are necessary for adipocyte differentiation. During keratinocyte differentiation, Jagged1 increased PPARγ expression and PPARγ in turn inhibited NF-κB by physical association between NF-κBp65 and PPARγ. This inhibition induced keratinocyte undergo to terminal differentiation [113].



Although Notch signaling pathway and PPARγ have been suggested to regulate macrophage functions, in particular during macrophage polarization, it is not known whether they crosstalk to regulate macrophage effector function. In this research, the crosstalk between Notch signaling and PPARγ was explored to understand the interaction between these signaling pathways. In addition, the impacts of this crosstalk in human macrophages was investigated in the context of tumor cell induced macrophages migration.

# CHAPTER III

# MATERIALS AND METHODS

## 3.1 Cell culture

### 3.1.1 Cell line

THP-1, a human leukemia cell line cell line (reference no. JCRB0112, Japanese Collection of Research Bioresources Cell Bank, Japan) was used in this study. Cells were maintained in Roswell Park Memorial Institute (RPMI) 1640 (Hyclone, UK) which was supplemented with 10% (v/v) fetal bovine serum (Hyclone, UK), 1% (w/v) sodium pyruvate (Hyclone, UK), 1% (w/v) HEPES (Hyclone, UK), 50 uM β-mercapto-ethanol, 100 U/ml penicillin and 0.25 mg/ml streptomycin (Hyclone, UK) and incubated at 37˚C in a humidified 5% (v/v) $CO_2$ incubator.

HEK293T, a human embryonic kidney cell line (ATCC no CRL-1573) was maintained in Dulbecco's Modified Eagle Medium (DMEM) supplemented with supplements with 10% (v/v) fetal bovine serum (Hyclone, UK), 1% (w/v) sodium pyruvate (Hyclone, UK), 1% (w/v) HEPES (Hyclone, UK), 100 U/ml penicillin and 0.25 mg/ml streptomycin (Hyclone, UK). Cell was cultured at 37˚C in a humidified 5% (v/v) $CO_2$ incubator.



### 3.1.2 Cell preparation

THP-1 and HEK293T were cultured in cell culture treated flask (T 25$cm^2$ flask) (Nunc, USA). For preparing THP-1 cells for experiment, cells were collected into 15 ml tube and centrifuged at 1000 rpm for 5 min (Hettich ROTOFIX 32 Benchtop Centrifuge, USA). The culture supernatant was discarded, and cell pellets were resuspended in complete RPMI1640 complete medium.

Viable cell numbers were counted using trypan blue dye (Hyclone, UK) exclusion method and plated into the tissue culture treated plates.

3.1.3 Cell preservation for storage

THP-1 was resuspended in RPMI1640 or DMEM freezing medium containing 10% DMSO (v/v) (Sigma Aldrich, USA) in complete medium, respectively. Cells were kept in cryogenic vials (Corning Incorporation, USA). The vials were stored at -80$^{o}$C for short term storage. For long term storage, the vials were kept at -80$^{o}$C overnight and transferred to the liquid nitrogen tank (Taylor Wharton, USA).

3.1.4 Thawing cells

Stored THP-1 and HEK293T were rapidly thawed in the water bath (Memmert, Germany) at 37$^{o}$C. Cells were added into 9 ml of serum-free RPMI1640 or DMEM media, respectively. Cells suspension was centrifuged at 1000 rpm for 5 min. The supernatant was discarded and replaced with fresh complete media. Cells were maintained and cultured as described above.

3.2 Human CD14+ monocytes isolation

The use of healthy donor blood was granted for ethic approval by the Institutional Review Board, Faculty of Medicine, Chulalongkorn University (IRB No. 055/60). Whole blood from healthy donors were gently overlaid on ficoll reagent (GE Healthcare, UK) at ratio blood: ficoll reagent is 2:1 and centrifuged at 3,000 rpm for 20 min. Peripheral blood mononuclear cells (PBMCs) were transferred to 15 ml centrifuge tube containing cold wash buffer (Appendix A). Cells were centrifuged to washed out the remaining ficoll reagent at 1,200 rpm for 5 min. Red blood cell was removed by incubating with red blood cell lysis buffer for 5 min. PBMCs were added wash buffer to stop activity of red blood cell lysis buffer, then centrifuged at 1,200 rpm for 5 min. One hundred million of PBMCs was used to isolate CD14+ monocytes. In brief, $100x10^{6}$ PBMCs was resuspended in 90 μl of the cold MACs buffer (Appendix A). Ten microliters of human CD14 MicroBeads (MACS Miltenyi Biotec, Germany) were added to the cells, incubated with occasional shaking for 15 min. Cells were immediately add MACs buffer 10 ml and centrifuged at 1,200 rpm for 5 min to remove unbound antibody. Cells were resuspended with 500 μl MACs buffer before subjecting to MACs MS column (MACS Miltenyi Biotec, Germany). The column was placed into

magnetic field and rinsed with 500 μl MACs buffer before applying sample. Then, the column was washed three times with 500 μl of MACs buffer. CD14+ monocytes were eluted by adding 1 ml MACs buffer and gently push plugger on the column. CD14+ monocytes were counted and seed the desired cell number to cell culture container.

To differentiate CD14+ monocytes to macrophages, monocytes were maintained in M-CSF (20 ng/ml) (Biolegend, USA) in complete medium Iscove's Modified Dulbecco's Media (iMDM media (Hyclone, UK) supplemented with 5% human serum, 100 U/ml penicillin and 0.25 mg/ml streptomycin) Cells were incubated at 37˚C in a humidified 5% (v/v) $CO_2$ incubator for 7 days. Media were changed half volume every 2 days.

3.3 Western Blot

3.3.1 Protein extraction and measurement

Cells were treated as indicated in each experiment. Cell lysates were extracted using method that described previously by Palaga et al. (2003). In short, culture supernatant was removed from plate and cells were washed by 1 ml of cold PBS and subsequently by appropriate volume of buffer A (Appendix A). The proteins were extracted using buffer B containing phosphatase inhibitor (Sigma Aldrich, USA). Cell lysates were transferred to 1.5 ml microcentrifuge tubes (Axygen Scientific, USA) and mixed by vortex mixer for 1 min before centrifugation at 8,000Xg for 5 min at 4$^{o}$C. The clear supernatants were kept on ice until analysis or -80$^{o}$C for further analysis.



BCA (bicinchoninic acid)$^{TM}$ protein assay kit (PIERCE, USA) was used to measure protein concentration in samples , according to manufacturer’s instruction. Bovine serum albumin (BSA) was used as protein standard at 1, 0.5, 0.25, 0.125, 0.063 and 0.031 mg/ml and the samples were diluted in sterile double distilled water at 1:10 in 96-well microtiter plate (Corning Incorporation, USA). Reagent A and reagent B were mixed at the ratio of 50:1 before adding 250 μl into each well. The plate was incubated at 37˚C for 30 min before measuring the absorbance at 540 nm using microplate reader (Anthos 2010, UK).

3.3.2 Sodium dodecyl sulfate polyacrylamide gel electrophoresis (SDS-PAGE)

SDS-PAGE gels were prepared following the recipe shown in Appendix A. Protein samples were mixed with Laemmli buffer (Appendix A) and heated at 100˚C for 5 min in the heat box (Thermomixer Compact, Eppendorf, Germany) before loading to the gels. Protein ladder (New England Biolab, UK) was used as a reference of molecular weight. The samples were separated using a constant volt for at least 90 min in running buffer for SDS-PAGE using mini Protein III system (Bio-Rad, USA).

3.3.3 Western Blot

SDS-PAGE gels were equilibrated in transfer buffer (Appendix A) for 5 min. Polyvinylidene fluoride (PVDF) membranes (GE Healthcare, USA) were prepared by soaking in absolute methanol (Merck, Germany). Excess methanol was removed by rinsing with double distilled water twice. The membrane was submerged in transfer buffer. Whatman filter papers (6 pieces) were prepared and immersed in the transfer buffer. For protein transfer, three pieces of filter paper, PVDF membrane, gel and 3 pieces of filter paper were set up in the semi-dry transfer Transfer-Blot® SD (Bio-Rad, USA) instrument and air bubbles were carefully removed. The transfer was performed using a constant current at 80 mA (for one gel) or 150 mA (for two gels) for 105 min.

3.3.4 Antibody probing



PVDF membranes from previously process were blocked twice in blocking solution (Appendix A) for 5 min each on rocking platform (Labnet Rocker 25, Labnet International Inc, USA). The PVDF membranes were later probed with primary antibody at 4$^{o}$C in refrigerator overnight. The working dilution of the primary antibodies that were used in this study was summarized in Table 3.1. After this step, the membranes were gently shaken for 1 h on a rocking platform at room temperature. Primary antibody was removed and washed unbound antibody with PBST (Appendix A) for 5 min and 15 min twice for each step. Secondary antibody that conjugated with horse-radish peroxidase (Amersham Biosciences, UK) was added to the membrane. The working dilution of the secondary antibodies that were used in this study was summarized in Table 1. The membranes were shaken for 1 h on the rocking platform.

Unbound and non-specific binding of antibody were washed with PBST 5 min twice and 15 min for 3 times before detection.

3.3.5 Signal detection by chemiluminescence and autoradiography

Substrates for chemiluminescent detection was prepared with the recipe in Appendix A. In brief, solution A and solution B was freshly prepared and mixed immediately before incubation for 1 min with the membranes. The membranes were wrapped with plastic wrap and set in Hypercassette (Amersham Bioscience, UK) for X-Ray film (for High Performance Chemiluminescence Film: Amersham Hyperfilm$^{TM}$ ECL (Amersham Bioscience, UK) exposure in the dark room. The exposure time of each protein varied depend on experiment. The exposed film was developed in an X-ray film developer solution for 5 seconds, washed with water, and immersed in X-ray film fixer solution for 1 min and washed again with water in the final step.

Table 1 Antibodies used in Western Blot

| Antigen | Working Dilution of primary antibody | Working Dilution of secondary antibody |
|---|---|---|
| Cleaved Notch1 (Val 1744) | 1:1000 | 1:2000 (Goat anti rabbit IgG) |
| Notch1 | 1:2000 | 1:4000 (Goat anti rabbit IgG) |
| β-actin | 1:10000 | 1:5000 (Sheep anti mouse IgG) |
| Phosphor-AKT (Ser473) | 1:2000 | 1:4000 (Goat anti rabbit IgG) |
| Total-AKT | 1:2000 | 1:4000 (Goat anti rabbit IgG) |
| Phosphor-STAT6 (Tyr641) | 1:2000 | 1:4000 (Goat anti rabbit IgG) |
| Total-STAT6 | 1:2000 | 1:4000 (Goat anti rabbit IgG) |
| PPARγ | 1:1000 | 1:2000 (Goat anti rabbit IgG) |
| NEDD4L | 1:2000 | 1:2000 (Goat anti rabbit IgG) |

3.4 RNA extraction

Cells were treated as indicated experiment, RNA was extracted using TRIzol® (Invitrogen, UK). In brief, cells were lysed directly using 0.5 ml TRIzol®. Cell lysate were aspirated up and down for 7-8 times and the total cell lysates were transferred to the microcentrifuge tubes. Samples were centrifuged at 12,000Xg for 10 min at 4°C to reduce genomic DNA contamination in further step. Clear lysates were transfer to the new microcentrifuge tube. The samples were left at room temperature for 5 min before adding 100 µl chloroform per 0.5 ml TRIzol®. The mixture was vigorously shaken for 15 seconds and incubated at room temperature for 3 min. Samples were centrifuged at 12,000Xg for 15 min at 4°C. The aqueous phase was carefully transferred to the new microcentrifuge tube. Two hundred microliters of iso-propanol (Merck, Germany) per 0.5 ml TRIzol® was added to the samples. The tubes were inverted to mix before incubating at room temperature for 10 min prior to centrifugation at 12,000Xg for 10 min at 4°C. Supernatants were discarded and washed with 75% ethanol (Merck, Germany) in DEPC water (Invitrogen, UK). The samples were mixed by vortexing and centrifuged at 7,500Xg for 10 min at 4°C. Finally, RNA were air dried at room temperature before adding 20 µl DEPC water and incubated for 10 min at 60°C to dissolve an RNA pellet. Total RNA samples were kept at -80°c until use. RNA were measured OD260 and OD280 using Nanodrop (Thermoscientific, USA)



3.5 Reverse transcription for complementary DNA (cDNA) synthesis

One hundred ng to 1 µg of sample RNA were used as template to synthesize cDNA by mixing with 0.2 µg Random hexamers (Qiagen, Germany). The reaction volume was adjusted to 12.5 µl by DEPC water. The samples were heated at 65°C for 5 min and cooled down to 4°C on ice. The sample was later added 1xRT buffer (Fermentas, Canada), 1 mM dNTP mix (Fermentas, Canada), 20U of RNase inhibitor (Fermentas, Canada) and 200U of Reverse transcriptase (Fermentas, Canada). All samples were mixed well and spun down before putting into the PCR machine Bioer Life Express (Bioer Technology, China) The PCR machine was set as follows; 25°C for 10 min, 42°C for 60 min and 70°C for 10 min. The cDNA was stored at -20°C until use.

3.6 Semi-Quantitative polymerase chain reaction (qPCR)

The qPCR was carried out using according to iQ™ SYBR® Green Supermix (BioRad, USA) manufacturer's protocol. Two µl of cDNA solution was added to qPCR solution that composed of 5 µl of iQ™ SYBR® Green Supermix, 0.3 µM forward and reverse primer and 2.25 µl of nuclease free water (each sample was analyzed in duplicate). The qPCR was performed in the Bio-Rad CFX Connected Real Time System (BioRad, USA). The nucleotide sequences of primers used in this study and the annealing temperatures of qPCR conditions were summarized in Table 2. The relative expressions of mRNA levels were calculated according to Livak K.J., *et al* 2001 [114].

Table 2 The nucleotide sequence of primers and annealing temperature of qPCR condition.

| Gene | Primer sequence (5'→3') | Annealing Temp (°C) | PCR product (bp) | Reference |
|---|---|---|---|---|
| *ACTIN* | For ACCAACTGGGACGACATGGAG | 55 | 385 | Palaga T., *et al*, 2008 [115] |
| | Rev GTGGTGGTGAAGCTGTAGCC | | | |
| *h_NOTCH1* | For CAGCCTGCACAACCAGACAGA | 55 | 298 | Kuncharin Y., *et al*, 2011 [116] |
| | Rev TGAGTTGATGAGGTCCTCCAG | | | |
| *h_NOTCH2* | For TGAGTAGGCTCCATCCAGTC | 55 | 530 | Kuncharin Y., *et al*, 2011 [116] |
| | Rev TGGTGTCAGGTAGGCATGCT | | | |
| *h_NOTCH3* | For GGACATGCAGGATAGCAAGGA | 60 | 105 | Fung E., *et al*, 2007 [117] |
| | Rev GATCTCACGGTTGGCAAAGTG | | | |
| *h_NOTCH4* | For TGGGAGCTTGCGGTTCTG | 60 | 92 | Fung E., *et al*, 2007 [117] |
| | Rev GACCACAGTCAAGTTGAGGTGATC | | | |
| *h_JAGGED1* | For AAGGGGTGCGGTATATTTCC | 57 | 104 | Kongkavitoon P., *et al*, 2016 [118] |
| | Rev TCCCGTGAAGCCTTTGTTAC | | | |

| Gene | Primer sequence (5'→3') | Annealing Temperature (°C) | PCR product (bp) | Reference |
|---|---|---|---|---|
| *h_JAGGED2* | For AGCTGGAACGAGACGAGTGT | 60 | 222 | Choi, J.H., *et al*, 2008 [119] |
| | Rev TCTTGCCACCAAAGTCATCA | | | |
| *h_DLL1* | For CCACGCAGATCAAGAACACC | 55 | 336 | Kongkavitoon P., *et al*, 2016 [118] |
| | Rev TTGCTATGACGCACTCATCC | | | |
| *h_DLL3* | For CACTCCCGGATGCACTCAA | 60 | 148 | - |
| | Rev GCTACCTCCCGAGCGTAGATG | | | |
| *h_HEY1* | *For* AACTGTTGGTGGCCTGAATC | 55 | 160 | Li, HCH., *et al*, 2016 [120] |
| | *Rev* GCGGTAAATGCAGGCGTAT | | | |
| *h_PPARG* | *For* TGACAGATGTGATCTTAACT | 60 | 111 | - |
| | *Rev* AACCTGATGGCATTATGA | | | |
| *h_NEDD4L* | *For* TCCAATGGTCCTCAGCTGTTTA | 60 | 147 | Kuratomi G. et al, 2005 [121] |
| | *Rev* ATTTTCCACGGCCATGAGA | | | |

3.7 Retrovirus and lentivirus transduction



HEK293T cell line ($1x10^6$ cells/4ml) were seed in 35 $mm^3$ petri dish overnight. The retroviral vectors for NIC1 (encodes for amino acid from position 1770 to 2556 of *Homo sapiens* NOTCH1, accession no. AF308602.1) (MSCV-GFP-Myc-NIC1), which was a kind gift of Dr. Barbara A. Osborne (University of Massachusetts Amherst, USA), the retroviral vector for DNMAML (MSCV-Mam(12–74)-EGFP), which was a kind gift from Dr. Warren Pear (University of Pennsylvania, USA) and packaging construct pCL-Ampho (Imagenex, Canada) were co-transfected into HEK293T cells using the FuGene®HD transfection reagent (Roche, USA) according to the manufacturer's instructions. In brief, 2 μg of pCL-Ampho and 2 μg of the retroviral vector were added in the microcentrifuge tube (tube A) containing serum free medium (Opti-MEM, Gibco, USA). Another microcentrifuge tube was prepared by adding 6 μl

of FuGene®HD transfection (tube B). Both tubes were mixed well before transferring solution from tube A to tube B. The tubes (A+B) were briefly vortexed, spun down and incubated at room temperature for 15 min. During this step, culture medium were carefully removed from HEK293T cells, cells were gently washed with warm PBS. Two milliliters of fresh medium were carefully added to HEK293T cells. Eight hundred microliters of DMEM complete media were added to the tubes (A+B), mixed by pipetting and dropped-wise to HEK293T cells. The transfected cell was observed for GFP expression under inverted fluorescence microscope before transduction. Culture supernatants containing retroviruses were harvested twice at 48 and 72 h after transfection and used to transduce THP-1 cells, as described previously [116]. Breifly, culture supernatant containing virus was filtrated through 0.45 μm filter. The filtrated supernatant were aliquoted to 1.2 ml in microcentrifuge tube. These tubes were added 6 μl of FuGene ® HD transfection reagent, mix by vortexing and dropped-wise into THP-1 cells. Cells were centrifuged at 2,200 rpm, with no break, for 1 h at room temperature. Cells were put back into 5% $CO_2$ incubator for 1 h before filling up with 1 ml of RPMI1640 complete media. Transduction efficiency was confirmed by fluorescent microscopy and flow cytometry.

For lentivirus transduction, two set of lentiviral vectors, that were the lentiviral plasmid vector for NEDD4L knockout and for NIC1 overexpression. The lentiviral plasmid vector for NEDD4L knockout (N4L#1KO and N4L#2KO) had plentiCRISPR as control vector, which were purchased from GenScript, USA. The lentiviral plasmid vector NIC1 overxpression (EF1α-CMV-hN1-GFP) and empty vector (EF1α-CMV-DEST-GFP) obtained from Dr. Dilip Kumar (A*STAR, Singapore). The lentiviral vector packaging construct containing gene encoding VSVG was obtained from Dr. Barbara A. Osborne and psPAX2 was purchased from Addgene, USA. The lentivirus transduction protocol was similar to retrovirus transduction described above, except lentiviral vector packaging construct was used 0.5 μg of VSVG, 0.5 μg of psPAX2 to mix with 1 μg of lentiviral vector.

3.8 RNA sequencing (RNAseq)

3.8.1 Sample preparation

CTRL, NIC1 and DNMAML overexpressing THP-1 cells were pretreated with PMA (5 ng/ml) for 48 h, before stimulating with IL-4 (20 ng/ml) for 3 h. RNA were extracted by RNeasy mini kit (QIAGEN, USA). In brief, RNA were collected in RLT buffer, then centrifuge at 12,000Xg for 10 min at 4$^{o}$C. Clear RNA lysates were transferred to new microcentrifuge tube. Two hundred and fifty microliters of absolute ethanol were added to RNA sample, mixing by pipetting and transferred to RNeasy mini spin column. The columns were centrifuged at 8,000Xg for 15 seconds at room temperature. The flow through fraction were discarded. The columns were added 350 µl of buffer RW1 and centrifuged at 8,000Xg for 15 seconds at room temperature, discarded the flow through. DNaseI solution was directly to RNeasy column membrane and incubated for 15 min at room temperature. The columns were added 350 µl of buffer RW1 and centrifuged at 8,000Xg for 15 seconds at room temperature, discarded the flow through. Five hundred microliter of buffer RPE was added to column to wash the column twice. The columns were centrifuged at 8,000Xg for 15 seconds for the first washing and for 2 min for the second. The remaining liquid in the column was removed by centrifugation at 17,900Xg for 1 min. Thirty microliters of RNase-free water were directly added to RNeasy column membrane and incubated for 1 min before centrifugation at 8,000Xg for 1 min. RNA were kept at -80 $^{o}$C until used.



3.8.2 Sequencing library construction

Integrity of Total RNA was assessed using Agilent 2100 Bioanalyzer (Agilent, USA). Five hundred nanogram of the total RNA from each sample was used to create individually indexed strand-specific RNA-seq libraries using Truseq stranded mRNA library preparation kit (Illumina, USA). Briefly, poly-A containing mRNA molecules was captured using magnetic oligo (dT) beads, purified and directed to cDNA synthesis. AMPure XP beads (Beckman Coulter Genomic, USA) were used to separate the cDNA from reaction mix. Indexing adapters were ligated to the cDNA, and subsequently all cDNA libraries were checked for quality using Agilent 2100 Bioanalyzer (Agilent,

USA) and quantified with DeNovix fluorometer (DeNovix, USA). The indexed sequencing libraries were pooled in equimolar quantity and subjected to cluster generation and paired-end 2x75 nucleotide read sequencing on Illumina NextSeq 500 sequencer. The sequencing process was carried out at Omics Sciences and Bioinformatics Center, Bangkok, Thailand.

3.8.3 Differential expression analyses of RNA-seq data

Bioinformatics analyses comprised an initial quality check of the raw reads data files using FASTQC software. Adapter and poor-quality reads were removed using Trimmomatic. The filtered reads were aligned to Human reference genome (EnsembleXX) using HISAT2 aligner software. HTSeq program was implemented to obtain raw counts for all human genes. Subsequently, the gene counts were used for differential expression analysis with the DESeq2 package.

3.8.4 Pearson correlation coefficient matrix (PCCM)

Correlation analysis was the analytical process to evaluate the association between two or more variable. Correlation coefficient was computed using Pearson correlation method which measured linear dependent between two variables in the case that samples had normal distribution. In this study, correlation matrix was used to investigate the dependence between multiple variables at the same time. The result is a table containing the correlation coefficients between each variable and the others. The PCCM was computed and visualized in RStudio by following guideline from Statistical tools for high-throughput data analysis (STHTDA) (http://www.sthda.com).

3.8.5 Principle component analysis (PCA)

PCA aims to identify directions along which the maximal variation in the data. This analysis extracted the important information from the complicated data table and presented this information as a set of few new variables that is called principal components. These new variables similar to a linear combination of the original data, that could be visualized graphically, with minimal loss of information. PCA was

computed and visualized in RStudio by following guideline from STHTDA (http://www.sthda.com).

3.8.6 RNAseq visualization

Differential expressed genes were represented in log2 transformed values. Heatmaps were generated using MORPHEUS, and differentially expressed genes were clustered using hierarchical clustering with complete linkage on one minus Pearson correlation metric. (https://software.broadinstitute.org/morpheus)

3.8.7 GSEAPreranked analysis

GSEAPreranked was performed using Broad Institute GSEA software version 3.0 and Molecular Signature Database (MSigDB) version 6.1. Gene set database was h.all.v6.1.symbol.gmt [Hallmark]. Weight scoring was applied for ranking statistic of data set.

3.8.8 Network analysis

Interested genes target was submitted to STRING version 10.5 (https://string-db.org), Network was clustered using k-mean clustering. Connected line represented evidence base interaction (in 5 criteria; text meaning, experiments, database, gene-fusion, neighborhood and co-occurrence).



3.9 Lipid staining

Cells were stimulated as indicated and the culture medium was removed. Cells were washed twice with PBS to remove extracellular lipid. Cells were fixed in 10% formaldehyde (Sigma Aldrich, USA) for 10 min and 100% formaldehyde for 1 h. The fixed cells were washed twice with water and incubated with 60% isopropanol in water for 5 min before completely dry. The cells were stained with oil red o (Sigma Aldrich, USA) solution (Appendix A) for 10 min, excessive dye was washed off with water for 4 times. Cells were visualized under an inverted microscope (Olympus, Olympus Corporation, Japan). Oil red O staining lipid in cells was eluted by 50 μl of 100%

isopropanol to measure the absorbance at 492 nm (the recommended wavelength was 500 nm) using microplate reader (Anthos 2010, UK).

3.10 Flow cytometry

Cells were treated as indicated. For cell surface staining, cells were harvested and FC receptor was blocked with human serum. Cells were washed with 1% FBS in PBS before staining with the fluorochrome conjugated antibody. For intracellular staining, Cells were washed with 1% FBS in PBS after blocking the FC receptor. Cells were fixed in 3% formaldehyde in PBS at 37$^{o}$C for 10 min and permeated by cold methanol on ice, followed by antibody staining. Cell were wash twice with 1% FBS in PBS before subjecting to analyze by flow cytometer (FC500, Beckman Coulter, USA). The antibodies and isotype control antibody, that were used in this study, were showed in Table 3. The acquired data were analyzed using FlowJo data analysis software (Tree Star, Inc., USA)

3.11 Statistical analysis

All statistical analyses except RNAseq analysis was performed using GraphPad Prism software Statistical significance was determined using two-way ANOVA, one-way ANOVA or unpaired t-test. *p*-value of less than 0.05 were considered significant.



Table 3 Antibodies used in flow cytometry

| Antibody lists | Used amount (μl) | Isotype control antibody | Company |
|---|---|---|---|
| Anti-CD14-PE | 2.5 | mIgG1κ-PE | BioLegend |
| Anti-CD163/PECy7 | 2.5 | mIgG1κ-PE/Cy7 | BioLegend |
| Anti-IL-4Rα-PE | 3 | mIgG1-PE | Immunotools |
| Anti-CD36-PE | 2.5 | mIgG1-PE | Immonotools |
| 7AAD (live/dead dye) | 1 | - | BioLegend |

# CHAPTER IV

# RESULTS

## 4.1. Phenotype of human M(IL-4)

### 4.1.1. M(IL-4) phenotype in THP-1 cell line

IL-4 stimulated macrophages receive signaling through IL-4Rα to activate STAT6 and AKT by phosphorylation. Phosphorylated STAT6 and AKT translocate to nucleus to regulate M(IL-4) signature target genes such as *TGM2*, *PPARG* [22, 122]. In this study, a human monocytic cell line (THP-1) was pretreated with PMA for 48 h to induce differentiation from monocytes to macrophages before stimulating with IL-4. To test that the dose of IL-4 at 20 ng/ml is sufficient to activate macrophages, IL-4R downstream signaling molecules and the target genes were examined by Western blot [123]. The results showed clearly that 20 ng/ml of IL-4 is sufficient to activate STAT6 and AKT by phosphorylation after activation as early as 15 min post treatment with IL-4 (Figure 5).

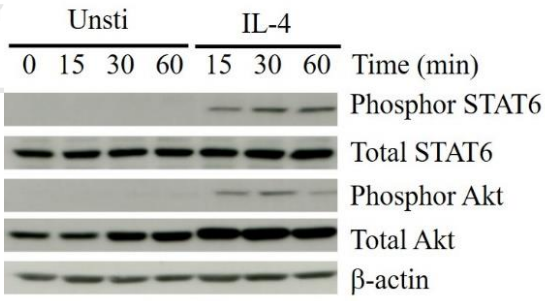


Figure 5 Activation of IL-4 signaling in THP-1 upon receiving IL-4.
THP-1 cell was pretreated with PMA (5 ng/ml) for 48 h before stimulating with IL-4 (20 ng/ml) for 0, 15, 30 and 60 min. Phosphorylated form and total protein of STAT6 and AKT were detected by Western blot. β-actin was used as loading control. The result was representative of three independent experiments.

When the two M(IL-4) signature proteins, TGM2 and PPARγ were examined, increasing of TGM2 and PPARγ protein level was observed in a time dependent manner (Figure 6A). To confirm this result, the band density from Western blot were measured by ImageJ program and was normalized with β-actin as the loading control. Normalized protein expression level was calculated relative to that of the unstimulation condition at each time point (Figure 6B and 6C). Significant upregulation of TGM2 and PPARγ protein level was detected over 18 h of IL-4 stimulation. This result confirmed that IL-4 (20 ng/ml) is sufficient to induce expression of IL-4 target proteins. Therefore, this IL-4 concentration will be used for further experiment.

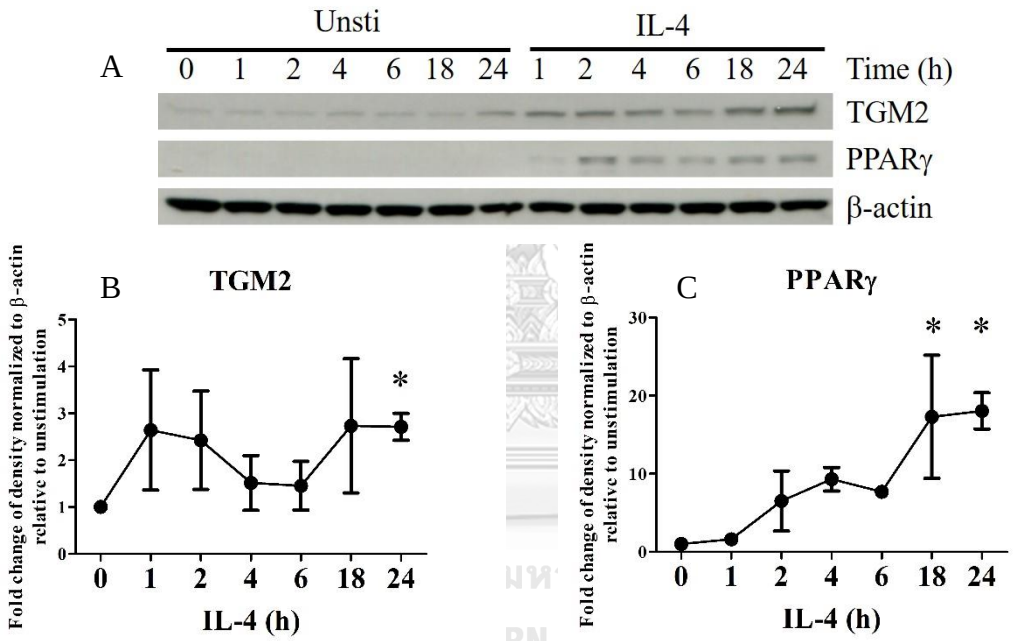


Figure 6 The phenotype of human M(IL-4) in THP-1.

THP-1 cell was pretreated with PMA (5 ng/ml) for 48 h before stimulating with IL-4 (20 ng/ml) for indicated time. (A) TGM2 and PPARγ were detected by Western blot. β-actin was used as loading control. The result was representative of three independent experiments. Relative protein level of TGM2 (B) and PPARγ (C) normalized by unstimulation at each time point was shown. The results are mean ± SEM of 5-6 independent experiments. *indicated statistically significant differences when compared with the unstimulated condition at $p < 0.05$.

4.1.2 Phenotypes of M(IL-4) in primary human monocyte derived macrophages (HMDMs)

4.1.2.1 Purity of CD14+ monocytes after isolation from PBMCs

The results obtained in THP-1 was confirmed in HMDMs. Human monocytes in PBMCs are divided into 3 subsets i.e. CD14+CD16$^{low}$, CD14+CD16+ and CD14$^{low}$CD16+ [124]. These major monocyte subsets have distinct phenotypes and functions [125]. This study used CD14+ monocytes because they are the major population (up to 90% of monocytes) in PBMCs [124]. CD14 monocytes were isolated from healthy blood donor. CD14+ is expressed mainly in granulocytes and monocytes. However, CD14+ granulocytes were excluded by ficoll density gradient centrifugation. CD14+ mononuclear cells were further isolated from PBMCs by positive selection using human CD14 MicroBeads. Purity of CD14+ monocytes after isolation was more than 97.4% as examined by flow cytometer (Figure 7).

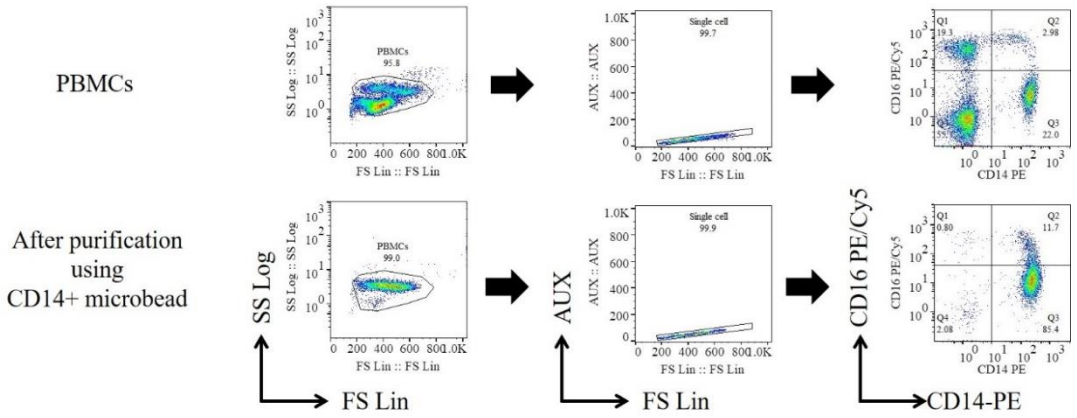


Figure 7 Gating strategy and the purity of CD14+ monocyte after isolation from PBMCs.

PBMCs were isolated white blood cells from healthy donor by ficoll gradient centrifugation. CD14+ monocytes were purified from PBMC by human CD14 MicroBeads. PBMCs and CD14+ cells after purification were stained for CD14 and CD16 and examined by flow cytometer. The result is representative of three independent healthy donors.

4.1.2.2 Macrophage markers

Purified CD14+ human monocytes were differentiated with M-CSF for 7 days. HMDMs were subjected for detection of macrophage markers prior to performing further experiments. In this study, human monocytes and monocytes derived macrophages were examined for CD163 and CD14 by flow cytometry. Consistent with previous studies, upregulation of CD163 and downregulation of CD14 were observed in M-CSF treated human macrophages compared with undifferentiated monocytes (Figure 8). This result indicated that HMDMs were successfully obtained.

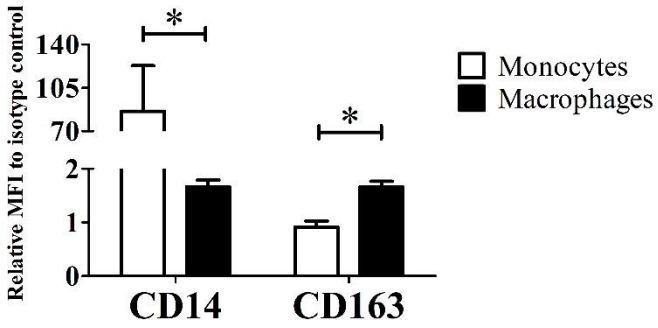




Figure 8 Human macrophages marker determination.
CD14+ monocytes were differentiated with 20 ng/ml M-CSF for 7 days. Culture medium was changed with fresh medium containing M-CSF every 2-3 days in half volume. Monocytes (day 0) and monocytes derived macrophages (day 7) were collected to examine for CD163 and CD14 by flow cytometry. The results are mean ± SEM of two independent healthy donors. *indicated statistically significant differences when compared with monocytic stage condition at $p < 0.05$.

4.1.2.3 Phenotypes of M(IL-4) from HMDMs

HMDMs were stimulated with IL-4 (20 ng/ml) for indicated times. The signaling downstream of IL-4 was examined by Western blot. Phosphorylation of STAT6 and AKT were increased with the similar kinetic as in IL-4 activated THP-1 cell (Figure 9A). This result, together with the upregulation of PPARγ confirmed that IL-4 dose and activation protocol in HMDMs was suitable to study the effect of IL-4 on macrophages activation (Figure 9B).

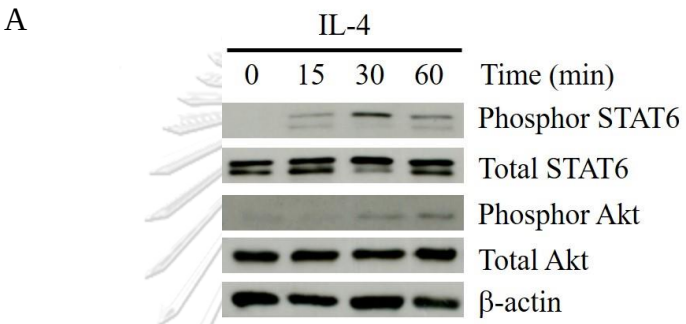


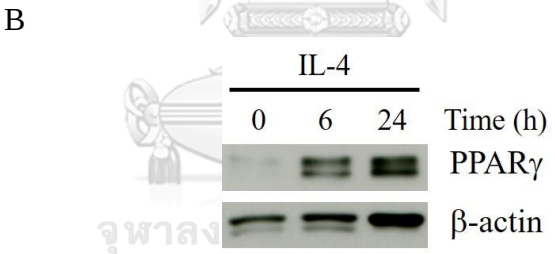




Figure 9 M(IL-4) macrophages activation and phenotype in HMDMs.
HMDMs were stimulated with IL-4 (20 ng/ml) for indicated time in each experiment. (A and B). Phosphorylation and total protein of STAT6 and AKT and PPARγ was detected by Western blot. β-actin was used as loading control. The result is representative of three healthy donors.

4.2 Notch signaling was activated in human M(IL-4)

4.2.1 Notch ligands and receptors expression in M(IL-4) (THP-1)

Upon IL-4 treatment, early (1-6 h) and late (24 h) responses were monitored for the expression of Notch receptors and ligands by qPCR. All mRNA expression of Notch ligands and receptors except *JAGGED1* and *NOTCH1*, were downregulated upon IL-4 stimulation (Figure 10). *NOTCH4* could not be detected. Therefore, IL-4 stimulation increased mRNA of *NOTCH1* and *JAGGED1* but decreased the expression of other receptors and ligands.

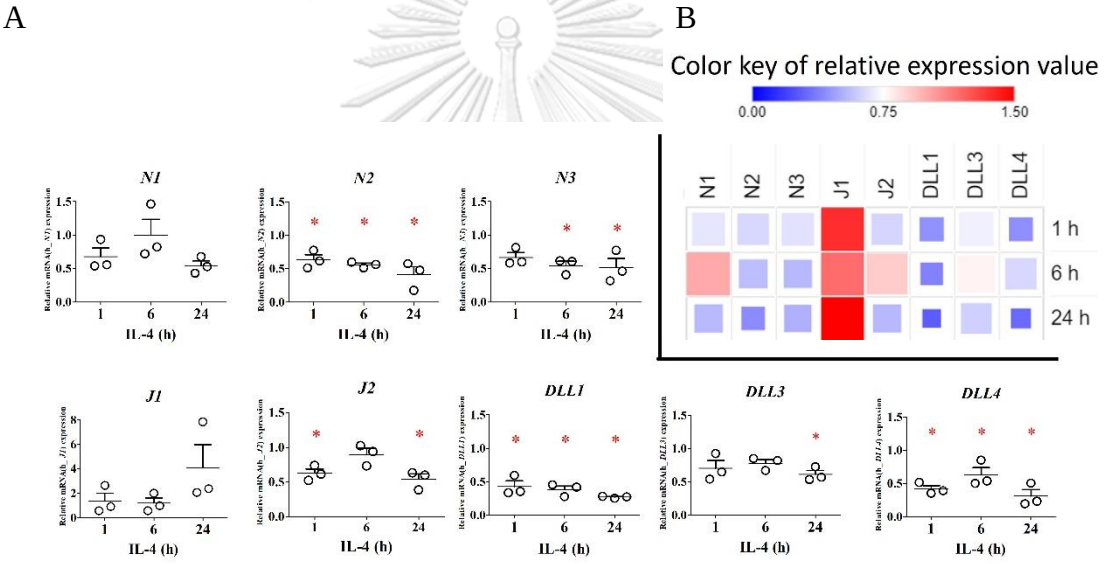




Figure 10 mRNA expression of Notch ligands and receptors in IL-4 activated THP-1. THP-1 cell was pretreated with PMA (5 ng/ml) for 48 h before stimulating with IL-4 (20 ng/ml) for 1, 6 and 24 h. (A) RNA were collected to examine Notch ligands and receptors mRNA expression by qPCR. *β-ACTIN* was used as housekeeping gene. (B) Summary of relative mRNA was shown in a heatmap. The box size correlated with expression level. The results are mean ± SEM of three independent experiments. *indicated statistically significant differences when compared with unstimulated condition at $p < 0.05$.

4.2.2 IL-4 treatment induced activation of Notch1 in THP-1

To investigate whether activation of Notch signaling was induced in IL-4 activated THP-1, cleaved Notch1 was detected by Western blot using antibody specific for cleavage site of Notch1 (Val1744). Rapid activation of Notch1 was clearly detected within 15-30 min upon IL-4 stimulation (Figure 11A-B). Additionally, expression of *HEY1* (one of the Notch target gene) was increased at 6 h (Figure 11C). However, *HES1* mRNA expression was decreased (data not shown) Similar observation was obtained from IL-4 activated HMDMs (Figure 12). Furthermore, when DAPT (γ-secretase inhibitor, GSI) was used, cleaved Notch1 was completely disappeared. These results strongly indicated that IL-4 stimulation activated Notch signaling in human macrophages at early time point both in human macrophages cell line and primary macrophages and this activation requires the activity of γ-secretase.

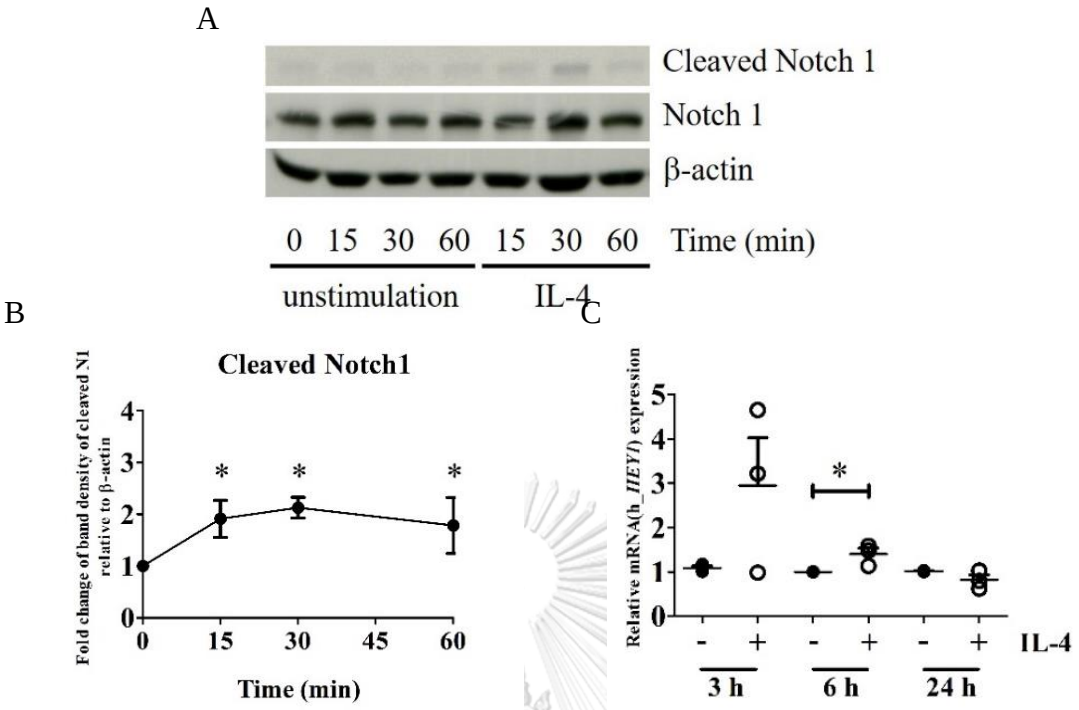


Figure 11 IL-4 activated Notch signaling in THP-1.

THP-1 cell was pretreated with PMA (5 ng/ml) for 48 h before stimulating with IL-4 (20 ng/ml) for indicated time. (A) Cleaved Notch1 (Val1744) and Notch1 were detected by Western blot. β-actin was used as loading control. The result is representative of three independent experiments. (B) The band density of cleaved Notch1 was normalized to β-actin and the relative level was calculated by comparing with unstimulating cell at each time point. (C) *HEY1* expression was determined by qPCR. *β-ACTIN* was used as housekeeping gene. The results are mean ± SEM of three independent experiments. *indicated statistically significant differences when compared with unstimulated condition at each time point at $p < 0.05$.

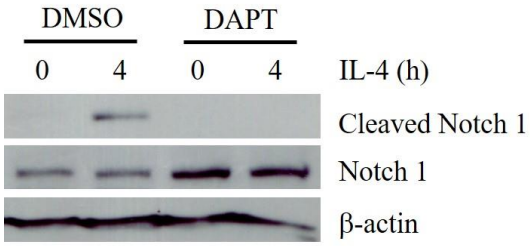


Figure 12 IL-4 activated Notch signaling in HMDMs.
HMDMs pretreated with DAPT (50 μM) or vehicle control (DMSO) for 1 h before stimulating with IL-4 (20 ng/ml) for 4 h. Cleaved Notch1 and Notch1 protein expression were examined by Western blot. β-actin was used as loading control. The result is representative of three healthy donors.

4.3 Notch signaling modulated PPARgamma expression in M(IL-4)

To understand how Notch signaling plays role in M(IL-4), THP-1 was engineered to increase or decrease Notch signaling by two strategies. First, in the pharmacological approach, DAPT was used to inhibit γ-secretase activity and abolish the releasing of cleaved Notch1 from transmembrane, [126]. Second, a genetic modification approach using retroviral vector containing DNA encoding Notch1 intracellular domain (for amino acid from position 1770 to 2556 of human *NOTCH1*) or dominant Negative Mastermind-like (DNMAML) were performed to retrovirally transduce into THP-1. Empty vector was used as control plasmid (CTRL). NIC1 overexpressing cells represented Notch hyperactivation. In contrast, DNMAML lacking the co-activator recruitment domain of MAML, interfered with the activity of canonical Notch signaling [116]. The phenotype of NIC1 and DNMAML overexpressing THP-1 was validated by detecting *HEY1* level after IL-4 stimulation. IL-4 stimulated CTRL increased *HEY1* expression (Figure 13). NIC1 overexpressing THP-1 increased *HEY1* in the presence or absence of IL-4 (Figure 13). In contrast, DNMAML overexpressing THP-1 fail to induce *HEY1* expression (Figure 13). These results confirmed that overexpression of NIC1 and DNMAML had hyperactive and hypoactive Notch signaling, respectively.

Next, to address whether Notch signaling is important for IL-4-induced PPARγ expression, NIC1 or DNMAML overexpressing THP-1 were activated with IL-4 and

PPARγ was monitored by Western blot. NIC1 overexpression increased PPARγ□level, while DNMAML overexpression had no effect on PPARγ expression at all time points tested (Figure 14). The effect of NIC1 on PPARγ was stronger at 24 h than at 4 h after IL-4 stimulation.

To confirm that activation of Notch signaling was important for increasing PPARγ protein expression, THP-1 and HMDMs were pretreated with DAPT to inhibit Notch activation before stimulating with IL-4. Consistent with NIC1 overexpressing phenotype, DAPT pretreatment decreased PPARγ protein expression in both cells (Figure 15A and 15B). These results strongly indicated that cleavage of Notch receptor was essential for increasing PPARγ protein expression in M(IL-4).

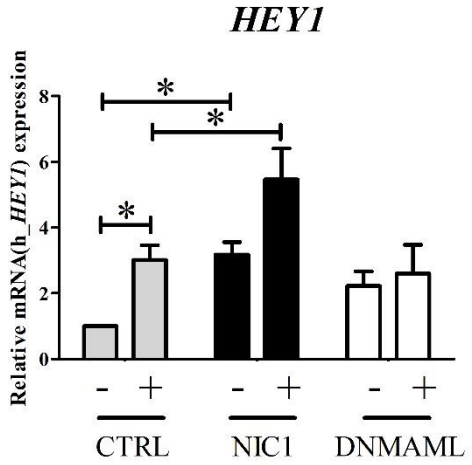




Figure 13 IL-4 activated Notch signaling in THP-1.
CTRL, NIC1 and DNMAML modified THP-1 were pretreated with PMA (5 ng/ml) for 48 h before stimulating with IL-4 (20 ng/ml) for 3 h. *HEY1* expression was determined by qPCR. *β-ACTIN* was used as housekeeping gene. The results are mean ± SEM of three independent experiments. *indicated statistically significant differences at $p < 0.05$.

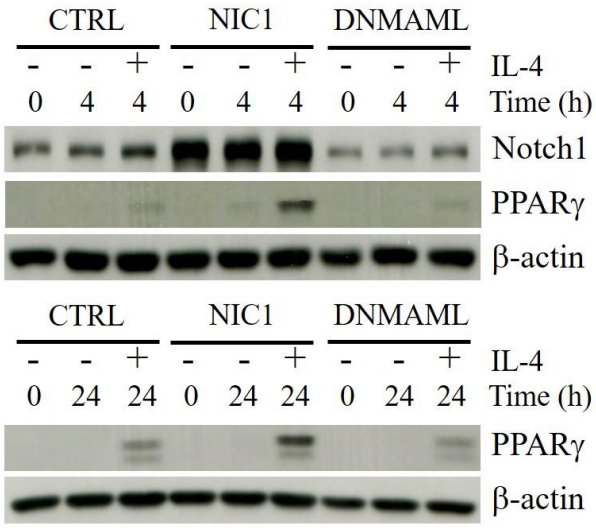


Figure 14 PPARγ expression in IL-4 activated Notch modified THP-1.

CTRL, NIC1 and DNMAML overexpressing THP-1 were pretreated with PMA (5 ng/ml) for 48 h before stimulating with IL-4 (20 ng/ml) for 4 or 24 h. PPARγ and Notch1 protein expression were examined by Western blot. β-actin was used as loading control. The result is representative of three independent experiments.

A **THP-1**

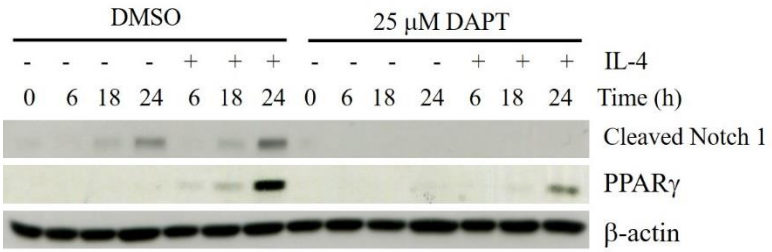


B **HMDMs**

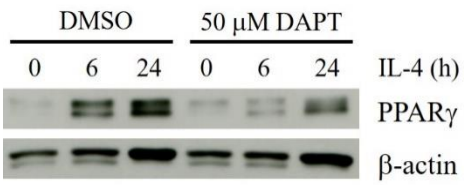


Figure 15 DAPT treatment decreased PPARγ in M(IL-4).

(A) THP-1 cell was pretreated with PMA (5 ng/ml) for 48 h. Cells were pretreated with DAPT (25 μM) or vehicle control (DMSO) for 1 h before stimulating with IL-4 for 0, 6, 18 and 24 h. Cleaved Notch1 and PPARγ protein expression were examined by Western blot. β-actin was used as loading control. The result is representative of three independent experiments (B) HMDMs were pretreated with DAPT (50 μM) for 1 h before stimulating with IL-4 (20 ng/ml) for 6 and 24 h. PPARγ protein expression was examined by Western blot. β-actin was used as loading control. The result is representative of three healthy donors.

4.4 Molecular mechanism how Notch signaling regulates PPARgamma in M(IL-4)

In order to understand how Notch signaling is involved in regulation of PPARγ in M(IL-4), the potential mechanism that may affect PPARγ expression was investigated. The mechanisms, including IL-4R expression, IL-4 downstream signaling, transcriptional regulation and protein degradation, were explored.

4.4.1 Effect of Notch signaling on IL-4 receptor alpha expression in IL-4-activated THP-1.

Feedback mechanism of IL-4 signaling in macrophages is responsible for reduction of IL-4R after IL-4 activation [42]. IL-4Rα expression was measured in IL-4-activated NIC1 and DNMAML overexpressing THP-1. IL-4Rα protein expression was decreased after 18 h of IL-4 activation in THP-1 cell which is consistent with previous report in U937 (Figure 16) [42]. No difference were found in the level of IL-4Rα at the basal or after IL-4 treatment among NIC1 or DNMAML overexpressing THP-1. This result indicated that Notch signaling did not interfere with IL-4Rα.

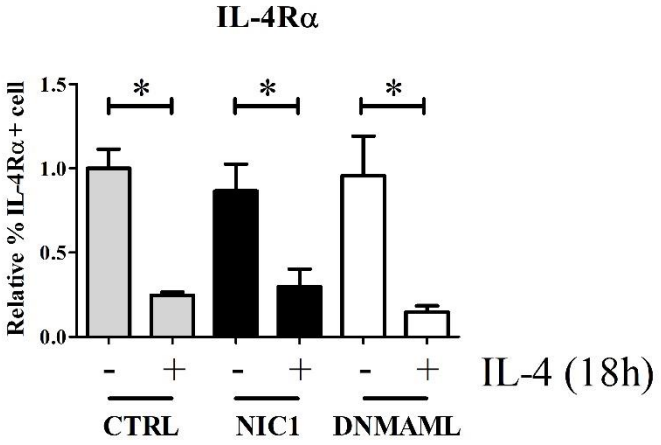


Figure 16 IL-4Rα expression in IL-4 activated Notch modified THP-1.
CTRL, NIC1 and DNMAML modified THP-1 were pretreated with PMA (5 ng/ml) for 48 h before stimulating with IL-4 (20 ng/ml) for 18 h. IL-4Rα expression was examined by flow cytometer. The results are mean ± SEM of three independent experiment. *indicated statistically significant differences at $p < 0.05$.

4.4.2 Effect of Notch signaling on IL-4 downstream signaling in macrophages.

IL-4 signaling pathway was well known to activate by phosphorylation of STAT6 and AKT. To examine that effect of Notch signaling on IL-4 downstream signaling, THP-1 was pretreated with DAPT and activated with IL-4. DAPT effectively inhibited Notch signaling in IL-4 activated THP-1 (Figure 17A and 17B). DAPT treated cell did not change STAT6 phosphorylation level but slight reduction in AKT phosphorylation level were detected by Western blot (Figure 17A). Similar result was obtained from HMDMs that DAPT did not change STAT6 phosphorylation level but decreased AKT (phosphorylation level) upon IL-4 activation (Figure 18). DAPT pretreated HMDMs decreased AKT phosphorylation more than in THP-1. These results might be because of the different dose of DAPT used. HMDMs were treated with higher dose (50 μM) because lower dose could not inhibit Notch target gene mRNA expression in our preliminary experiment (data not shown).

The contradictory reports showed that wortmannin and LY29004 (both are PI3K inhibitor) treated IL-4 stimulated mouse macrophages had opposite effect to PPARγ [30, 31]. Wortmannin treatment had no effect [30]. In contrast, LY294002 treatment decreased PPARγ expression [31]. Moreover, these results could not rule out the effect of multiple substrates of γ-secretase. Therefore, further investigation has to be addressed to clearly identify the mechanism underlying the effect of Notch on PPARγ.

A

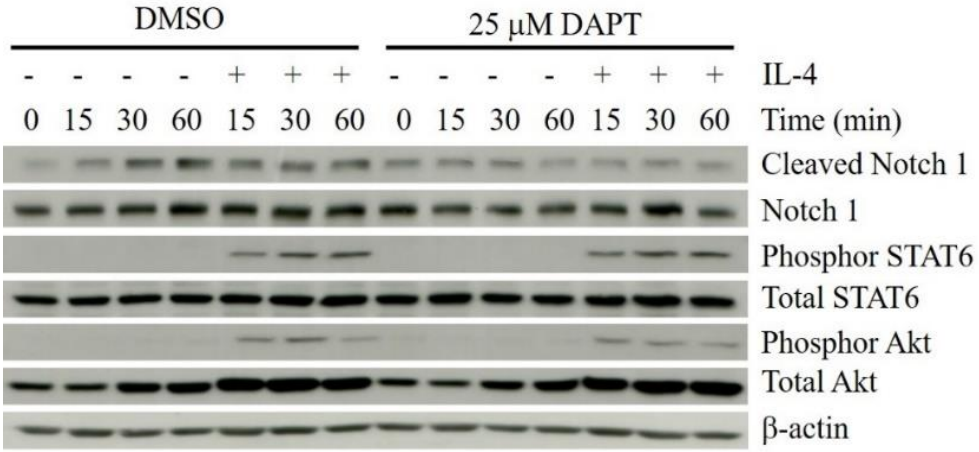


B

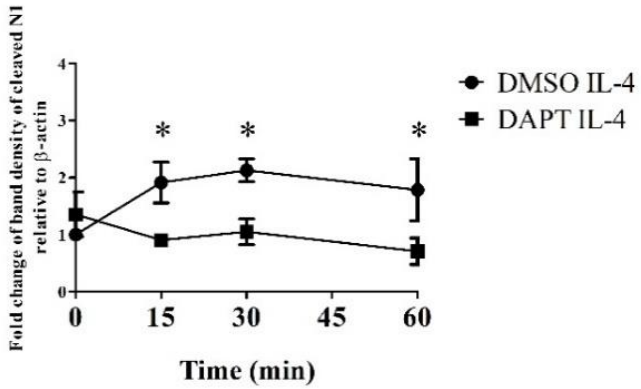


Figure 17 Effect of DAPT on IL-4 downstream signaling in THP-1.

(A) THP-1 cell was pretreated with PMA (5 ng/ml) for 48 h. Cell was pretreated with DAPT (25 μM) or vehicle control (DMSO) for 1 h before stimulating with IL-4 (20 ng/ml) for 0, 15, 30 and 60 min. Cleaved Notch1, Notch1, phosphorylation and total protein of STAT6 and AKT were detected by Western blot. β-actin was used as loading control. The result is representative of three independent experiments. (B) Band density of cleaved Notch1 was measured and the relative normalized protein expression level of cleaved Notch1 to unstimulation of each time point were calculated. The results are mean ± SEM of three independent experiments. *indicated statistically significant differences when compared with unstimulated condition at $p < 0.05$.

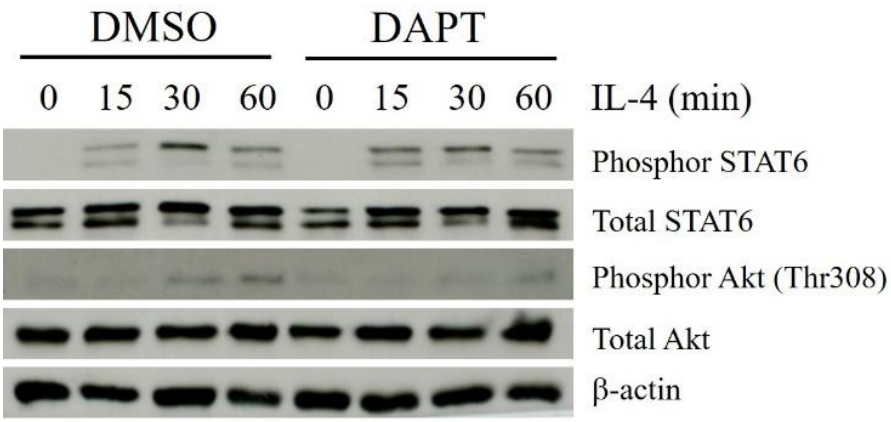


Figure 18 Effect of DAPT on IL-4 downstream signaling in HMDMs.
HMDMs were pretreated with DAPT (50 μM) or vehicle control (DMSO) for 1 h before stimulation with IL-4 (20 ng/ml) for 0,15, 30 and 60 min. Phosphorylation and total protein of STAT6 and AKT were detected by Western blot. β-actin was used as loading control. The result is representative of three independent healthy donors.

4.4.3 Effect of Notch signaling on *PPARG* mRNA expression in M(IL-4).

To examine whether Notch regulate PPARγ at the transcriptional level, *PPARG* mRNA expression in NIC1 and DNMAML overexpressing THP-1 cell in the presence or absence with IL-4 was investigated by qPCR. *PPARG* mRNA expression was increased at 3 h after IL-4 activation (Figure 19A). IL-4 stimulation increased *PPARG* mRNA at both 3 or 6 h in NIC1 or DNMAML overexpressing THP-1 similar to CTRL (Figure 19A and 19B). These results indicated that Notch signaling did not regulate PPARγ protein expression by increasing the transcription of mRNA.

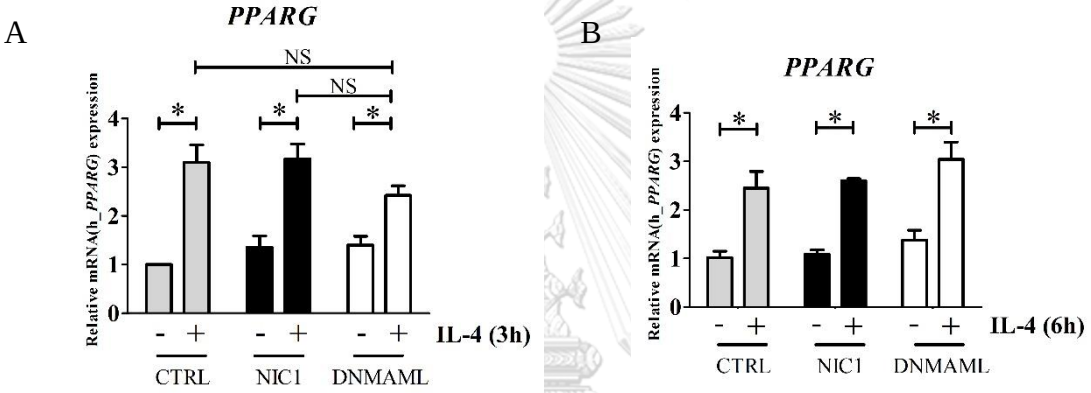


Figure 19 *PPARG* mRNA expression in IL-4 activated THP-1.

CTRL, NIC1 and DNMAML overexpressing THP-1 cell was pretreated with PMA (5 ng/ml) for 48 h before stimulating with IL-4 (20 ng/ml) for 3 (A) and 6 h (B). *PPARG* mRNA expression was determined by qPCR. *β-ACTIN* was used as housekeeping gene. The results are mean ± SEM of three independent experiments. *indicated statistically significant differences at $p < 0.05$. NS indicated that no statistically significant differences.

4.4.4 Effect of Notch signaling on *PPARG* mRNA stability in M(IL-4)

Because increasing PPARγ protein level, but not *PPARG* mRNA was observed when Notch signaling is hyperactivated, we hypothesized that Notch may increase mRNA stability of *PPARG*. Several factors including poly A tail, 3'untranslated region, mRNase etc., were reported to affect mRNA stability [127]. To address the hypothesis that Notch1 signaling increases *PPARG* mRNA, leading to increase protein level, NIC1 overexpressing THP-1 cell was stimulated with IL-4 for 3 h before blocking of mRNA transcription by actinomycin D (transcription inhibitor). The remaining of *PPARG* mRNA was monitored by qPCR. *PPARG* mRNA half-life in IL-4 activated CTRL cell was 104.3 ± 16.47 min (Figure 20). The half-life was not different from IL-4-activated NIC1 overexpressing cells which was 94.91 ± 7.58 min (Figure 20). From these results, Notch signaling did not regulate *PPARG* mRNA stability.

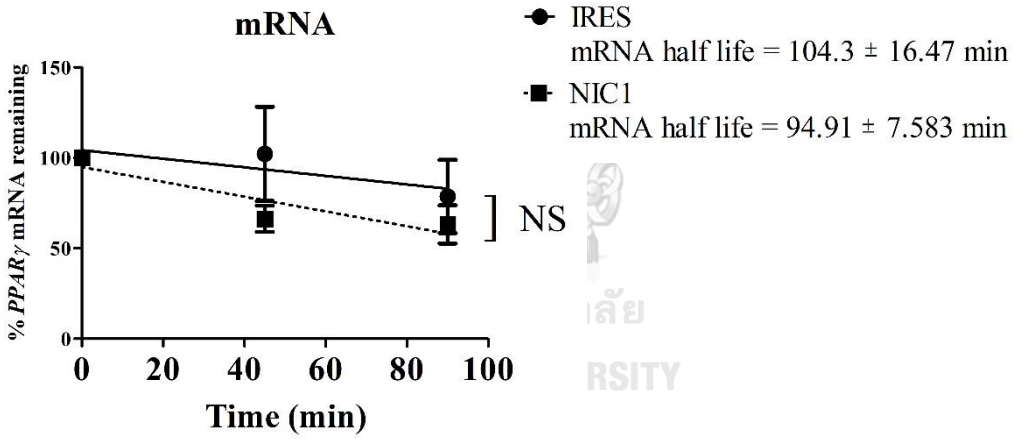


Figure 20 *PPARG* mRNA stability in IL-4 activated NIC1 overexpressing THP-1. CTRL and NIC1 overexpressing THP-1 cell were pretreated with PMA (5 ng/ml) for 48 h. Cells were stimulated with IL-4 (20 ng/ml) for 3 h, subsequently treated with actinomycin D (1 μM) for 0, 45 and 90 min. *PPARG* mRNA expression was determined by qPCR. *β-ACTIN* was used as housekeeping gene. The results are mean ± SEM of three independent experiments. NS indicated that no statistically significant differences.

4.4.5 Effect of Notch signaling on PPARgamma protein synthesis and degradation.

The results obtained until now, indicated that NIC1 increased PPARγ protein expression in IL-4 stimulation and the regulation mechanism was not through IL-4Rα expression, downstream signaling of IL-4, *PPARG* mRNA expression and stability. Previous reports found that PPARγ was degraded by proteasome in adipocytes [101, 102]. Therefore, synthesis and degradation of PPARγ were examined in M(IL-4). NIC1 or DNMAML overexpressing THP-1 was pretreated with MG132 (a proteasome inhibitor) to inhibit protein degradation via proteasome. After this treatment cells were stimulated with IL-4 for 4 h. Consistent with previous reports, MG132 treatment of IL-4 stimulated THP-1 delayed PPARγ degradation by proteasome (Figure 21A and 21B). Indeed, if Notch1 hyperactivation increase PPARγ level via proteasome mediated degradation, MG132 treatment would yield similar result as CTRL cells. NIC1 overexpression and MG132 cotreatment did not further increase the level of PPARγ when compared with MG132 treatment of CTRL This result indicated that NIC1 overexpressing THP-1 was decreased PPARγ protein degradation via proteasome because inhibition of proteasome did not enhance this effect.

IL-4 stimulated DNMAML overexpressing THP-1 had comparable PPARγ level as IL-4 stimulated CTRL with or without MG132 treatment (Figure 21A and 21B), indicating that DNMAML overexpressing THP-1 did not regulate PPARγ protein synthesis and degradation. These results suggested that Notch signaling did not control PPARγ protein synthesis, whereas Notch1 hyperactivation increased PPARγ stability, possibly through delay protein degradation.

A

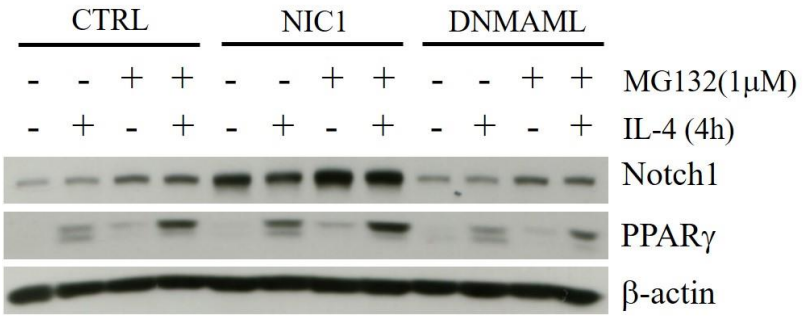


B

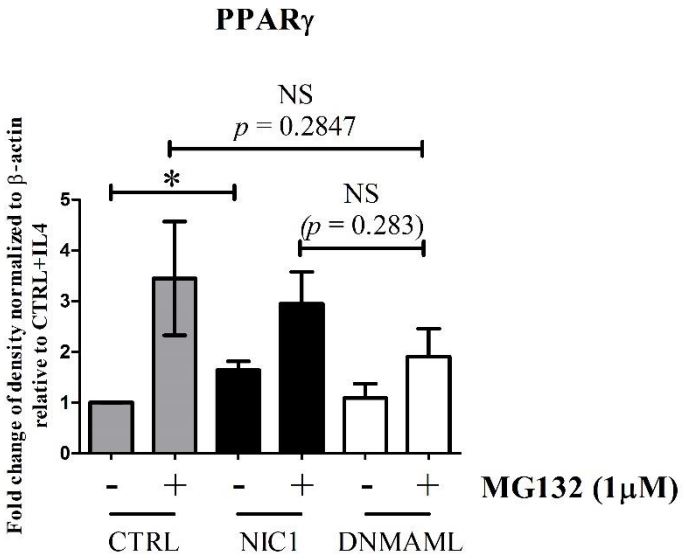


Figure 21 NIC1 decreased proteasome degrade PPARγ.

(A) THP-1 cell was pretreated with PMA (5 ng/ml) for 48 h. Cell was pretreated with MG132 (1 μM) for 1 h, subsequently stimulated with IL-4 (20 ng/ml) for 4 h. PPARγ and Notch1 protein expression was examined by Western blot. β-actin was used as loading control. (B) PPARγ band density from IL-4 stimulated condition in (A) was normalized to β-actin. The results are mean ± SEM of three independent experiments. *indicated statistically significant differences at $p < 0.05$.

In this study, PMA was used to induce differentiation of THP-1 to macrophages state. Therefore, NIC1 might modulate PMA signaling and caused increasing of PPARγ. To exclude this possibility, PPARγ protein expression was directly investigated in NIC1 or DNMAML overexpressing THP-1 without PMA treatment. Similar result with PMA treatment was obtained. NIC1 overexpression increased PPARγ protein expression compared with CTRL (Figure 22), while DNMAML still had no effect on PPARγ protein expression (Figure 22). These results indicated that NIC1 alone is sufficient for increasing PPARγ even in the absence of IL-4.

To examine whether NIC1 overexpressing THP-1 cell increases PPARγ protein stability, PPARγ protein half-life was examined in IL-4-activated NIC1 overexpressing THP-1 compared with IL-4 activated CTRL. Protein half-life of PPARγ was 69.93 ± 27.86 min in IL-4-activated CTRL, while IL-4-activated NIC1 overexpressing cells showed approximately twice longer half-life of PPARγ (122.75 +/- 37.21 min) (Figure 23).

Collectively, these results indicated that NIC1 overexpression by itself extends the half-life of PPARγ in regardless of signal from IL-4.



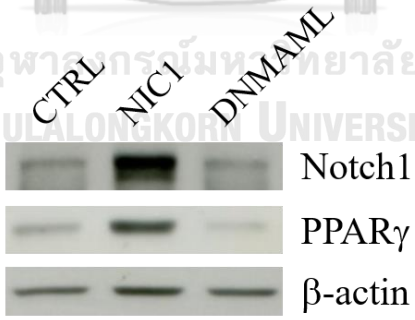


Figure 22 NIC1 alone is sufficient in increasing PPARγ protein**.**
PPARγ and Notch1 protein expression was detected in NIC1, DNMAML and CTRL overexpressing THP-1 by Western blot. β-actin was used as loading control. The result is representative of three independent experiments.

A

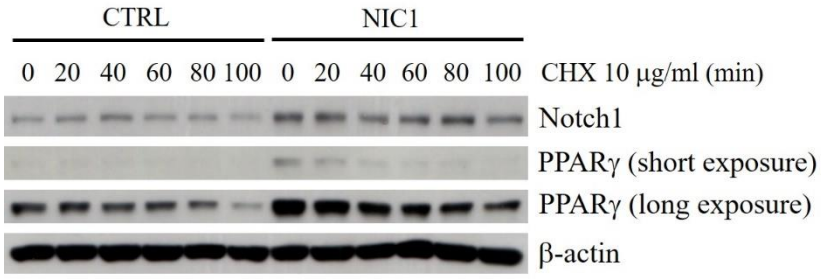


B

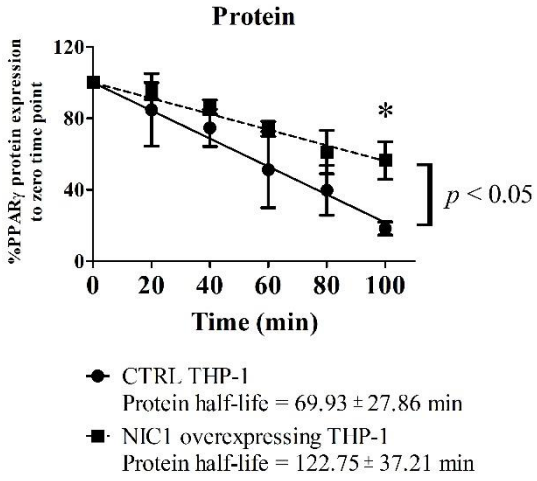


Figure 23 NIC1 prolonged PPARγ protein half-life in THP-1.

CTRL and NIC1 overexpressing THP-1 cell were pretreated with PMA (5 ng/ml) for 48 h. Cells were stimulated with IL-4 (20 ng/ml) for 4 h, followed by treatment with cycloheximide (CHX, 10 μg/ml). Protein lysate was collected every 20 min for total 100 min. (A) PPARγ and Notch1 protein expression was examined by Western blot. β-actin was used as loading control. (B) Graph depicting PPARγ protein stability in IL-4 activated CTRL or NIC1 overexpressing THP-1. PPARγ band density in (A) was normalized with β-actin. The normalized expression was calculated as % PPARγ expression relative to 0 min of CHX treatment. The results are mean ± SEM of three independent experiments. *indicated statistically significant differences at $p < 0.05$.

4.5 Transcriptomic analysis of NIC1 or DNMAML overexpressing M(IL-4)

To obtain detailed mechanism how Notch signaling functions in M(IL-4), RNAseq analysis was performed. Unstimulated and IL-4-stimulated CTRL, NIC1 and DNMAML overexpressing THP-1 cells were subjected to transcriptomic profile analysis by RNAseq.

4.5.1 Sample profile similarity

Similarity across sample groups was determined by Pearson correlation coefficient matrices (PCCM). PCCM results revealed transcriptomic profile among all samples was quite similar which had correlation coefficient close to 1 (Figure 24). There was less similarity between NIC1 overexpressing THP-1 background compared to other samples. The most dissimilarity were found between NIC1 and DNMAML overexpressing THP-1 samples, indicating that these samples were transcriptionally distinct. The CTRL and DNMAML overexpressing THP-1 data set on both unstimulation and IL-4 stimulation was similar. Therefore, NIC1 overexpression had stronger impact on the transcriptomic profile of M(IL-4) than DNMAML overexpression.

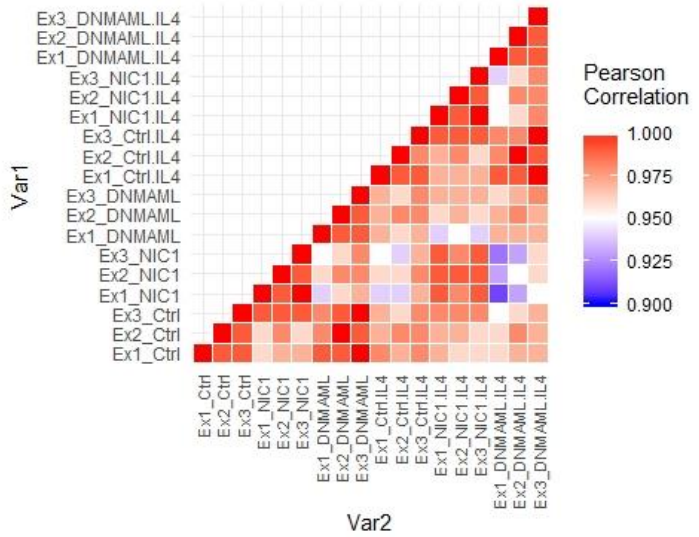


Figure 24 Heatmap of Pearson correlation coefficient matrix (PCCM).
Pearson correlation coefficients are standardized from 0.9 to 1.0.

4.5.2 Variation in datasets by principle component analysis (PCA)

PCA was performed to determine variation in the datasets [128]. The PCA plot showed that unstimulation set and IL-4 stimulation located in the separated dimension in all conditions (Figure 25), indicating that IL-4 stimulation changed the gene expression profile which was different from unstimulation. NIC1 overexpression datasets (both unstimulation and IL-4) was clearly separated from CTRL or DNMAML overexpression datasets (Figure 25). Data set of DNMAML and CTRL often clustered together, suggesting that DNMAML overexpression had minimal impact on transcriptomic data, compared with CTRL (Figure 25). This result suggested that hyperactivation of Notch signaling has stronger impact on M(IL-4) than its inhibition by DNMAML. This may suggest the important of non-canonical Notch signaling in M(IL-4)

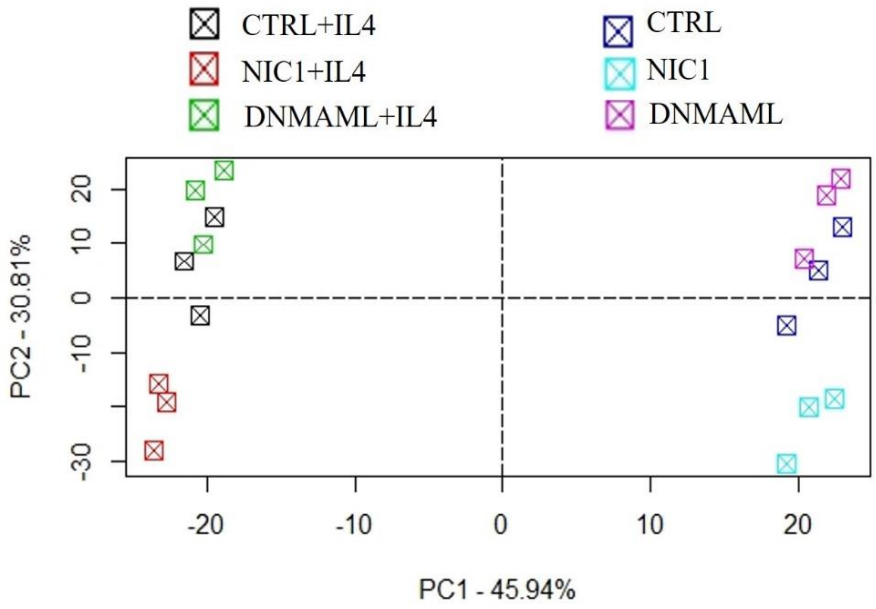


Figure 25 Principle component analysis of RNA-seq data.
Dim1 (PCA dimension 1, x-axis) represented 45.94% and Dim2 (PCA dimension 2, y-axis) represented 30.81% of total variation in the data.

4.5.3 Genes regulated by IL-4 in M(IL-4)

To determine which genes were under the influence of IL-4 in IL-4 activated THP-1, all raw counts from IL-4 activated CTRL (CTRL M(IL-4)) were compared with CTRL unstimulation (CTRL) using DESeq2 on Galaxy web-based analysis platform. IL-4 treatment induced change in 402 genes changing (Table 5 Appendix B), which mostly upregulated (71.64%) and 28.64% was down regulated during IL-4 activation. (Figure 26A and 26B). To select the potential target(s) which had statistically significance with high fold change, the volcano plot between CTRL and CTRL M(IL-4) was generated (Figure 27). The blue dot indicated genes which had strongly up-or downregulated from dataset. The well known IL-4 target such as cytokine inducible SH2-containing protein (CISH), suppressor of cytokine signaling 1 (SOCS1) had been reported to be upregulated in IL-4-activated human and mouse macrophages and well as in breast cancer [129]. These results implied that IL-4 acitvated THP-1 had consistent phenotype with previously described for M(IL-4).

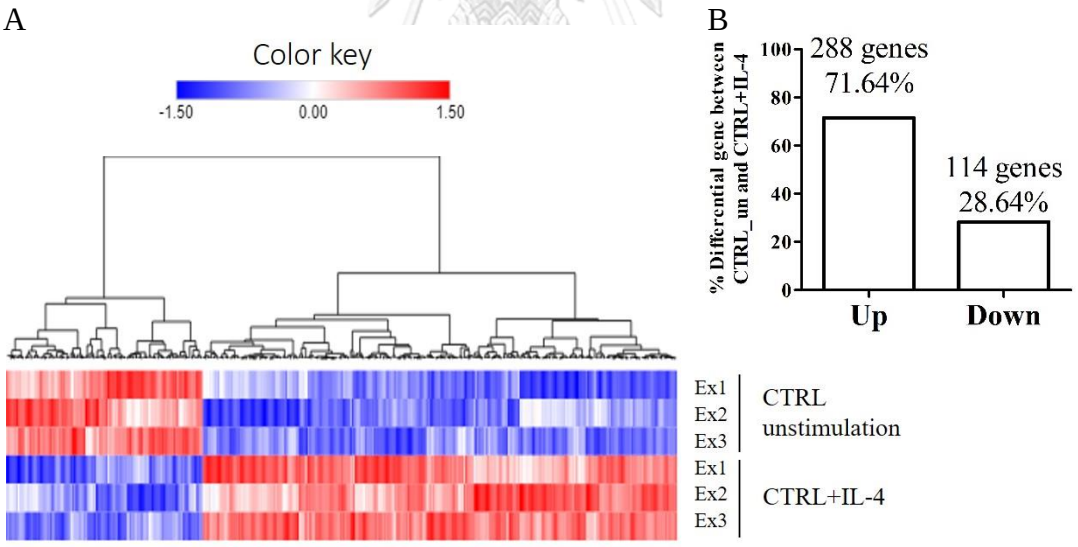


Figure 26 Heat map of gene transcript differential expression during IL-4 activated THP-1.

Heat map of gene expression was represented in log2 transformed values; red represented expression greater than mean and blue represented expression lower than mean, as shown in color key scale. (B) The percentage of up-and down-regulation of differential gene expression between CTRL unstimulation and CTRL M(IL-4).

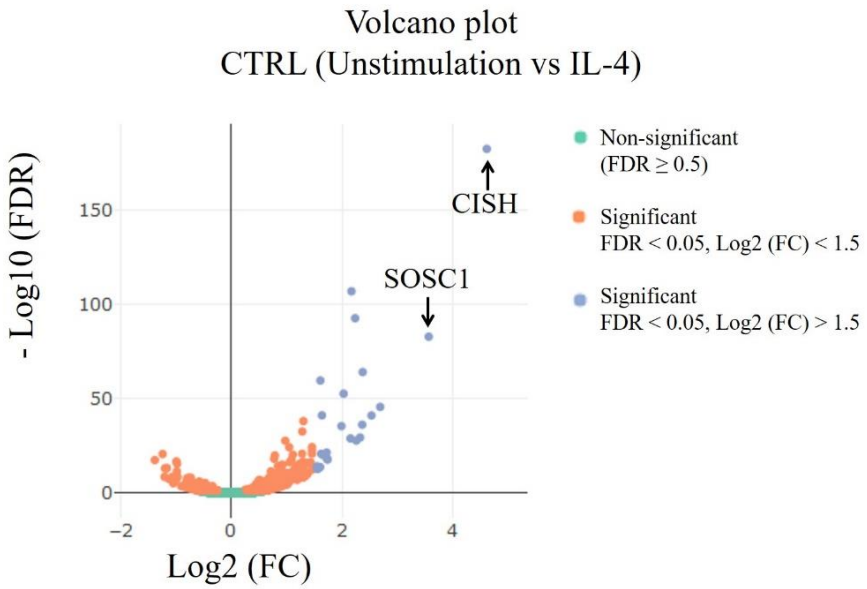


Figure 27 Volcano plot of the transcriptomes between CTRL M(IL-4) compared with CTRL.

X-axis represented log2(fold change). Y-axis represented -log10(FDR). Green dots represented not significant different genes (FDR ≥ 0.05). Orange dots represented differential gene expression (FDR < 0.5) but log2(fold change) less than 1.5. Blue dots represented differential gene expression (FDR < 0.5) and log2(fold change) greater than 1.5.

4.5.4 Transcriptomic changing in NIC1 overexpressing M(IL-4)

The volcano plot between NIC1 overexpressing M(IL-4) and unstimulation (Figure 28) showed upregulated and downregulated genes similar to the upregulated IL-4 target form CTRL M(IL-4) such as CISH and SOCS1. This result implies that IL-4 stimulation induced M(IL-4) profile in the presence of NIC1 overexpression and had M(IL-4) phenotype. The overall differential expressed genes was showed in Table 6 (Appendix C).

To explore which genes were more affected by NIC1 overexpression, dataset of IL-4 stimulated condition from NIC1 was compared to dataset of CTRL. Heatmap in Figure 29A showed differential gene expression in both conditions. Ninety-one genes were found differentially expressed. Among these genes, 90.11 % was upregulated and 9.89 % was down regulated (Figure 29B). NIC1 overexpressing M(IL-4) predominantly upregulated HES4 and DTX1, the two known of Notch target genes [130] (Figure 29A and 30). Many studies used HES1 and HEY1 as indicator for Notch signaling activation [131]. This study as indicated HES4 and DTX1 as another indicators for Notch activation in M(IL-4). HES4 was poor prognostic marker for chemotherapy in osteosarcoma, due to it increased tumor metastasis [131]. DTX1 function as positive and negative regulator of Notch [132]. Among these differentially upregulated genes, some were related to inflammation. For example, Aryl hydrocarbon nuclear transporter 2 (ARNT2), was a late response gene, the level of which increased upon TNFα stimulation in human macrophages [133].



In addition, the differential expressed genes of IL-4 stimulated condition between NIC1 and CTRL was subjected to gene ontology (GO) analysis based on molecular (Figure 31) and biological function (Figure 32). The signaling receptor binding including Notch1, DTX1, ARTN2, were presented at the top of molecular function of GO. The next involved in lipid antigen binding and T cell receptor binding which found CD1A, CD1C and CD1D in these data set. CD1 family member is atypical MHCII that presents lipid antigen to immune cells [134]. CD1A, CD1C and CD1D presents antigen to reactive T cell, B cell and NK T cell, respectively [134]. Therefore, the upregulating of these genes enhances T cell activation and immune response as found in biological

function of GO. Interestingly, adhesion and response to wounding were other biological function that found in IL-4 stimulated NIC1 overexpressing M(IL-4) compared with CTRL M(IL-4). These results indicated that Notch regulates lipid antigen presentation to lymphocytes, cell adhesion and response to wounding in M(IL-4).

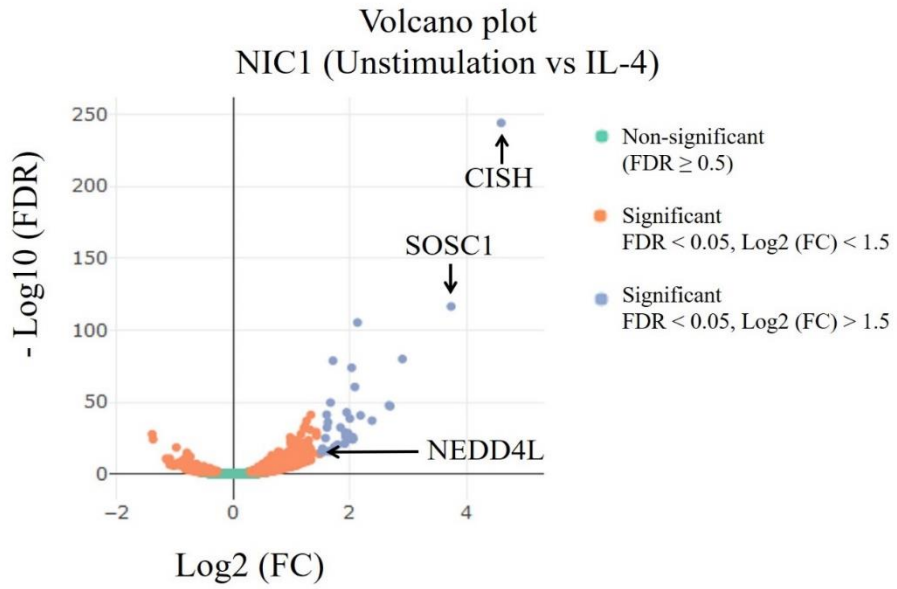


Figure 28 Volcano plot of transcriptomic data between NIC1 overexpressing M(IL-4) and unstimulation.

X-axis represents log2(fold change). Y-axis represents -log10(FDR). Green dots are genes with no significant difference (FDR ≥ 0.05). Orange dots are differentially expressed gene (FDR < 0.5) with log2(fold change) less than 1.5. Blue dots are differentially expressed gene (FDR < 0.5) with log2(fold change) greater than 1.5.

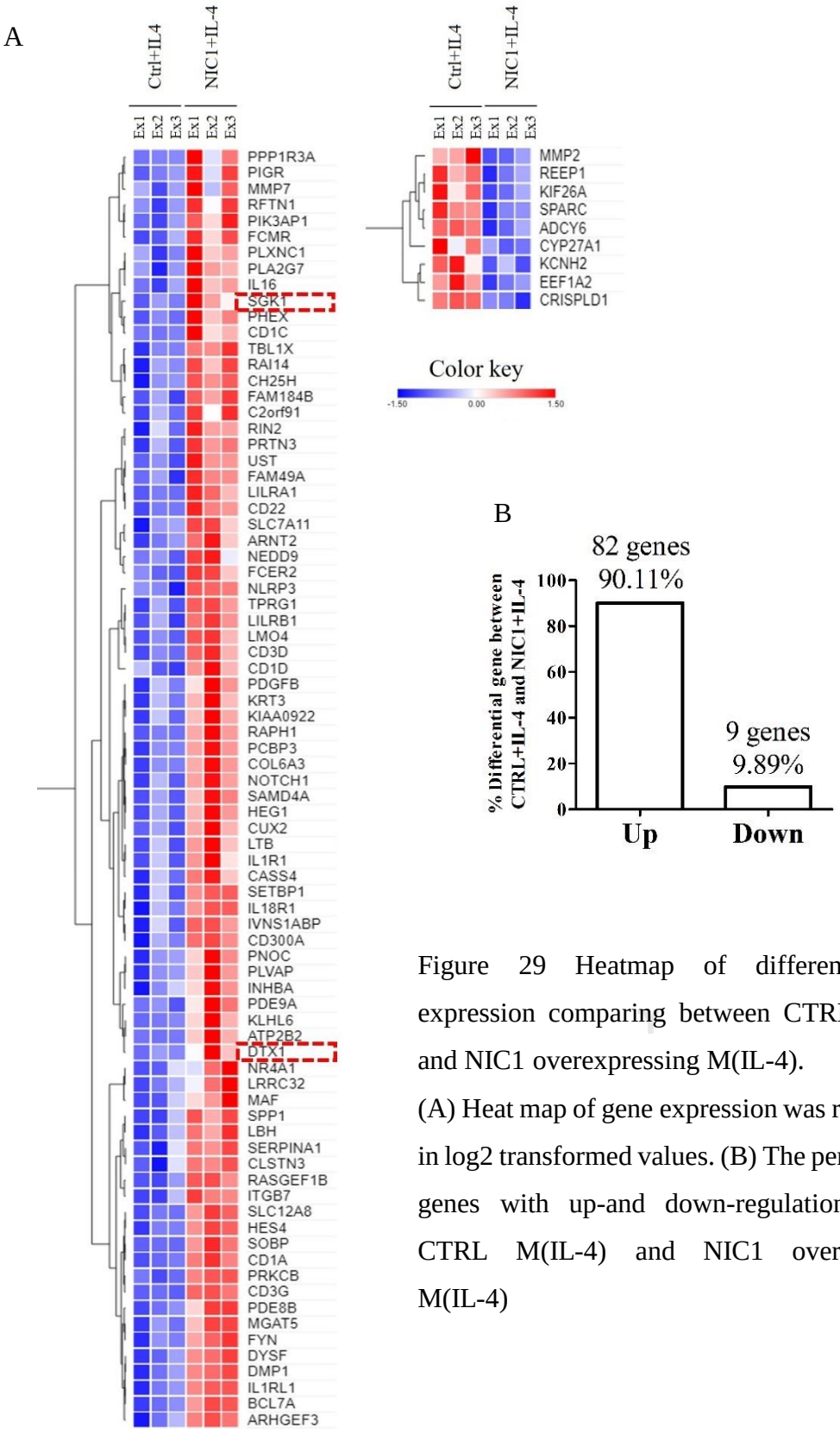


Figure 29 Heatmap of differential gene expression comparing between CTRL M(IL-4) and NIC1 overexpressing M(IL-4).

(A) Heat map of gene expression was represented in log2 transformed values. (B) The percentage of genes with up-and down-regulation between CTRL M(IL-4) and NIC1 overexpressing M(IL-4)

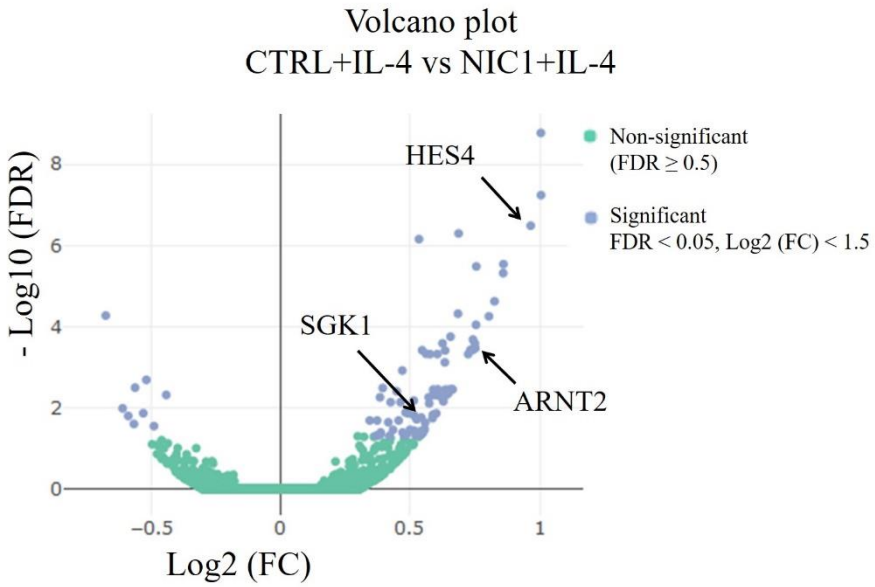


Figure 30 Volcano plot of transcriptomes between CTRL (MIL-4) compared and NIC1 overexpressing M(IL-4).

X-axis represents log2(fold change). Y-axis represents -log10(FDR). Green dots are genes with no significant difference (FDR ≥ 0.05). Blue dots are differentially expressed gene (FDR < 0.5) with log2(fold change) less than 1.5.

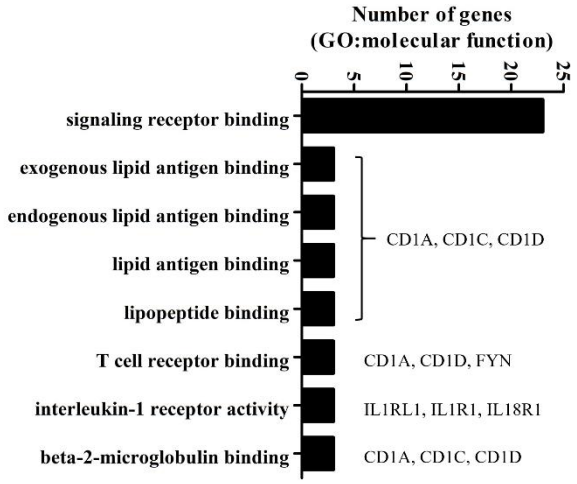


Figure 31 Gene ontology analysis based on molecular function of the differential expressed genes between CTRL (MIL-4) compared and NIC1 overexpressing M(IL-4). X-axis represents number of genes in each molecular function. Y-axis represents the molecular function of GO analysis that $p < 0.05$.

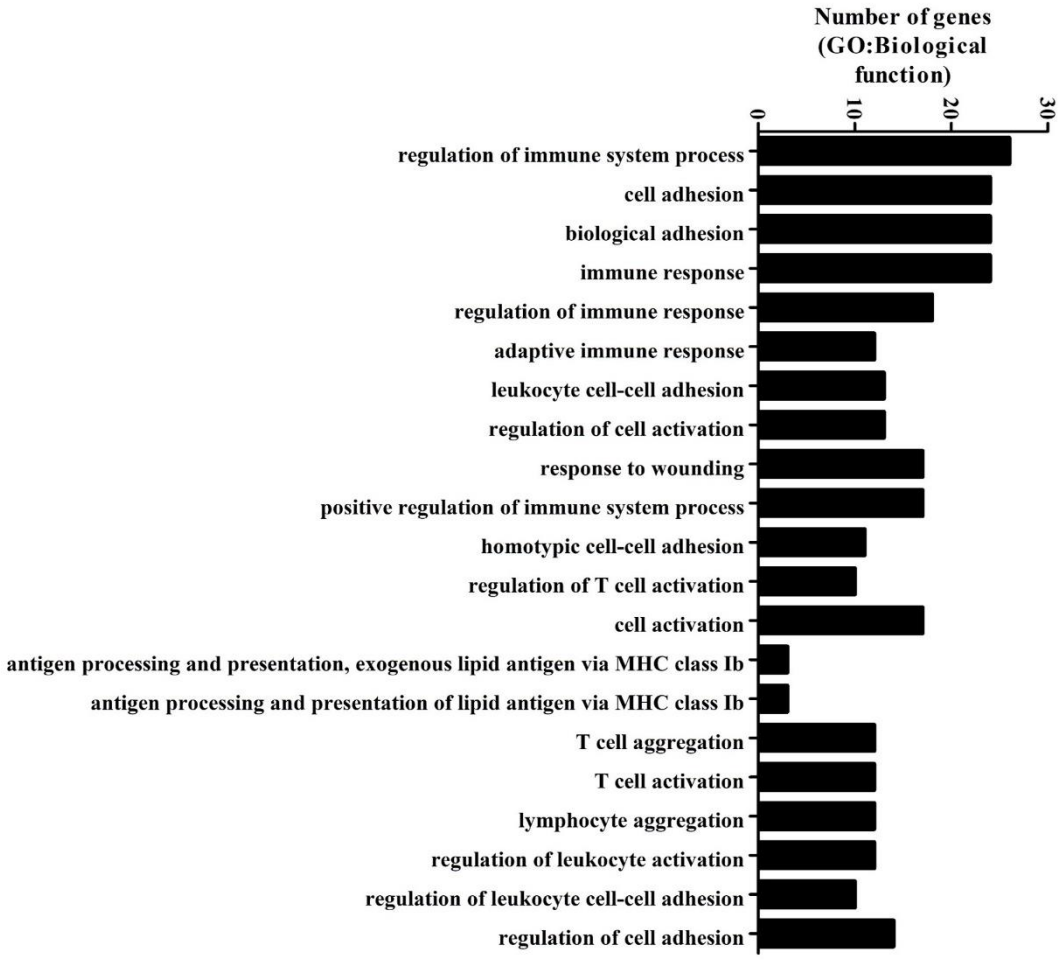




Figure 32 Gene ontology analysis based on biological function of the differential expressed genes between CTRL (MIL-4) compared with NIC1 overexpressing M(IL-4).

The top 20 of biological function of GO was selected to present. X-axis represents number of genes in each biological function. Y-axis represents the biological function of GO analysis $p < 0.05$.

4.5.5 Transcriptomic changing in DNMAML overexpressing M(IL-4)

The volcano plot between DNMAML overexpressing M(IL-4) and unstimulation (Figure 33) showed upregulated and downregulated genes similar to the upregulated IL-4 target form CTRL M(IL-4) such as CISH and SOCS1. This result implies that IL-4 stimulation induced M(IL-4) profile in the presence of DNMAML overexpression and had M(IL-4) phenotype.

In contrast to NIC1 overexpressing M(IL-4), DNMAML overexpressing M(IL-4) dataset showed minimal impact comparing with IL-4 stimulated CTRL. Acid Phosphatase 5, Tartrate Resistant (ACP-5) was the only one differentially expressed gene (Figure 34). However, comparing IL-4 stimulated dataset with unstimulated dataset in DNMAML overexpression identified 461 genes with differential expression, and had similar heat map pattern to IL-4 stimulated CTRL, except for ACP5 (Figure 34), which significantly different in unstimulated condition of DNMAML compared to CTRL.

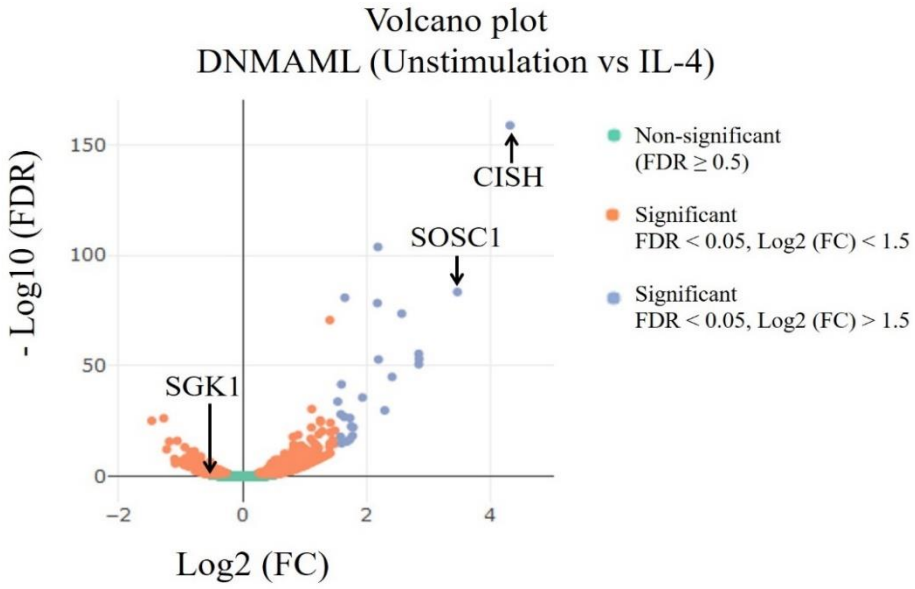


Figure 33 Volcano plot of transcriptomic data between DNMAML overexpressing M(IL-4) compared with DNMAML unstimulation.

X-axis represents log2(fold change). Y-axis represents -log10(FDR). Green dots are genes with no significant difference (FDR ≥ 0.05). Orange dots are differentially expressed gene (FDR < 0.5) with log2(fold change) less than 1.5. Blue dots are differentially expressed gene (FDR < 0.5) with log2(fold change) greater than 1.5.

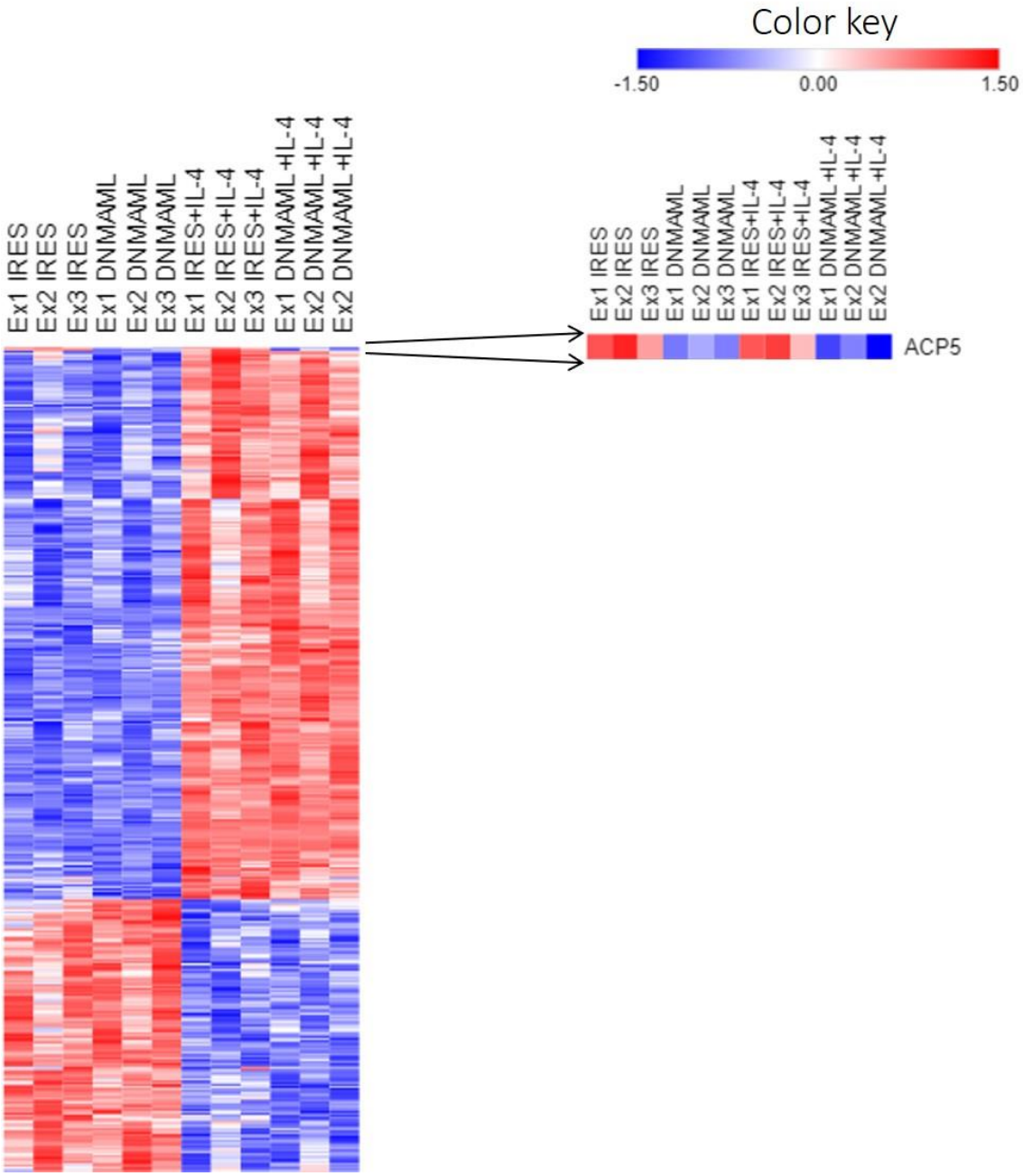


Figure 34 Heatmap of differentially expressed genes in DNMAML overexpressing M(IL-4).

Heat map of gene expression was represented in log2 transformed values.

4.5.6 Enrichment gene sets of NIC1 overexpressing M(IL-4) compared with CTRL M(IL-4).

To select gene sets with biological significance between CTRL M(IL-4) and NIC1 overexpressing M(IL-4), the gene raw counts of both sets were subjected to GSEAPreranked tool in the GSEA software. In this comparison, hall mark of interferon alpha (IFNα) was dominant in CTRL M(IL-4) which was reported before that IFNα enhanced IL-4-mediated STAT6 function (Table 4) [135]. Hyperactivation of Notch1 clearly enriched Notch signaling pathway (Table 4). IL-4 stimulated NIC1 showed increased inflammatory property gene set, including TNFα signaling via NF-κB, inflammatory response, KRAS signaling and IL-6 JAK-STAT3 signaling [136]. Some involved in anti-inflammation such as androgen receptor signaling [137, 138]. Hypoxia condition which was enriched in NIC1 overexpressing M(IL-4), was the common feature of several diseases such as atherosclerosis, cancer, infection, ischemic heart failure etc [139]. The genes in hypoxia hallmark was matched to differential gene expression from DESeq2 analysis (log2 fold change greater than 1.5 or less than -1) to select the potential target. NEDD4L was found upregulated in NIC1 overexpressing M(IL-4) (compared with NIC1 unstimulation) (Figure 28 and 35).

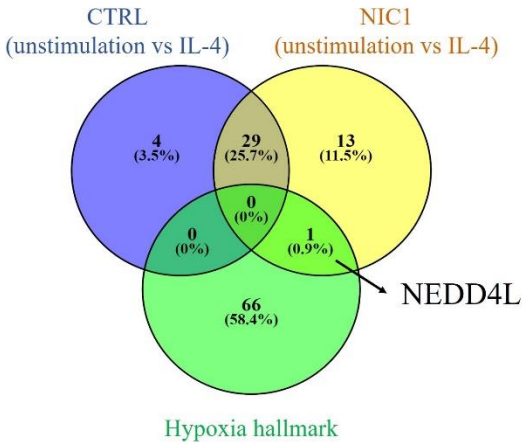


Figure 35 Venn diagram.

The differential gene expression from DESeq2 of IL-4 from CTRL M(IL-4) and NIC1 overexpressing M(IL-4) were compared with the significant enrichment genes from hypoxia hallmark of GSEAPreranked analysis. The result is showed in venn diagram.

Table 4 Enrichment gene set in NIC1 overexpressing M(IL-4) from GSEAPreranked analysis comparing between CTRL (MIL-4) and NIC1 overexpressing M(IL-4)

| NAME | NES* | FDR |
|---|---|---|
| HALLMARK_TNFA_SIGNALING_VIA_NFKB | -2.23261 | 0 |
| HALLMARK_INFLAMMATORY_RESPONSE | -2.10527 | 0 |
| HALLMARK_IL2_STAT5_SIGNALING | -1.89539 | 4.00E-04 |
| HALLMARK_KRAS_SIGNALING_UP | -1.89511 | 3.00E-04 |
| HALLMARK_ALLOGRAFT_REJECTION | -1.83354 | 8.82E-04 |
| HALLMARK_ANGIOGENESIS | -1.80401 | 9.42E-04 |
| HALLMARK_NOTCH_SIGNALING | -1.73873 | 0.003234 |
| HALLMARK_COMPLEMENT | -1.71673 | 0.003496 |
| HALLMARK_P53_PATHWAY | -1.59989 | 0.013222 |
| HALLMARK_ANDROGEN_RESPONSE | -1.55659 | 0.020283 |
| HALLMARK_IL6_JAK_STAT3_SIGNALING | -1.54132 | 0.022609 |
| HALLMARK_HEDGEHOG_SIGNALING | -1.47749 | 0.04138 |
| HALLMARK_HYPOXIA | -1.47474 | 0.039183 |
| HALLMARK_COAGULATION | -1.44364 | 0.049053 |



*NES is normalized enrichment score. A significant NES value was set at FDR (false discovery rate) < 0.05. A negative NES value indicates that the members of the gene set tend to show at the bottom of the ranked transcriptome data, indicating that these gene sets are up-regulated and a significant positive NES indicates the opposite [140].

4.5.7 Network analysis

To understand how Notch interacts with NEDD4L which may play a role in controlling PPARγ expression, Notch1, NEDD4L and PPARγ was subjected to string-db network analysis (Figure 36). The result revealed that these genes linked together through serum glucocorticoid kinase 1 (SGK1). SGK1 was significant upregulated in NIC1 overexpressing M(IL-4) compared with CTRL M(IL-4) (Figure 30) NEDD4L had been reported to stabilize PPARγ in 3T3-L1 cell. Moreover, NIC1 was the target of NEDD4L for degradation [101]. This emphasized the possibility of NEDD4L to be good candidate target that link Notch to PPAPγ. We hypothesized that NIC1 hyperactivation increases NEDD4L for the stabilization of PPARγ.

Collectively, RNA-seq analysis provided the following information; 1) inhibition of Notch signaling by DNMAML was low influent to M(IL-4) macrophages. 2) hyperactivation of Notch1 increased both inflammatory and anti-inflammatory respond of M(IL-4). 3) NIC1 was important for IL-4 stimulation rather than Notch target genes. For further study, how Notch1 controls PPARγ through NEDD4L was investigated in the next experiment.

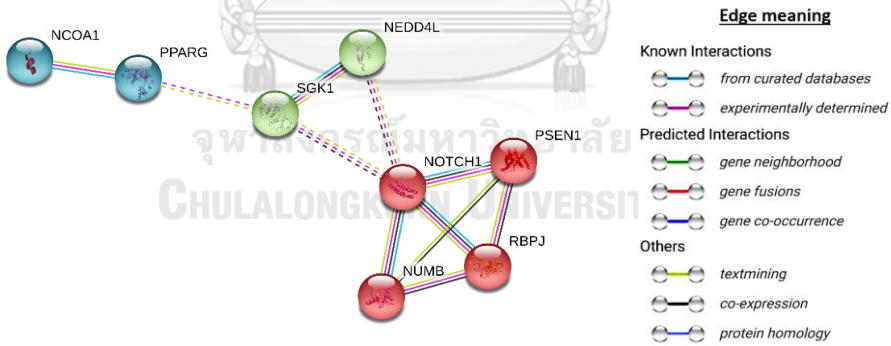


Figure 36 Network analysis.

Notch1, PPARγ and NEDD4L name were subjected to string-db network analysis web based. Edge represented protein-protein association. Edge color represented the characteristic of association. The network was clustered by k-mean clustering method. Solid line represented network linkage of protein in the same cluster. Dot line represented network linkage of protein in the different cluster.

4.6. NEDD4L expression in M(IL-4)

From the transcriptomic data, NEDD4L was increased in IL-4-stimulated NIC1 overexpressing THP-1 cell line. *NEDD4L* mRNA expression in IL-4 stimulated THP-1 was validated by qPCR. The result showed that *NEDD4L* mRNA was increased at 3 h after IL-4 stimulation (Figure 37). In addition, IL-4 stimulated NIC1 overexpressing THP-1 increased *NEDD4L* expression higher than CTRL (Figure 37). In contrast, IL-4 stimulated DNMAML overexpressing THP-1 only slightly increased *NEDD4L* expression but did not reach the statistical significance. Therefore, the effect of NIC1 on *NEDD4L* expression from RNA-seq was confirmed by qPCR. Next, NEDD4L protein expression was detected by Western blot. The level of NEDD4L did not change at 4 h after IL-4 stimulation (Figure 38A). NIC1 and DNMAML also had no effect on NEDD4L expression at this period. Consistent result in HMDMs showed that DAPT pretreatment did not alter NEDD4L expression at 4 h after IL-4 stimulation (Figure 38B and 38C). These results indicated that NIC1 increased *NEDD4L* at mRNA level but not protein level at the time tested but the effect at longer time point can not be excluded.

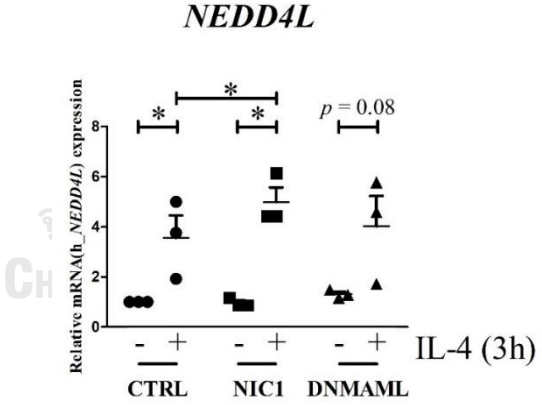


Figure 37 NEDD4L expression in NIC1 or DNMAML overexpressing THP-1 upon IL-4 stimulation.

CTRL, NIC1 and DNMAML overexpressing THP-1 were pretreated with PMA (5 ng/ml) for 48 h. After that cells were stimulating with IL-4 (20 ng/ml) for 3 h. *NEDD4L* mRNA expression was detected by qPCR. *β-ACTIN* was used as housekeeping gene. The results are mean ± SEM of three independent experiment. *indicated statistically significant differences at $p < 0.05$.

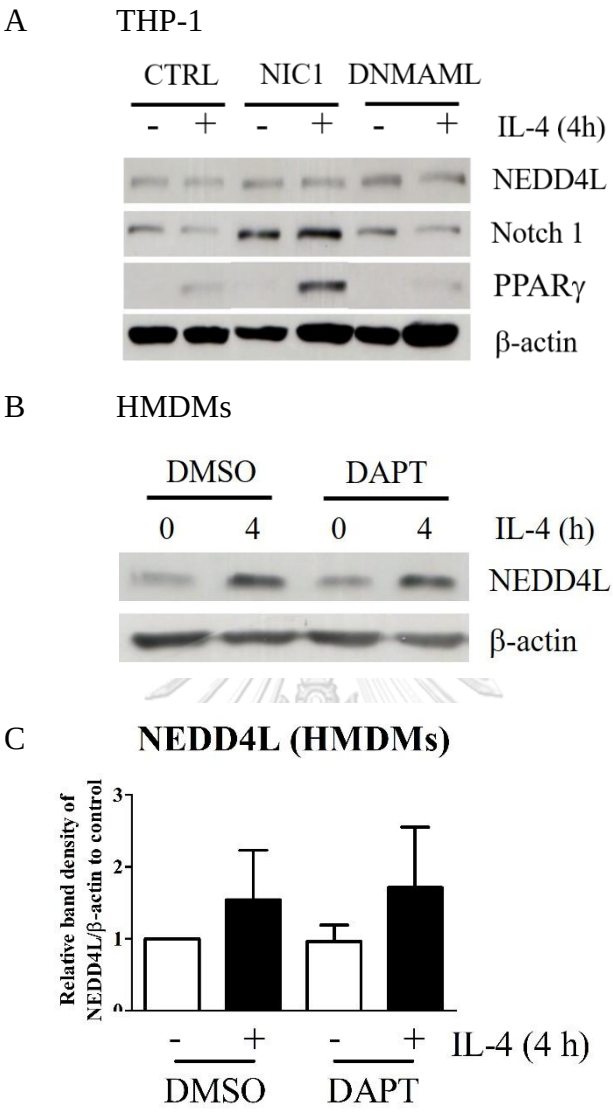


Figure 38 NEDD4L expression in NIC1 or DNMAML overexpressing THP-1 upon IL-4 stimulation.

(A) CTRL, NIC1 and DNMAML overexpressing THP-1 were pretreated with PMA (5 ng/ml) for 48 h. After that cells were stimulating with IL-4 (20 ng/ml) for 4 h. The result is representative of three independent experiments. (B) HMDMs were pretreated with DAPT (50 μM) for 1 h before stimulation with IL-4 (20 ng/ml) for 4 h. Notch1, PPARγ, NEDD4L were detected by Western blot. β-actin was used as loading control. The result is representative of three independent healthy donors. (C) Band density of NEDD4L was normalized with β-actin. Relative expression was calculated to unstimulated condition. The results are mean ± SEM of three independent healthy donors.

4.7. CRISPR/Cas9-mediated *NEDD4L* knockout in THP-1 cell

To understand the crosstalk among Notch1/PPAR□/NEDD4L in IL-4-stimulated THP-1, *NEDD4L* was deleted by CRISPR/Cas9 technique. To avoid the off target effect of CRISPR/Cas9 mediated gene knockout, two guide RNAs targeting NEDD4L (N4L#1KO and N4L#2KO) were used to confirm the knockout phenotype. Deletion of NEDD4L was confirmed by Western blot. Complete knockout of NEDD4L was detected in NEDD4L-knockouted THP-1 (Figure 39), indicating that *NEDD4L* knockout was successful. Because previous reports indicated that NEDD4L enhanced degradation of Notch [141-144], the level of cleaved Notch1 and Notch1 were detected by Western blot. *NEDD4L* deletion did not alter Notch1 or cleaved Notch1 protein level in THP-1 cell (Figure 39 and 40). Thus, Notch1 protein is not regulated by NEDD4L in M(IL-4). The level of PPARγ also was not different in *NEDD4L* knockout compared to the control at tested time point. Therefore, NEDD4L knockout alone had no effect on PPARγ expression or Notch/cleaved Notch1 of PPARγ in IL-4 stimulation.

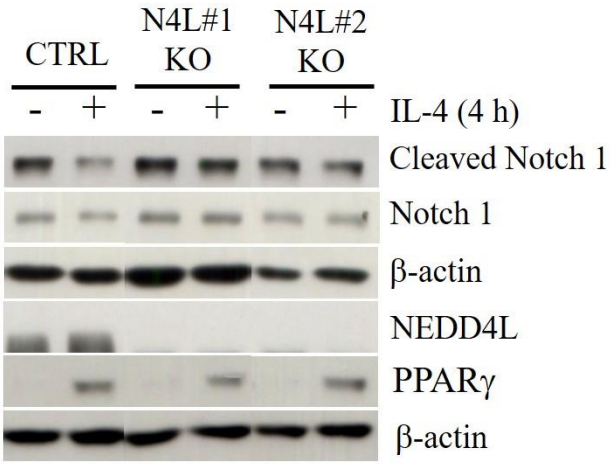


Figure 39 PPARγ and Notch1 expression in NEDD4L knockout THP-1 cell.
NEDD4L knockout THP-1 cell were pretreated with PMA (5 ng/ml) for 48 h, subsequently stimulated with IL-4 (20 ng/ml) for 4 h. NEDD4L, cleaved N1, Notch1 and PPARγ protein expression was examined by Western blot. β-actin was used as loading control. The result is representative of three independent experiments.

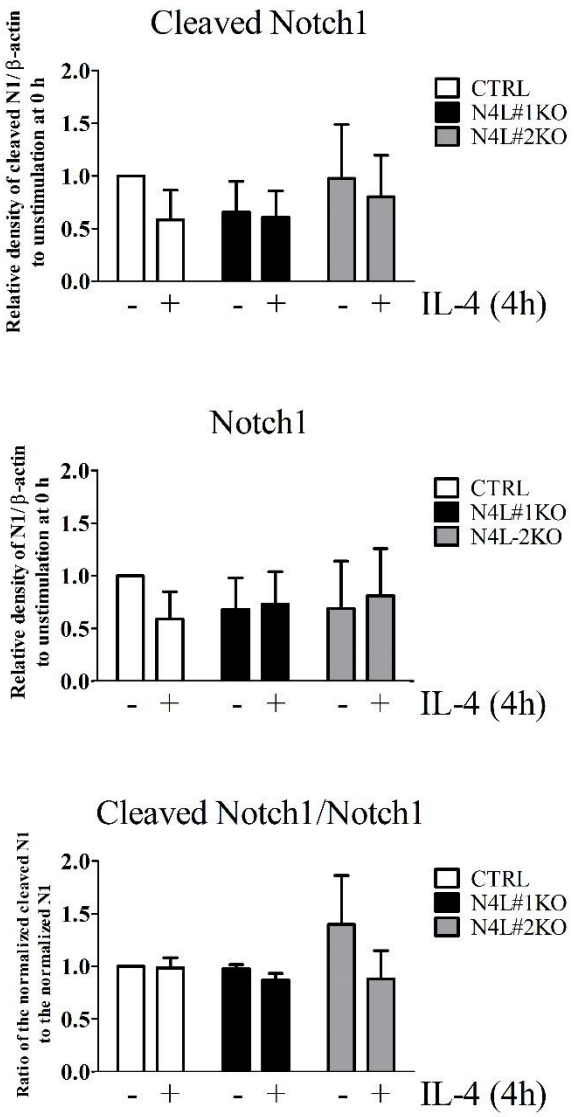


Figure 40 Cleaved Notch1, Notch1 and cleaved Notch1/Notch1 ratio in IL-4 stimulated NEDD4L knockout THP-1 cell.

Band density of cleaved Notch1 and Notch1 were normalized with β-actin. Relative expression was calculated to unstimulation. The results are mean ± SEM of three independent experiments. These data sourced from experiment in Figure 39.

4.8. Effect of NIC1 overexpression on PPARgamma expression in M(IL-4) in *NEDD4L*-KO cell

The results obtained thus far indicated that Notch activation in IL-4 stimulated THP-1 was not sufficient to see the effect of *NEDD4L* knockout on PPARγ. Therefore, NIC1 or control plasmid was lentivirally transduced to *NEDD4L* knockout THP-1 (called N4L-KO+NIC1 for NIC1 overexpression in *NEDD4L* knockout THP-1 and N4L-KO+Ctrl for control). Notch1 was detected to confirm that NIC1 was overexpressed in the transduced cells. N4L-KO+NIC1 exhibited high Notch1 and loss of NEDD4L in both *NEDD4L* knockout background (N4L-1#KO+NIC1 and N4L-2#KO+NIC1). These results indicated that N4L-KO+NIC1 cell line were successfully generated (Figure 41).

PPARγ expression was examined in these cell lines by Western blot. The result showed that PPARγ was reduced in N4L-KO+NIC1 in both NEDD4L-KO background, with and without IL-4 stimulation, suggesting that Notch/PPARγ/NEDD4L crosstalk and NIC1 regulated PPARγ through NEDD4L (Figure 41).

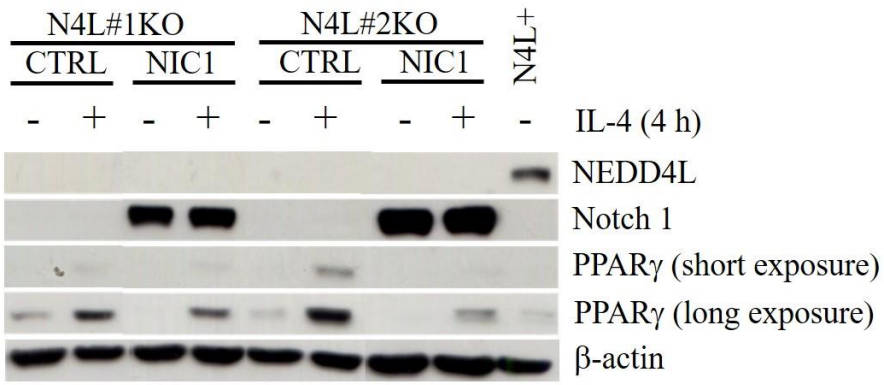


Figure 41 PPARγ expression in NIC1 overexpressing THP-1 with NEDD4L-KO background.

N4L-KO+NIC1 THP-1 cell were pretreated with PMA (5 ng/ml) for 48 h, subsequently stimulated with IL-4 (20 ng/ml) for 4 h. NEDD4L, Notch1, PPARγ protein expression was examined by Western blot. β-actin was used as loading control. The result is representative of three independent experiments.

Next, the effect of NIC1 overexpression in *NEDD4L* knockout THP-1 on *PPARG* mRNA was examined in NIC1 overexpressing cell. *PPARG* mRNA was investigated by qPCR. Unexpectedly, *PPARG* was decreased in both unstimulation and IL-4 stimulation of N4L-KO+NIC1 THP-1 cell (Figure 42). The decreasing *PPARG* mRNA correlated with reducing protein level, indicating that NIC1 regulated *PPARG* at transcriptional level via NEDD4L. This effect was not observed when NEDD4L is present.

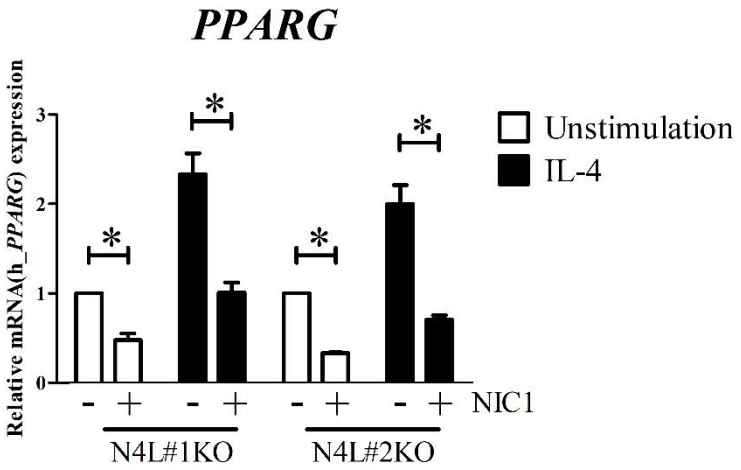


Figure 42 PPARG expression in NIC1 overexpression on NEDD4L-KO background THP-1 cell.

N4L-KO+NIC1 THP-1 cell were pretreated with PMA (5 ng/ml) for 48h, subsequently stimulated with IL-4 (20 ng/ml) for 3 h. *PPARG* mRNA expression was examined by qPCR. *β-ACTIN* was used as housekeeping gene. The results are mean ± SEM of three independent experiment. *indicated statistically significant differences at $p < 0.05$.

4.9 NEDD4L deletion reduced IL-4 induced AKT phosphorylation in NIC1 overexpressing cell.

The results of both *PPARG* mRNA and PPARγ protein level in N4L-KO+NIC1 THP-1 cell showed that combination of NEDD4L knockout and NIC1 overexpression strongly affect the PPARγ in the presence or absence of IL-4.

According to network analysis, Notch1, PPARγ, NEDD4L were linked through SGK1 and SGK1 was increased in NIC1 overexpressing M(IL-4) compared with CTRL M(IL-4). SGK1 is activated by PI3K/mTORC2 [145]. It shares approximately 45-55% homology at the catalytic domain and common downstream substrates with AKT [145, 146]. Therefore, the involvement of AKT was examined.

4.10 AKT phosphorylation in NIC1 overexpression on NEDD4L knockout THP-1

To explore how Notch regulated PPARγ through NEDD4L, AKT phosphorylation was determined by Western blot. The result showed that N4L-KO+NIC1 overexpressing THP-1 decreased AKT phosphorylation in the presence or absence of IL-4 (Figure 43). This result was consistent with the report that knockdown NEDD4L in H157 (squamous cell lung carcinoma) impaired AKT phosphorylation because NEDD4L required to control the dynamic of PI3KCA, a kinase upstream of AKT. In conclusion, Notch requires NEDD4L for AKT phosphorylation. However, the possibility that this mechanism control *PPARG* at transcriptional level in THP-1 cell need more further investigation.

Summary of the level of PPARγ, phosphor-/total-AKT ratio and NEDD4L in IL-4 stimulated NIC1 and DNMAML overexpressing THP1 in NEDD4L or NEDD4L KO background were shown in Figure 44.

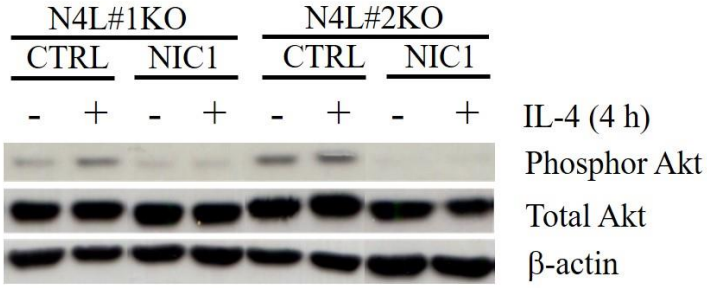


Figure 43 AKT phosphorylation in NIC1 overexpression on NEDD4L-KO background THP-1 cell.

N4L-KO+NIC1 THP-1 cell were pretreated with PMA (5 ng/ml) for 48 h, subsequently stimulated with IL-4 (20 ng/ml) for 4 h. Phosphor-and total AKT was examined by Western blot. β-actin was used as loading control. The result is representative of three independent experiments.

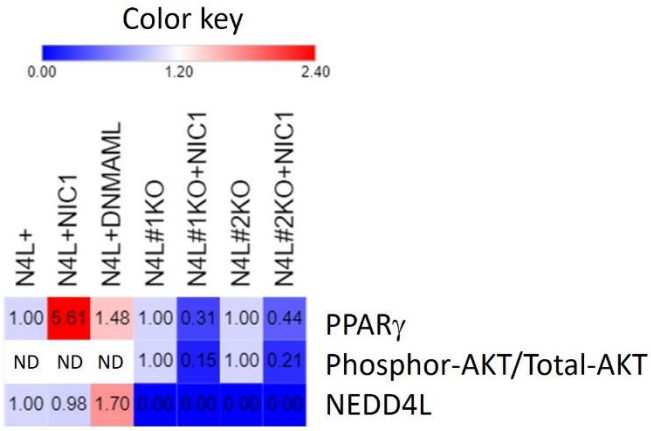


Figure 44 Heatmap summarization of PPARγ, ratio between phosphor- and total AKT and NEDD4L expression in each genetic modify THP-1 under IL-4 stimulation.

Band density of PPARγ and NEDD4L was normalized with β-actin. Phosphorylated AKT band density was ratio to total AKT. These data sourced from experiment in Figure 38, 41 and 43)

4.10 Biological impacts of Notch signaling on the function of M(IL-4)

4.10.1 The effect of Notch signaling on lipid uptake of M(IL-4)

This study found that Notch signaling was important for PPARγ expression in M(IL-4). Previous studies reported that PPARγ level correlated with its activity [77]. RNA-seq data was analyzed for PPARγ signaling pathway according to Biocarta database. Matched differential genes in all comparisons between RNA-seq and Biocarta database were summarized in the heatmap (Figure 45). CD36 (a PPARγ target gene) was highly expressed in NIC1 overexpressing THP-1 in the presence or absence of IL-4 as shown in Figure 37. However, CD36 did not reach the statistical significant difference from RNA-seq data. This may be because it requires some ligand provided from IL-4 regulated genes such as the derivative of ALOX15 to activate PPARγ transcriptional activity [81, 88].

Next, CD36 expression was determined in IL-4 stimulated NIC1 and DNMAML overexpressing THP-1. Rosiglitazone, a PPARγ synthetic ligand, was used as positive control to activate PPARγ. Consistent with the previous reports that rosiglitazone activated PPARγ to increase CD36 expression (Figure 46A) [97]. NIC1 overexpressing THP-1 only slightly increased CD36 surface expression but the level decreased in rosiglitazone treatment. DNMAML overexpression was unable to increase CD36 expression upon rosiglitazone treatment.



This result raised the question why NIC1 overexpressing THP-1 stabilized PPARγ could not increase CD36. Based on the CD36 function, CD36 expression on cell surface binds to lipid and flips itself and the lipid to intracellular side [147]. Therefore, CD36 on the cell surface decrease during its physiological function of lipid uptake. To examine the possibility that CD36 in NIC1 overexpressing cells function more than control by flipping intracellulary, the intracellular CD36 level was determined by flow cytometer. As expected, the intracellular CD36 expression was increased in NIC1 overxpressing THP-1 in unstimulation and rosiglitazone treatment (Figure 46B). However, IL-4 or rosiglitazone did not alter the intracellular CD36 level in CTRL or

DNMAML overexpressing THP-1. These results suggested that NIC1 increased intracellular CD36 in macrophages, as indicative of increasing functions.

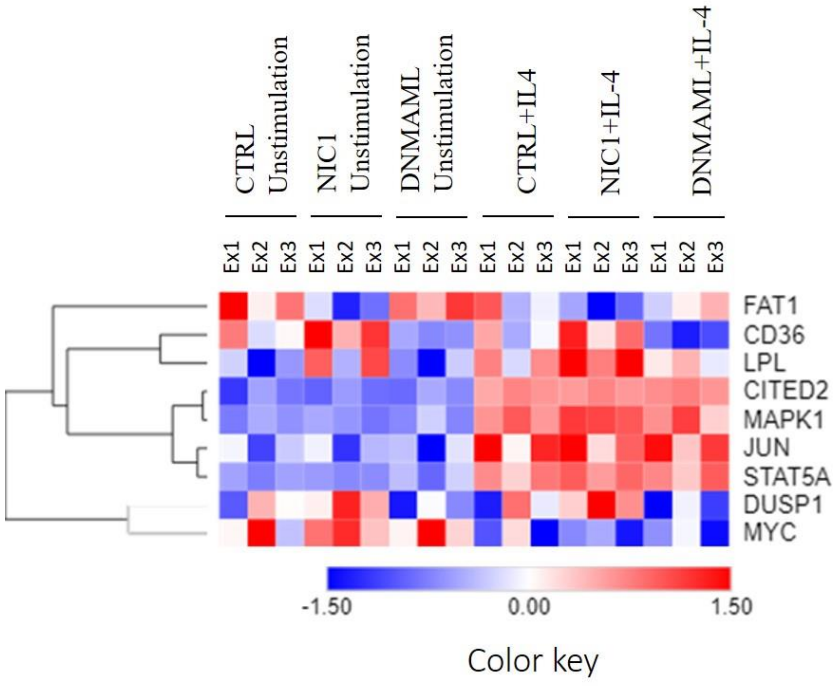




Figure 45 Heatmap of the significant differential expressed gene from RNA-seq data in PPARγ pathway from Biocarta database.

Differential expressed genes in all comparison was picked up the genes that found on PPARγ signaling genes from Biocarta database.

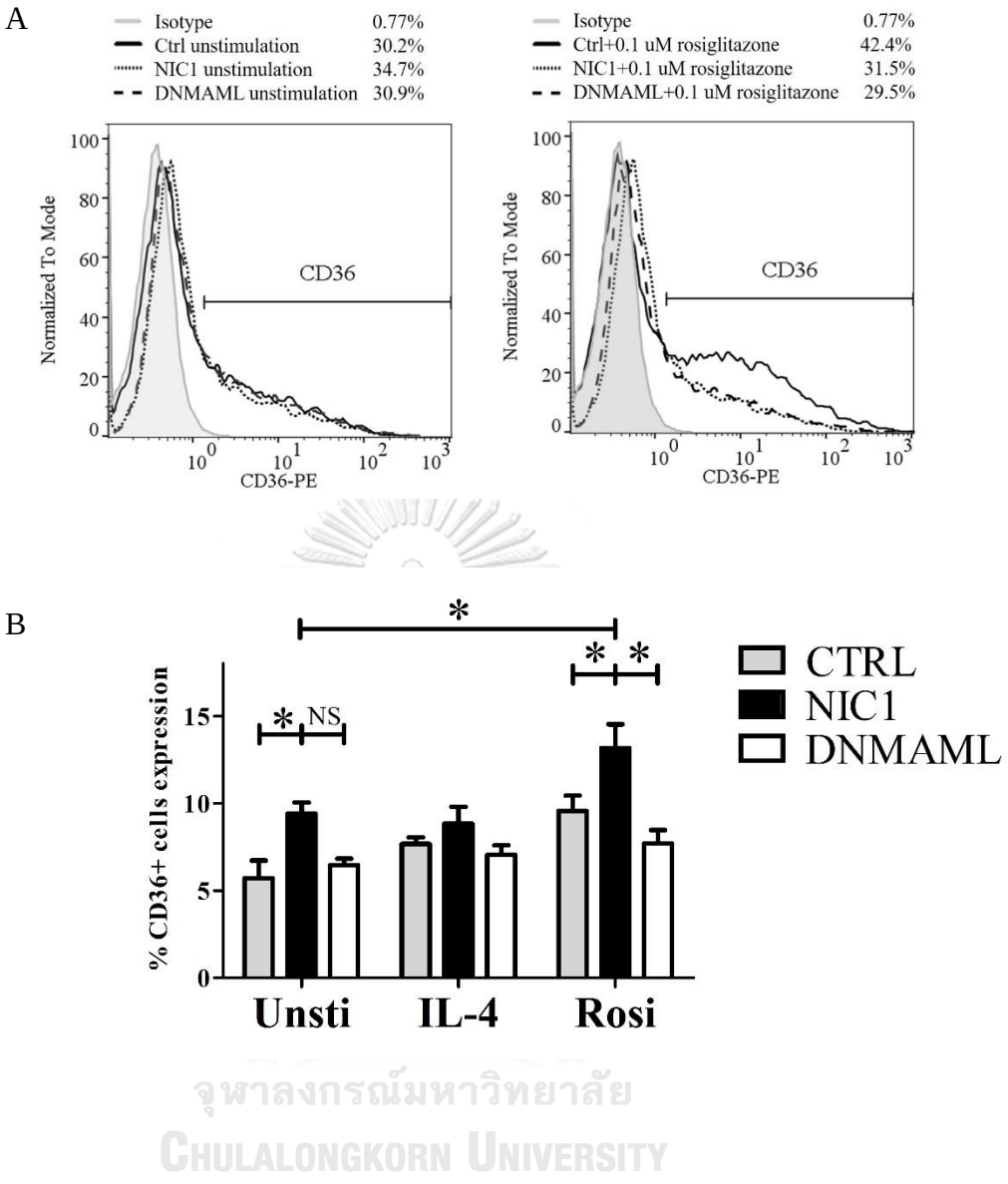




Figure 46 CD36 expression in IL-4 and rosiglitazone stimulated Notch or DNMAML overexpressing THP-1.

CTRL, NIC1 and DNMAML overexpressing THP-1 were treated with PMA (5 ng/ml) for 48 h before stimulating with IL-4 (20 ng/ml) for 18 h. (A) Surface and (B) intracellular CD36 were detected by flow cytometer. (A) The result is representative of three independent experiments. (B) The results are mean ± SEM of three independent experiment. *indicated statistically significant differences at $p < 0.05$. NS indicated that no statistically significant differences.

To confirm that increasing intracellular CD36 was because of higher biological activity, lipid uptake was examined in oxLDL stimulated-NIC1 or-DNMAML overexpressing THP-1. In unstimulated and IL-4 stimulated condition, NIC1 overexpressing THP-1 had the highest intracellular lipid accumulation (Figure 47). oxLDL increased lipid uptake in CTRL and DNMAML, but, did not increased in NIC1. This may be because lipid already highly accumulated at the high level in unstimulated NIC1 overexpressing cells (Figure 47). Stimulation with IL-4 increased lipid accumulation in THP-1 cells similar to oxLDL treatment (Figure 47). These results confirmed that Notch signaling increased PPARγ, leading to increase CD36 expression and its function.

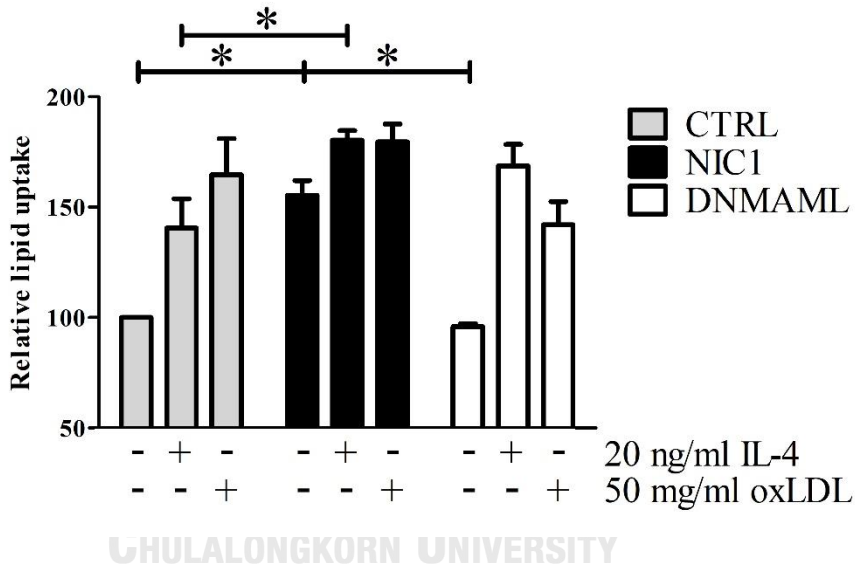




Figure 47 Lipid accumulation in IL-4 and oxLDL stimulated NIC1 and DNMAML overexpressing THP-1 cell.

CTRL, NIC1 and DNMAML overexpressing THP-1 were treated with PMA (5 ng/ml) for 48 h before stimulating with IL-4 (20 ng/ml) or oxLDL (50 mg/ml) for 24 h. Intracellular lipid was stained followed Oil red O lipid staining method. Lipid staining was dissolved with 100% isopropanol for measurement absorbance at 492 nm. The results are mean ± SEM from three independent experiment. * indicated statistically significant differences at $p < 0.05$.

# CHAPTER V

# DISCUSSION

*The role of Notch signaling in IL-4 stimulated macrophages*. IL-4 stimulation induced Notch1 activation, resulting in increased *HEY1* mRNA expression. The consistent result from Foldi J., et al, 2016, reveal the requirement of RBPJκ in pro-healing murine M(chitin) [69]. This study however did not identify responsible Notch receptors/ligands. In contrast, DLL4 co-stimulation with IL-4 caused macrophages apoptosis and impaired expression of M(IL-4) markers [70]. *DLL4* mRNA was decreased in our study, suggesting that DLL4 may not be responsible Notch ligand for Notch signaling activation in human M(IL-4). Recent studies reported the distinct biological activities triggered by different Notch ligands (3). Moreover, JAGGED and DLL tend to express on different cells because NIC inhibits DLL expression via HES1 in mouse neural progenitors cell [148] and increases JAGGED though miR-200 in human prostate cancer [149, 150]. Additionally, some ligands have specific property such as DLL3 which inhibits Notch signaling rather than activation (1, 2). For example, HCC827 cell (lung adenocarcinoma cell line) expressed JAGGED1 and JAGGED2, but only JAGGED1 depletion induced cell apoptosis (3). In contrast, JAGGED2 depletion induced expression of high inflammatory cytokines-related genes (3). This study indicated that Notch1 was activated in human M(IL-4), possibly via JAGGED1. Definitive proof of the ligand or receptor in M(IL-4) needs further investigation.

*Effect of Notch signaling on PPARγ expression in M(IL-4).* Gain and loss of Notch signaling highlighted on the importance of Notch signaling in increasing the level of PPARγ in the presence or absence of IL-4. Due to different mechanism of inhibition, DNMAML and DAPT treatment can yield the different outcomes. DNMAML overexpressing M(IL-4) had no effect to PPARγ level, while DAPT pretreatment decreased its level. In addition, DAPT inhibited γ-secretase activity which has multiple

substrates. The results of DAPT pretreatment could not rule out this possibility. Previous studies reported that Notch target gene, HES1, directly binds to *PPARG* promoter to inhibit its expression in pancreatic cancer (4). Our result showed that DNMAML overexpressing THP-1 which has Notch transcriptional activity defect, did not effect to PPARγ level (Figure 10), indicating that the influence of Notch signaling to PPARγ may be from non-canonical pathway. Non-canonical Notch signaling pathway is reported in various cell types. For example, Notch signaling function independent of γ-secretase to regulate synaptic vesicle proteins, synaptophysin 1 and VGLUT1, in excitatory neurons [151].

*Mechanism of NIC1 modulates PPARγ expression.* The experiment to address how Notch modulate PPARγ in M(IL-4) reveal that it was not from the alteration of IL-4Rα and its downstream signaling. DAPT pretreatment had minor effect on AKT phosphorylation in IL-4 stimulated THP-1 but had stronger effect on HMDMs. These different results may be due to the DAPT dose in HMDMs is higher than the used in THP-1. This study applied DAPT (50 μM) in primary macrophages at higher dose than THP-1 (25 μM), because it could not inhibit Notch target gene transcription in the preliminary result. AKT control M(IL-4) target genes (6) but there was no direct evidence showed that it regulates PPARγ expression. Pharmacological inhibitors of AKT, wortmannin and LY29004, showed inconsistent results on PPARγ expression in murine M(IL-4) [30, 31]. On the other hands, AKT regulates PPARγ transcriptional activity by phosphorylated CBP/p300 (PPARγ co-activator) and enhanced its acetyltransferase activity in adipocytes (7, 8). Nevertheless, *PPARG* mRNA level and stability did not alter in NIC1 and DNMAML overexpressing THP-1, compared with control, suggesting that Notch signaling did not regulate PPARγ at the transcriptional level.

Previous studies revealed that, PPARγ is degraded by proteasome [101]. MG132 pretreatment had similar PPARγ level compare to control in M(IL-4), implying that Notch signaling delays PPARγ degradation, resulting in increased PPARγ half-life. Previous study showed that NIC1/HES1 induced Ngn3 destabilization to control endocrine program in hepatic progenitor (9). However, NIC1 stabilized PPARγ

phenotype might not require transcriptional activity of Notch, according to DNMAML and DAPT results. This result strongly indicates that NIC1 domain is necessary to modulate PPARγ stability via diminishing proteasome degradation. These effects may be because the decreasing of seven-in-absentia homolog 2 (SIAH2), an E3 ubiquitin ligase that directly interacts with PPARγ and targets PPARγ for proteasome degradation in mature adipocytes. SIAH2 was found in our transcriptomic data upon comparison of NIC1 overexpressing M(IL-4) and unstimulation ($p$ = 0.096, Table 6, Appendix C). However, the exact mechanism whether NIC1 regulates PPARγ stability need further investigation.

*Notch signaling influences IL-4 inducible genes in THP-1*. Transcriptomic analysis provided how Notch signaling plays role in M(IL-4). Hyperactivation and hypoactivation of Notch signaling did not interfere with macrophages polarization to M(IL-4) phenotype because both had similar pattern of M(IL-4) markers. The overall impact of NIC1 overexpressing M(IL-4) was revealed by the enrichment of gene set involving in wounding, cell adhesion and lymphocytes activation by lipid antigen presentation. Interestingly, we found that NIC1 hyperactivation in IL-4 stimulation activated mixed macrophages phenotypes in the presence of IL-4. This result is contradictory to previous studies which stated that hyperactivation of NIC1 in TAM forced TAM to become proinflammatory macrophages (10). DNMAML overexpressing M(IL-4) found only ACP5 that was differentially expressed when compared with CTRL M(IL-4). ACP5 (Acid Phosphatase 5, Tartrate Resistant) regulates two enzymes; tartrate resistant acid phosphatase 5b (TRAP5b, expresses in bone-resorbing osteoclasts) and TRAP5a (expresses in macrophages and dendritic cells) [152]. IL-4 increased ACP5 in STAT6 dependent manner in RAW264.7 [152]. However, ACP5 was not increased in CTRL M(IL-4) in our transcriptomic data (Figure 28, Appendix B) and Notch signaling may be required for IL-4 induced ACP5 expression. TRAP expression in murine alveolar-like macrophages was found in asthma and chronic obstructive pulmonary disease and participated in tissue remodeling [153]. This result is correlated with wounding (GO) from NIC1 overexpressing M(IL-4), indicating that Notch signaling may involve in tissue remodeling process.

*Notch and NEDD4L regulated PPARγ in IL-4 stimulated THP-1 cell.* IL-4. Transcriptomic data identified another mechanism by which Notch signaling regulates PPARγ. Differential expressed genes, NEDD4L, significantly found in NIC1 overexpressing M(IL-4) had a link with Notch1 and PPARγ through SGK1 which was another pro-healing macrophages marker [146]. NEDD4 which is a gene in NEDD4 family like NEDD4L had been reported to stabilized PPARγ in 3T3-L1 cell (14). NEDD4 and NEDD4L share 78% similarity [154] and have some overlapping functions as negative regulator of Notch signaling [108, 109, 143, 144]. There is the possibility NEDD4L that was induced for controlling hyperactivation status of Notch signaling, has another effect to increase PPARγ stability. However, deletion of *NEDD4L* in THP-1 cell did not affect the level of cleaved Notch1 or Notch1 in the presence or absence of IL-4. There may be a compensatory mechanism from other ubiquitin ligase enzymes such as Su(dx) (in Drosophila, it is ITCH, WWP1 and WWP2 in mammalian) (16, 17). In addition, *NEDD4L* knockout alone in THP-1 did not alter PPARγ. In contrast, NIC1 overexpression on *NEDD4L* knockout THP-1 strongly decreased PPARγ mRNA and protein level in the present or absent with IL-4. Therefore, NIC1 overexpressing M(IL-4) may require NEDD4L for removing unknown suppressor from the transcriptional regulation of *PPARG*. Moreover, NIC1 overexpression in NEDD4L knockout cell impaired AKT phosphorylation. Previous report described that loss of NEDD4L impaired AKT phosphorylation (18). However, AKT phosphorylation was detected in IL-4 stimulated NIC1 overexpression on *NEDD4L* knockout THP-1 at late time point (4h). Therefore, this effect may be because of the secondary metabolite of M(IL-4). Recent study showed that, DAPT pretreatment decreased AKT phosphorylation in LPS stimulated RAW264.7 cell line [65]. There is the possibility that Notch signaling may control AKT phosphorylation in M(IL-4).

*Notch regulated M(IL-4) biological functions.* Our study found novel role of Notch signaling in regulating PPARγ expression in M(IL-4) and one of its target gene, CD36, was overrepresented in NIC1 overexpressing THP-1 dataset. CD36 mediated lipid uptake and internalized lipid-receptor complex into the cell (19). Therefore, intracellular CD36 reflected its activity. Intracellular CD36 was increased in unstimulated NIC1 overexpressing cell, correlated with lipid accumulation, suggesting

that NIC1 increased CD36 expression and function through the stability of PPARγ. However, IL-4 stimulation caused lipid accumulation independent of CD36 because IL-4 alone did not induce CD36 expression. These results emphasized the important of Notch signaling to PPARγ mediated lipid uptake in M(IL-4) macrophages.

In conclusion, this study proposes two mechanisms of which Notch signaling regulate M(IL-4) (Figure 48). First, non-canonical Notch signaling stabilized PPARγ to delay proteasome degradation by unknown mechanism. Second, NIC1 requires NEDD4L to degrade unknown suppressor of transcription regulation of PPARG. These finding emphasize the selectively activated Notch receptor in M(IL-4) and fulfill the knowledge gap that Notch signaling regulates lipid uptake mediated through PPARγ regulation in human macrophages.

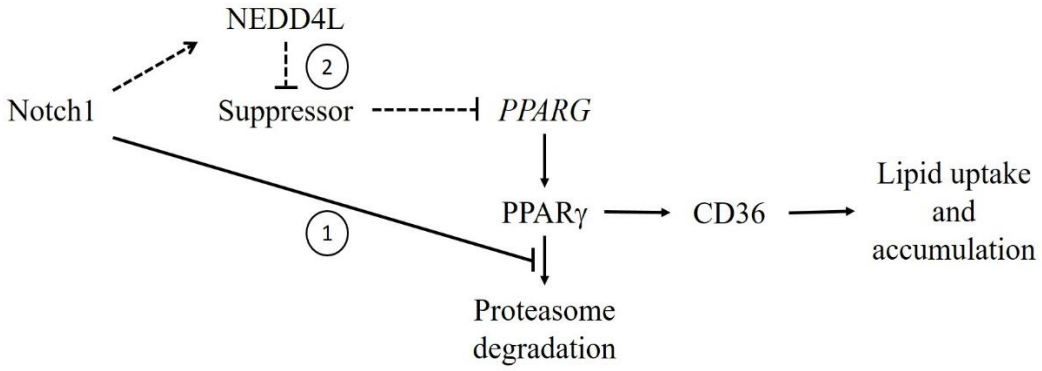




Figure 48 The role of Notch signaling in M(IL-4).

# CHAPTER VI

# CONCLUSIONS

6.1 IL-4 stimulated macrophages activated Notch1 receptor and *HEY1*.

6.2 NIC1 hyperactivation increased PPARγ. Inhibit NIC1 cleavage by DAPT pretreatment declined PPARγ, DNMAML mediated Notch inhibition had no effect to PPARγ. These results indicate the role of non-canonical Notch signaling regulates PPARγ.

6.3 This study proposed 2 mechanisms of Notch signaling to regulate PPARγ (Figure 48);

6.3.1 Notch signaling stabilizes PPARγ by decreasing its proteasome degradation.

6.3.2 Notch requires NEDD4L to control PPARγ by removing unknown suppressor that regulates *PPARG* transcription.

6.4 NIC1 overexpression in NEDD4L knockout THP-1 decreased AKT phosphorylation during IL-4 stimulation.

6.5 NIC1 overexpressing THP-1 regulated lipid uptake via CD36 in the present or absent with IL-4.

# REFERENCES


1. Stremmel, C., et al., *Yolk sac macrophage progenitors traffic to the embryo during defined stages of development.* Nature Communications, 2018. **9**(1): p. 75.

2. Wake, H., et al., *Microglia: actively surveying and shaping neuronal circuit structure and function.* Trends in Neurosciences, 2013. **36**(4): p. 209-217.

3. Aurora, A.B., et al., *Macrophages are required for neonatal heart regeneration.* The Journal of Clinical Investigation, 2014. **124**(3): p. 1382-1392.

4. Tondravi, M.M., et al., *Osteopetrosis in mice lacking haematopoietic transcription factor PU.1.* Nature, 1997. **386**: p. 81.

5. Epelman, S., K.J. Lavine, and G.J. Randolph, *Origin and Functions of Tissue Macrophages.* Immunity, 2014. **41**(1): p. 21-35.

6. Parisi, L., et al., *Macrophage Polarization in Chronic Inflammatory Diseases: Killers or Builders?* Journal of Immunology Research, 2018. **2018**: p. 25.

7. Borggrefe, T. and F. Oswald, *Keeping Notch Target Genes off: A CSL Corepressor Caught in the Act.* Structure, 2014. **22**(1): p. 3-5.

8. Schultze, J.L., A. Schmieder, and S. Goerdt, *Macrophage activation in human diseases.* Seminars in Immunology, 2015. **27**(4): p. 249-256.

9. Mosser, D.M. and J.P. Edwards, *Exploring the full spectrum of macrophage activation.* Nature Reviews Immunology, 2008. **8**: p. 958.

10. Murray, Peter J., et al., *Macrophage Activation and Polarization: Nomenclature and Experimental Guidelines.* Immunity, 2014. **41**(1): p. 14-20.

11. Stöger, J.L., et al., *Distribution of macrophage polarization markers in human atherosclerosis.* Atherosclerosis, 2012. **225**(2): p. 461-468.

12. Moore, K.J., F.J. Sheedy, and E.A. Fisher, *Macrophages in atherosclerosis: a dynamic balance.* Nature Reviews Immunology, 2013. **13**: p. 709.

13. Zheng, X., et al., *Redirecting tumor-associated macrophages to become tumoricidal effectors as a novel strategy for cancer therapy.* Oncotarget, 2017. **8**(29): p. 48436-48452.

14. Aras, S. and M.R. Zaidi, *TAMeless traitors: macrophages in cancer progression and metastasis.* British Journal Of Cancer, 2017. **117**: p. 1583.

15. Porta, C., et al., *Macrophages in cancer and infectious diseases: the 'good' and the 'bad'.* Immunotherapy, 2011. **3**(10): p. 1185-1202.

16. Shintani, Y., et al., *IL-4 as a Repurposed Biological Drug for Myocardial Infarction through Augmentation of Reparative Cardiac Macrophages: Proof-of-Concept Data in Mice.* Scientific Reports, 2017. **7**(1): p. 6877.

17. Jiang, H., M.B. Harris, and P. Rothman, *IL-4/IL-13 signaling beyond JAK/STAT.* Journal of Allergy and Clinical Immunology, 2000. **105**(6, Part 1): p. 1063-1070.

18. Gandhi, H., et al., *Dynamics and Interaction of Interleukin-4 Receptor Subunits in Living Cells.* Biophysical Journal, 2014. **107**(11): p. 2515-2527.

19. Bo-Jiang, S., H. Thorsten, and S. Walter, *Global and Local Determinants for the Kinetics of Interleukin-4/Interleukin-4 Receptor α Chain Interaction.* European Journal of Biochemistry, 1996. **240**(1): p. 252-261.

20. Bhattacharjee, A., et al., *IL-4 and IL-13 employ discrete signaling pathways for target gene expression in alternatively activated monocytes/macrophages.* Free Radical Biology and Medicine, 2013. **54**: p. 1-16.

21. Alfonso-García, A., et al., *Label-free identification of macrophage phenotype by fluorescence lifetime imaging microscopy.* Journal of Biomedical Optics, 2016. **21**(4): p. 046005.

22. Daniel, B., et al., *The IL-4/STAT6/PPARγ signaling axis is driving the expansion of the RXR heterodimer cistrome, providing complex ligand responsiveness in macrophages.* Nucleic Acids Research, 2018: p. gky157-gky157.

23. Chen, H., et al., *Macrophage peroxisome proliferator-activated receptor γ deficiency delays skin wound healing through impairing apoptotic cell clearance in mice.* Cell Death & Disease, 2015. **6**(1): p. e1597.

24. Hasegawa-Moriyama, M., et al., *Peroxisome proliferator-activated receptor-gamma agonist rosiglitazone attenuates inflammatory pain through the induction of heme oxygenase-1 in macrophages.* PAIN®, 2013. **154**(8): p. 1402-1412.

25. Ahmadian, M., et al., *PPAR[gamma] signaling and metabolism: the good, the bad and the future.* Nat Med, 2013. **99**(5): p. 557-566.

26. Cathcart, M.K. and A. Bhattacharjee, *Monoamine oxidase A (MAO-A): a signature marker of alternatively activated monocytes/macrophages.* Inflammation and cell signaling, 2014. **1**(4): p. e161.

27. Huang, Stanley C.-C., et al., *Metabolic Reprogramming Mediated by the mTORC2-IRF4 Signaling Axis Is Essential for Macrophage Alternative Activation.* Immunity, 2016. **45**(4): p. 817-830.

28. Günthner, R. and H.-J. Anders, *Interferon-Regulatory Factors Determine Macrophage Phenotype Polarization.* Mediators of Inflammation, 2013. **2013**: p. 8.

29. Ruffell, D., et al., *A CREB-C/EBPβ cascade induces M2 macrophage-specific gene expression and promotes muscle injury repair.* Proceedings of the National Academy of Sciences, 2009. **106**(41): p. 17475-17480.

30. Szanto, A., et al., *STAT6 Transcription Factor Is a Facilitator of the Nuclear Receptor PPARγ-Regulated Gene Expression in Macrophages and Dendritic Cells.* Immunity, 2010. **33**(5): p. 699-712.

31. Kapoor, N., et al., *Transcription Factors STAT6 and KLF4 Implement Macrophage Polarization via the Dual Catalytic Powers of MCPIP.* The Journal of Immunology, 2015. **194**(12): p. 6011-6023.

32. Liao, X., et al., *Krüppel-like factor 4 regulates macrophage polarization.* The Journal of Clinical Investigation, 2011. **121**(7): p. 2736-2749.

33. Danuta, M., et al., *Interleukin-1-inducible MCPIP protein has structural and functional properties of RNase and participates in degradation of IL-1β mRNA.* The FEBS Journal, 2009. **276**(24): p. 7386-7399.

34. Matsushita, K., et al., *Zc3h12a is an RNase essential for controlling immune responses by regulating mRNA decay.* Nature, 2009. **458**: p. 1185.

35. Zheng, C., et al., *Local proliferation initiates macrophage accumulation in adipose tissue during obesity.* Cell Death &Amp; Disease, 2016. **7**: p. e2167.

36. Tung O. Chan, a. Susan E. Rittenhouse, and P.N. Tsichlis, *AKT/PKB and Other D3 Phosphoinositide-Regulated Kinases: Kinase Activation by Phosphoinositide-Dependent Phosphorylation.* Annual Review of Biochemistry, 1999. **68**(1): p. 965-1014.

37. Arranz, A., et al., *Akt1 and Akt2 protein kinases differentially contribute to macrophage polarization.* Proceedings of the National Academy of Sciences, 2012. **109**(24): p. 9517-9522.

38. Varin, A., et al., *Alternative activation of macrophages by IL-4 impairs phagocytosis of pathogens but potentiates microbial-induced signalling and cytokine secretion.* Blood, 2010. **115**(2): p. 353-362.

39. B., W.S., et al., *Alternative activation of macrophages by IL-4 requires SHIP degradation.* European Journal of Immunology, 2011. **41**(6): p. 1742-1753.

40. MacKinnon, A.C., et al., *Regulation of Alternative Macrophage Activation by Galectin-3.* The Journal of Immunology, 2008. **180**(4): p. 2650-2658.

41. Lu, X., et al., *PTP1B is a negative regulator of interleukin 4–induced STAT6 signaling.* Blood, 2008. **112**(10): p. 4098-4108.

42. Warren, K.J., et al., *The TORC1-activated Proteins, p70S6K and GRB10, Regulate IL-4 Signaling and M2 Macrophage Polarization by Modulating Phosphorylation of Insulin Receptor Substrate-2.* Journal of Biological Chemistry, 2016. **291**(48): p. 24922-24930.

43. Bray, S., *Notch signalling inDrosophila: three ways to use a pathway.* Seminars in Cell & Developmental Biology, 1998. **9**(6): p. 591-597.

44. Artavanis-Tsakonas, S., K. Matsuno, and M. Fortini, *Notch signaling.* Science, 1995. **268**(5208): p. 225-232.

45. Kanwar, R. and M.E. Fortini, *Notch Signaling: A Different Sort Makes the Cut.* Current Biology, 2004. **14**(24): p. R1043-R1045.

46. Cave, J.W., *Selective repression of Notch pathway target gene transcription.* Developmental Biology, 2011. **360**(1): p. 123-131.

47. Bray, S.J. and M. Gomez-Lamarca, *Notch after cleavage.* Current Opinion in Cell Biology, 2018. **51**: p. 103-109.

48. van Tetering, G. and M. Vooijs, *Proteolytic Cleavage of Notch: "HIT and RUN".* Current molecular medicine, 2011. **11**(4): p. 255-269.

49. Fryer, C.J., et al., *Mastermind mediates chromatin-specific transcription and turnover of the Notch enhancer complex.* Genes & Development, 2002. **16**(11): p. 1397-1411.

50. Johnson, J.E. and R.J. MacDonald, *Chapter three - Notch-Independent Functions of CSL*, in *Current Topics in Developmental Biology*, C. Birchmeier, Editor. 2011, Academic Press. p. 55-74.

51. Andersen, P., et al., *Non-Canonical Notch Signaling: Emerging Role and Mechanism.* Trends in Cell Biology, 2012. **22**(5): p. 257-265.

52. Hall, R.J. and C.A. Erickson, *ADAM 10: an active metalloprotease expressed during avian epithelial morphogenesis.* Developmental Biology, 2003. **256**(1): p. 147-160.

53. Groot, A.J. and M.A. Vooijs, *The Role of Adams in Notch Signaling.* Advances in experimental medicine and biology, 2012. **727**: p. 15-36.

54. Yan, Y., et al., *Defining the minimum substrate and charge recognition model of gamma-secretase.* Acta Pharmacologica Sinica, 2017. **38**: p. 1412.

55. Iso, T., et al., *HERP1 Is a Cell Type-specific Primary Target of Notch.* Journal of Biological Chemistry, 2002. **277**(8): p. 6598-6607.

56. Foldi, J., et al., *Autoamplification of Notch signaling in macrophages by TLR-induced and RBP-J-dependent induction of Jagged1.* Journal of immunology (Baltimore, Md. : 1950), 2010. **185**(9): p. 5023-5031.

57. Castel, D., et al., *Dynamic binding of RBPJ is determined by Notch signaling status.* Genes & Development, 2013. **27**(9): p. 1059-1071.

58. Ayaz, F. and B.A. Osborne, *Non-Canonical Notch Signaling in Cancer and Immunity.* Frontiers in Oncology, 2014. **4**: p. 345.

59. Jin, S., et al., *Non-canonical Notch signaling activates IL-6/JAK/STAT signaling in breast tumor cells and is controlled by p53 and IKKα/IKKβ.* Oncogene, 2012. **32**: p. 4892.

60. Ilagan, M.X.G., et al., *Real-Time Imaging of Notch Activation with a Luciferase Complementation-Based Reporter.* Science Signaling, 2011. **4**(181): p. rs7-rs7.

61. Kopan, R. and M.X.G. Ilagan, *The Canonical Notch Signaling Pathway: Unfolding the Activation Mechanism.* Cell, 2009. **137**(2): p. 216-233.

62. Foltz, D.R., et al., *Glycogen Synthase Kinase-3β Modulates Notch Signaling and Stability.* Current Biology, 2002. **12**(12): p. 1006-1011.

63. Wang, Y.-C., et al., *Notch Signaling Determines the M1 versus M2 Polarization of Macrophages in Antitumor Immune Responses.* Cancer Research, 2010. **70**(12): p. 4840.

64. Xu, H., et al., *Notch–RBP-J signaling regulates the transcription factor IRF8 to promote inflammatory macrophage polarization.* Nature Immunology, 2012. **13**: p. 642.

65. Sangphech, N., B.A. Osborne, and T. Palaga, *Notch signaling regulates the phosphorylation of Akt and survival of lipopolysaccharide-activated macrophages via regulator of G protein signaling 19 (RGS19).* Immunobiology, 2014. **219**(9): p. 653-660.

66. Fung, E., et al., *Delta-Like 4 Induces Notch Signaling in Macrophages.* Implications for Inflammation, 2007. **115**(23): p. 2948-2956.

67. Ruan, Z.-b., et al., *Effect of notch1,2,3 genes silicing on NF-κB signaling pathway of macrophages in patients with atherosclerosis.* Biomedicine & Pharmacotherapy, 2016. **84**: p. 666-673.

68. Zhao, J.-L., et al., *Forced Activation of Notch in Macrophages Represses Tumor Growth by Upregulating miR-125a and Disabling Tumor-Associated Macrophages.* Cancer Research, 2016. **76**(6): p. 1403-1415.

69. Foldi, J., et al., *RBP-J is required for M2 macrophage polarization in response to chitin and mediates expression of a subset of M2 genes.* Protein & Cell, 2016. **7**(3): p. 201-209.

70. Pagie, S., N. Gérard, and B. Charreau, *Notch signaling triggered via the ligand DLL4 impedes M2 macrophage differentiation and promotes their apoptosis.* Cell Communication and Signaling : CCS, 2018. **16**: p. 4.

71. Lemay, D.G. and D.H. Hwang, *Genome-wide identification of peroxisome proliferator response elements using integrated computational genomics.* Journal of Lipid Research, 2006. **47**(7): p. 1583-1587.

72. Sever, R. and C.K. Glass, *Signaling by Nuclear Receptors.* Cold Spring Harbor Perspectives in Biology, 2013. **5**(3): p. a016709.

73. Kim, T.-H., et al., *Modulation of the Transcriptional Activity of Peroxisome Proliferator-Activated Receptor Gamma by Protein-Protein Interactions and Post-Translational Modifications.* Yonsei Med J, 2013. **54**(3): p. 545-559.

74. Pott, S., et al., *PPARG Binding Landscapes in Macrophages Suggest a Genome-Wide Contribution of PU.1 to Divergent PPARG Binding in Human and Mouse.* PLOS ONE, 2012. **7**(10): p. e48102.

75. Oka, S.-i., et al., *Peroxisome Proliferator Activated Receptor-α Association With Silent Information Regulator 1 Suppresses Cardiac Fatty Acid Metabolism in the Failing Heart: CLINICAL PERSPECTIVE.* Circulation: Heart Failure, 2015. **8**(6): p. 1123-1132.

76. Zieleniak, A., M. Wójcik, and L.A. Woźniak, *Structure and physiological functions of the human peroxisome proliferator-activated receptor γ.* Archivum Immunologiae et Therapiae Experimentalis, 2008. **56**(5): p. 331.

77. Costa, V., et al., *PPARG: Gene Expression Regulation and Next-Generation Sequencing for Unsolved Issues.* PPAR Research, 2010. **2010**: p. 17.

78. Tagore, M., et al., *The Lineage-Specific Transcription Factor PU.1 Prevents Polycomb-Mediated Heterochromatin Formation at Macrophage-Specific Genes.* Molecular and Cellular Biology, 2015. **35**(15): p. 2610-2625.

79. Chen, Y., A.R. Jimenez, and J.D. Medh, *Identification and regulation of novel PPAR-γ splice variants in human THP-1 macrophages.* Biochimica et biophysica acta, 2006. **1759**(1-2): p. 32-43.

80. Lefterova, M.I., et al., *PPARγ and the global map of adipogenesis and beyond.* Trends in Endocrinology & Metabolism. **25**(6): p. 293-302.

81. Huang, J.T., et al., *Interleukin-4-dependent production of PPAR-γ ligands in macrophages by 12/15-lipoxygenase.* Nature, 1999. **400**: p. 378.

82. Gonzalez, Y.R., et al., *CITED2 Signals through Peroxisome Proliferator-Activated Receptor-γ to Regulate Death of Cortical Neurons after DNA Damage.* The Journal of Neuroscience, 2008. **28**(21): p. 5559-5569.

83. Kim, G.-D., et al., *CITED2 Restrains Proinflammatory Macrophage Activation and Response.* Molecular and Cellular Biology, 2018. **38**(5).

84. Barak, Y., et al., *PPARγ is required for placental, cardiac, and adipose tissue development.* Molecular Cell, 1999. **4**(4): p. 585-595.

85. Barish, G.D., *Peroxisome Proliferator-Activated Receptors and Liver X Receptors in Atherosclerosis and Immunity.* The Journal of Nutrition, 2006. **136**(3): p. 690-694.

86. Wang, H. and R.H. Eckel, *Lipoprotein lipase: from gene to obesity.* American Journal of Physiology-Endocrinology and Metabolism, 2009. **297**(2): p. E271-E288.

87. Huang, L.-H., et al., *Acyl-Coenzyme A:cholesterol Acyltransferase 1: Significance of Single Nucleotide Polymorphism at Residue 526 and Role of Proline 347 near the Fifth Transmembrane Domain.* The FEBS journal, 2014. **281**(7): p. 1773-1783.

88. Ricote, M., J.S. Welch, and C.K. Glass, *Regulation of Macrophage Gene Expression by the Peroxisome Proliferator-Activated Receptor-γ.* Hormone Research in Paediatrics, 2000. **54**(5-6): p. 275-280.

89. Ricote, M., et al., *Expression of the peroxisome proliferator-activated receptor γ (PPARγ) in human atherosclerosis and regulation in macrophages by colony stimulating factors and oxidized low density lipoprotein.* Proceedings of the National Academy of Sciences of the United States of America, 1998. **95**(13): p. 7614-7619.

90. Hasegawa-Moriyama, M., et al., *Peroxisome proliferator-activated receptor-gamma agonist rosiglitazone attenuates inflammatory pain through the induction of heme oxygenase-1 in macrophages.* PAIN, 2013. **154**(8): p. 1402-1412.

91. Bouhlel, M.A., et al., *PPARγ Activation Primes Human Monocytes into Alternative M2 Macrophages with Anti-inflammatory Properties.* Cell Metabolism, 2007. **6**(2): p. 137-143.

92. Spann, Nathanael J., et al., *Regulated Accumulation of Desmosterol Integrates Macrophage Lipid Metabolism and Inflammatory Responses.* Cell, 2012. **151**(1): p. 138-152.

93. Yue, L., et al., *Ligand-binding regulation of LXR/RXR and LXR/PPAR heterodimerizations: SPR technology-based kinetic analysis correlated with molecular dynamics simulation.* Protein Science : A Publication of the Protein Society, 2005. **14**(3): p. 812-822.

94. Bobryshev, Y.V., et al., *Macrophages and Their Role in Atherosclerosis: Pathophysiology and Transcriptome Analysis.* BioMed Research International, 2016. **2016**: p. 9582430.

95. Cheng, W.Y., et al., *Macrophage PPARγ inhibits Gpr132 to mediate the anti-tumor effects of rosiglitazone.* eLife, 2016. **5**: p. e18501.

96. Yu, J., et al., *DNMT1-PPARγ pathway in macrophages regulates chronic inflammation and atherosclerosis development in mice.* Scientific Reports, 2016. **6**: p. 30053.

97. Yu, M., et al., *Inhibition of Macrophage CD36 Expression and Cellular Oxidized Low Density Lipoprotein (oxLDL) Accumulation by Tamoxifen: A PEROXISOME PROLIFERATOR-ACTIVATED RECEPTOR (PPAR)γ-DEPENDENT MECHANISM.* Journal of Biological Chemistry, 2016. **291**(33): p. 16977-16989.

98. Kim, G. and G.H. Mahabaleshwar, *CITED2 Restrains Macrophage Pro-inflammatory Activation and Atherogenesis.* Atherosclerosis Supplements, 2018. **32**: p. 2.

99. Wright, H.M., et al., *A Synthetic Antagonist for the Peroxisome Proliferator-activated Receptor γ Inhibits Adipocyte Differentiation.* Journal of Biological Chemistry, 2000. **275**(3): p. 1873-1877.

100. Nakano, R., et al., *Antagonism of peroxisome proliferator-activated receptor γ prevents high-fat diet-induced obesity in vivo.* Biochemical Pharmacology, 2006. **72**(1): p. 42-52.

101. Li, J.J., et al., *Ubiquitin Ligase NEDD4 Regulates PPARγ Stability and Adipocyte Differentiation in 3T3-L1 Cells.* Scientific Reports, 2016. **6**: p. 38550.

102. Floyd, Z.E. and J.M. Stephens, *Interferon-γ-mediated Activation and Ubiquitin-Proteasome-dependent Degradation of PPARγ in Adipocytes.* Journal of Biological Chemistry, 2002. **277**(6): p. 4062-4068.

103. Shu, Y., et al., *Phosphorylation of PPARγ at Ser84 promotes glycolysis and cell proliferation in hepatocellular carcinoma by targeting PFKFB4.* Oncotarget, 2016. **7**(47): p. 76984-76994.

104. Hayat, M.A., *Chapter 1 - Introduction to Autophagy: Cancer, Other Pathologies, Inflammation, Immunity, Infection, and Aging, Volume 5*, in *Autophagy: Cancer, Other Pathologies, Inflammation, Immunity, Infection, and Aging*, M.A. Hayat, Editor. 2015, Academic Press: Amsterdam. p. 1-48.

105. Park, H.S., et al., *PPARγ neddylation essential for adipogenesis is a potential target for treating obesity.* Cell Death And Differentiation, 2016. **23**: p. 1296.

106. Goel, P., J.A. Manning, and S. Kumar, *NEDD4-2 (NEDD4L): The ubiquitin ligase for multiple membrane proteins.* Gene, 2015. **557**(1): p. 1-10.

107. Wang, Z., et al., *NEDD4L Protein Catalyzes Ubiquitination of PIK3CA Protein and Regulates PI3K-AKT Signaling.* Journal of Biological Chemistry, 2016. **291**(33): p. 17467-17477.

108. Totaro, A., et al., *YAP/TAZ link cell mechanics to Notch signalling to control epidermal stem cell fate.* Nature Communications, 2017. **8**: p. 15206.

109. Sakata, T., et al., *Drosophila Nedd4 Regulates Endocytosis of Notch and Suppresses Its Ligand-Independent Activation.* Current Biology, 2004. **14**(24): p. 2228-2236.

110. Maniati, E., et al., *Crosstalk between the canonical NF-κB and Notch signaling pathways inhibits Pparγ expression and promotes pancreatic cancer progression in mice.* The Journal of Clinical Investigation, 2011. **121**(12): p. 4685-4699.

111. Miyamoto, Y., et al., *Notch mediates TGFα-induced changes in epithelial differentiation during pancreatic tumorigenesis.* Cancer Cell, 2003. **3**(6): p. 565-576.

112. Fazio, C. and L. Ricciardiello, *Inflammation and Notch signaling: a crosstalk with opposite effects on tumorigenesis.* Cell Death &Amp; Disease, 2016. **7**: p. e2515.

113. Nickoloff, B.J., et al., *Jagged-1 mediated activation of notch signaling induces complete maturation of human keratinocytes through NF-kappaB and PPARgamma.* Cell Death And Differentiation, 2002. **9**(8): p. 842-855.

114. Livak, K.J. and T.D. Schmittgen, *Analysis of Relative Gene Expression Data Using Real-Time Quantitative PCR and the 2โ'ฮ"ฮ"CT Method.* Methods, 2001. **25**(4): p. 402-408.

115. Tanapat, P., et al., *Notch signaling is activated by TLR stimulation and regulates macrophage functions.* European Journal of Immunology, 2008. **38**(1): p. 174-183.

116. Kuncharin, Y., et al., *MAML1 regulates cell viability via the NF-κB pathway in cervical cancer cell lines.* Experimental Cell Research, 2011. **317**(13): p. 1830-1840.

117. Fung, E., et al., *Delta-Like 4 Induces Notch Signaling in Macrophages. Implications for Inflammation.* Circulation, 2007.

118. Kongkavitoon, P., et al., *Hepatitis B Virus HBx Activates Notch Signaling via Delta-Like 4/Notch1 in Hepatocellular Carcinoma.* PLOS ONE, 2016. **11**(1): p. e0146696.

119. Choi, J.-H., et al., *Jagged-1 and Notch3 juxtacrine loop regulates ovarian tumor growth and adhesion.* Cancer research, 2008. **68**(14): p. 5716-5723.

120. Li, H., et al., *Effect of IL-17 monoclonal antibody Secukinumab combined with IL-35 blockade of Notch signaling pathway on the invasive capability of hepatoma cells.* Genet Mol Res, 2016. **15**(2).

121. Kuratomi, G., et al., *NEDD4-2 (neural precursor cell expressed, developmentally down-regulated 4-2) negatively regulates TGF-β (transforming growth factor-β) signalling by inducing ubiquitin-mediated degradation of Smad2 and TGF-β type I receptor.* Biochemical Journal, 2005. **386**(Pt 3): p. 461-470.

122. Martinez, F.O. and S. Gordon, *The M1 and M2 paradigm of macrophage activation: time for reassessment.* F1000Prime Reports, 2014. **6**: p. 13.

123. Tarique, A.A., et al., *Phenotypic, Functional, and Plasticity Features of Classical and Alternatively Activated Human Macrophages.* American Journal of Respiratory Cell and Molecular Biology, 2015. **53**(5): p. 676-688.

124. Mukherjee, R., et al., *Non-Classical monocytes display inflammatory features: Validation in Sepsis and Systemic Lupus Erythematous.* Scientific Reports, 2015. **5**: p. 13886.

125. E., I., et al., *The Role of Different Monocyte Subsets in the Pathogenesis of Atherosclerosis and Acute Coronary Syndromes.* Scandinavian Journal of Immunology, 2015. **82**(3): p. 163-173.

126. Kornilova, A.Y., C. Das, and M.S. Wolfe, *Differential Effects of Inhibitors on the γ-Secretase Complex: MECHANISTIC IMPLICATIONS.* Journal of Biological Chemistry, 2003. **278**(19): p. 16470-16473.

127. Ross, J., *mRNA stability in mammalian cells.* Microbiological Reviews, 1995. **59**(3): p. 423-450.

128. Raghavachari, N., et al., *A systematic comparison and evaluation of high density exon arrays and RNA-seq technology used to unravel the peripheral blood transcriptome of sickle cell disease*. Vol. 5. 2012. 28.

129. !!! INVALID CITATION !!! (2, 18).

130. Kannan, S., et al., *Notch activation inhibits AML growth and survival: A potential therapeutic approach*. Vol. 210. 2013.

131. Madonna, M., et al., *Hes4: A potential prognostic biomarker for newly diagnosed patients with high-grade osteosarcoma.* Pediatric Blood & Cancer, 2017. **64**(5): p. e26318.

132. Radtke, F., N. Fasnacht, and H.R. MacDonald, *Notch Signaling in the Immune System.* Immunity, 2010. **32**(1): p. 14-27.

133. Huynh, L., et al., *Opposing regulation of the late phase TNF response by mTORC1-IL-10 signaling and hypoxia in human macrophages.* Scientific Reports, 2016. **6**: p. 31959.

134. Dowds, C.M., et al., *Lipid antigens in immunity.* Biological chemistry, 2014. **395**(1): p. 61-81.

135. Eriksen, K.W., et al., *Bi-phasic Effect of Interferon (IFN)-α: IFN-α UP- AND DOWN-REGULATES INTERLEUKIN-4 SIGNALING IN HUMAN T CELLS.* Journal of Biological Chemistry, 2004. **279**(1): p. 169-176.

136. Ferrarelli, L.K., *Mutant KRAS triggers an inflammatory attraction.* Science Signaling, 2015. **8**(361): p. ec20-ec20.

137. Becerra-Diaz, M., et al., *Unexpected role for androgen and androgen receptor as enhancers of M2 macrophage polarization.* The Journal of Immunology, 2018. **200**(1 Supplement): p. 44.18-44.18.

138. Bao, K. and R.L. Reinhardt, *The differential expression of IL-4 and IL-13 and its impact on type-2 Immunity.* Cytokine, 2015. **75**(1): p. 25-37.

139. Eltzschig, H.K. and P. Carmeliet, *Hypoxia and Inflammation.* New England Journal of Medicine, 2011. **364**(7): p. 656-665.

140. Kim, K., et al., *PIF1 Regulates Plastid Development by Repressing Photosynthetic Genes in the Endodermis.* Molecular Plant, 2016. **9**(10): p. 1415-1427.

141. T., N.J., M. Alison, and W. Gerry, *Notch Signaling – Constantly on the Move.* Traffic, 2007. **8**(8): p. 959-969.

142. Yamamoto, S., W.-L. Charng, and H.J. Bellen, *Chapter Five - Endocytosis and Intracellular Trafficking of Notch and Its Ligands*, in *Current Topics in Developmental Biology*, R. Kopan, Editor. 2010, Academic Press. p. 165-200.

143. Tanksley, J.P., X. Chen, and R.J. Coffey, *NEDD4L Is Downregulated in Colorectal Cancer and Inhibits Canonical WNT Signaling.* PLoS ONE, 2013. **8**(11): p. e81514.

144. Zhu, J.-y., et al., *The E3 ubiquitin ligase Nedd4/Nedd4L is directly regulated by microRNA 1.* Development (Cambridge, England), 2017. **144**(5): p. 866-875.

145. Di Cristofano, A., *Chapter Two - SGK1: The Dark Side of PI3K Signaling*, in *Current Topics in Developmental Biology*, A. Jenny, Editor. 2017, Academic Press. p. 49-71.

146. Yang, M., et al., *Serum-Glucocorticoid Regulated Kinase 1 Regulates Alternatively Activated Macrophage Polarization Contributing to Angiotensin II–Induced Inflammation and Cardiac Fibrosis.* Arteriosclerosis, Thrombosis, and Vascular Biology, 2012. **32**(7): p. 1675-1686.

147. Luiken, J.J.F.P., et al., *Post-translational modifications of CD36 (SR-B2): Implications for regulation of myocellular fatty acid uptake.* Biochimica et Biophysica Acta (BBA) - Molecular Basis of Disease, 2016. **1862**(12): p. 2253-2258.

148. Shimojo, H., T. Ohtsuka, and R. Kageyama, *Oscillations in Notch Signaling Regulate Maintenance of Neural Progenitors.* Neuron, 2008. **58**(1): p. 52-64.

149. Boareto, M., et al., *Jagged–Delta asymmetry in Notch signaling can give rise to a Sender/Receiver hybrid phenotype.* Proceedings of the National Academy of Sciences, 2015. **112**(5): p. E402-E409.

150. Vallejo, D.M., E. Caparros, and M. Dominguez, *Targeting Notch signalling by the conserved miR-8/200 microRNA family in development and cancer cells.* The EMBO Journal, 2011. **30**(4): p. 756-769.

151. Hayashi, Y., et al., *A novel non-canonical Notch signaling regulates expression of synaptic vesicle proteins in excitatory neurons.* Scientific Reports, 2016. **6**: p. 23969.

152. Yu, M., et al., *Complex Regulation of Tartrate-resistant Acid Phosphatase (TRAP) Expression by Interleukin 4 (IL-4): IL-4 INDIRECTLY SUPPRESSES RECEPTOR ACTIVATOR OF NF-κB LIGAND (RANKL)-MEDIATED TRAP EXPRESSION BUT MODESTLY INDUCES ITS EXPRESSION DIRECTLY.* Journal of Biological Chemistry, 2009. **284**(47): p. 32968-32979.

153. Boorsma, C.E., et al., *A Potent Tartrate Resistant Acid Phosphatase Inhibitor to Study the Function of TRAP in Alveolar Macrophages.* Scientific Reports, 2017. **7**(1): p. 12570.

154. Henshall, T.L. and S. Kumar, *NEDD4–2*, in *Encyclopedia of Signaling Molecules*, S. Choi, Editor. 2016, Springer New York: New York, NY. p. 1-6.

# APPENDICES

# APPENDIX A

**1. Completed media for tissue culture**

1.1 Completed DMEM 100 ml

| | | |
|---|---|---|
| DMEM | 90 | % |
| FBS | 10 | % |
| Penicillin | 100 | U/ml |
| Streptomycin | 0.4 | mg/ml |
| Sodium pyruvate | 1 | % |
| HEPES | 1 | % |

1.2 Completed RPMI1640 100 ml

| | | |
|---|---|---|
| RPMI1640 | 90 | % |
| FBS | 10 | % |
| Penicillin | 100 | U/ml |
| Streptomycin | 0.4 | mg/ml |
| Sodium pyruvate | 1 | % |
| HEPES | 1 | % |
| β-mercaptoethanol | 50 | μM |

1.3 Completed iMDM 100 ml

| | | |
|---|---|---|
| iMDM | 90 | % |
| Human serum | 10 | % |
| Penicillin | 100 | U/ml |
| Streptomycin | 0.4 | mg/ml |



**2. Freezing media 10 ml**

| | | |
|---|---|---|
| Completed media | 90 | % |
| DMSO | 10 | % |

**3. FBS and human serum inactivation**

Commercial FBS which were kept at -20°C was thawed at 4°C for overnight and inactivated at 56°C for 30 min. in water bath prior using.

**4. Buffer A for protein extraction**

| | | |
|---|---|---|
| 10 mM EGTA | 1 | ml |
| 10 mM DTT | 1 | ml |
| 500 mM Tris-HCl pH 7.2 | 1 | ml |
| 1.4 M KCl | 1 | ml |
| 25 mM $MgCl_2$ | 1 | ml |
| Sterile water | 5 | ml |
| Protease Inhibitor Cocktail Tablets | 1 | tablet |

**5. Buffer B for protein extraction**

| | | |
|---|---|---|
| Buffer A | 990 | µl |
| Nonidet P-40 | 10 | µl |

**6. 10% SDS-polyacrylamide gel 8 ml**

| | | |
|---|---|---|
| Sterile water | 4.236 | ml |
| 40% Acrylamide and Bis-acrylamide solution | 1.6 | ml |
| 1.5 M Tris-HCl pH 8.8 | 2 | ml |
| 10% SDS | 0.08 | ml |
| 10% APS | 0.08 | ml |
| TEMED | 0.004 | ml |

**7. 5% stacking gel 2 ml**

| | | |
|---|---|---|
| Sterile water | 1.204 | ml |
| 40% Acrylamide and Bis-acrylamide solution | 0.25 | ml |
| 1 M Tris-HCl pH 6.8 | 0.504 | ml |
| 10% SDS | 0.02 | ml |
| 10% APS | 0.02 | ml |
| TEMED | 0.002 | ml |

**8. 5×running bufferfor Western blot (1000 ml)**

| | | |
|---|---|---|
| Trisma base | 15.1 | g |
| Glycine | 94 | g |
| SDS | 5 | g |
| Deionized water was added to adjust volume into | 1000 | ml |

**9. 1.5M Tris-Cl pH 8.8 1000 ml**

One point five mole of Trisma-base was dissolved in sterile deionized water 800 ml, pH was adjusted into 8.8. Finally, the volume was adjusted into 1000 ml

**10. 2×Laemmli buffer (SDS-dye) 10 ml**

| | | |
|---|---|---|
| 1 M Tris-HCl pH 6.8 | 1 | ml |
| 10% SDS | 4 | ml |
| 99.5% glycerol | 2.01 | ml |
| Bromphenol blue | 0.001 | g |
| Deionized water was added to adjust volume into | 10 | ml |

**11. Transfer buffer for Western blot**

| | | |
|---|---|---|
| Trisma base | 5.08 | g |
| Glycine | 2.9 | g |
| SDS | 0.37 | g |

All reagents were dissolved in deionized water before adding absolute methanol 200 ml. The volume was adjusted into 1000 ml by deionized water.

**12. 1×PBS pH 7.4 1000 ml**

| | | |
|---|---|---|
| NaCl | 8 | g |
| KCl | 0.2 | g |
| $Na_2HPO_4$ | 1.44 | g |
| $KH_2PO_4$ | 0.24 | g |

Volume was adjusted into 1000 ml by deionized water before autoclaved at 121°C and pressure 15 psi for 15 min.

**13. PBST (washing buffer for Western blot)**

| | | |
|---|---|---|
| 1×PBS | 500 | ml |
| Tween20 | 0.05 | % |

**14. Blocking solution for Western blot**

| | | |
|---|---|---|
| PBST | 200 | ml |
| Non-fat dry milk | 6 | g |

**15. ECL substrate of HRP**

90mM of Coumaric acid was dissolved in 10 ml DMSO, aliquoted and kept at –20°C.

250 mM of Luminol was also dissolved in 10 ml DMSO, aliquoted and kept at –20°C.

**16. Solution A**

| | | |
|---|---|---|
| 100 mM Tris-HCl pH 8.5 (stored at 4˚C) | 2.5 | ml |
| 90 mM coumaric acid | 11 | µl |
| 250 mM luminol | 12.5 | µl |

**17. Solution B**

| | | |
|---|---|---|
| 100 mM Tris-HCl pH 8.5 (stored at 4˚C) | 2.5 | ml |
| 30% $H_2O_2$ | 1.5 | µl |

**18. Film developer and fixer**

Film developer and fixer were diluted in tap water at dilution 1:4.

**19. 0.01% DEPC water for RNA 100 ml**

One hundred ml of HPLC water was added into a clean bottle follow by 10 µl of DEPC (0.01% v/v). The bottle was swirled and incubated overnight at room temperature. Afterwards, DEPC water was sterile at 121°C, pressure 15 psi for 15 min.

**20. 75% Ethanol in DEPC 100 ml**

Twenty-five milliliters of 0.01% DEPC water was added in 75 ml of ethanol and kept at –20°C.

# APPENDIX B

Table 5 The differential expressed genes comparing between CTRL unstimulation and CTRL M(IL-4)

| GENES | Symbol | Base mean | log2(FC) | P-value | P-adj |
|---|---|---|---|---|---|
| ENSG00000114737 | CISH | 790.4813 | 4.62234 | 2.13E-187 | 3.31E-183 |
| ENSG00000106266 | SNX8 | 1820.017 | 2.172511 | 1.42E-111 | 1.11E-107 |
| ENSG00000100592 | DAAM1 | 766.249 | 2.239922 | 4.37E-97 | 2.26E-93 |
| ENSG00000185338 | SOCS1 | 368.3621 | 3.57183 | 3.64E-87 | 1.42E-83 |
| ENSG00000138134 | STAMBPL1 | 489.1123 | 2.376724 | 2.68E-68 | 8.34E-65 |
| ENSG00000166224 | SGPL1 | 2989.63 | 1.610252 | 9.64E-64 | 2.50E-60 |
| ENSG00000198743 | SLC5A3 | 2814.666 | 2.03033 | 1.06E-56 | 2.37E-53 |
| ENSG00000103044 | HAS3 | 730.0558 | 2.692616 | 1.29E-49 | 2.52E-46 |
| ENSG00000138821 | SLC39A8 | 823.3788 | 1.638144 | 4.29E-45 | 7.41E-42 |
| ENSG00000127863 | TNFRSF19 | 196.754 | 2.535233 | 5.42E-45 | 8.43E-42 |
| ENSG00000173198 | CYSLTR1 | 2989.208 | 1.303267 | 5.94E-42 | 8.39E-39 |
| ENSG00000168748 | CA7 | 380.5764 | 2.367843 | 5.33E-40 | 6.90E-37 |
| ENSG00000248187 | - | 280.4233 | 1.991013 | 3.18E-39 | 3.81E-36 |
| ENSG00000205730 | ITPRIPL2 | 3041.418 | 1.283424 | 2.50E-36 | 2.78E-33 |
| ENSG00000111729 | CLEC4A | 171.5708 | 2.329723 | 4.21E-33 | 4.36E-30 |
| ENSG00000161905 | ALOX15 | 78.04936 | 2.154454 | 1.37E-32 | 1.33E-29 |
| ENSG00000167641 | PPP1R14A | 48.75128 | 2.260514 | 2.09E-31 | 1.91E-28 |
| ENSG00000108262 | GIT1 | 3042.267 | 0.975472 | 2.65E-31 | 2.29E-28 |
| ENSG00000170448 | NFXL1 | 339.0572 | 1.458782 | 6.50E-28 | 5.32E-25 |
| ENSG00000171488 | LRRC8C | 4038.463 | 1.046018 | 7.88E-28 | 6.13E-25 |
| ENSG00000040531 | CTNS | 826.9113 | 1.459505 | 3.25E-26 | 2.41E-23 |
| ENSG00000171992 | SYNPO | 348.4624 | 1.723541 | 5.96E-25 | 4.21E-22 |
| ENSG00000169136 | ATF5 | 3197.873 | 1.279299 | 2.82E-24 | 1.83E-21 |
| ENSG00000243927 | MRPS6 | 1001.051 | 1.459116 | 2.72E-24 | 1.83E-21 |
| ENSG00000156127 | BATF | 282.1823 | 1.624542 | 2.94E-24 | 1.83E-21 |
| ENSG00000112773 | FAM46A | 1324.923 | -1.24529 | 4.23E-24 | 2.53E-21 |
| ENSG00000198829 | SUCNR1 | 7728.639 | 1.11266 | 9.50E-24 | 5.47E-21 |
| ENSG00000116514 | RNF19B | 2681.36 | 1.666011 | 1.99E-23 | 1.10E-20 |
| ENSG00000129625 | REEP5 | 2242.627 | 0.786769 | 2.60E-23 | 1.39E-20 |
| ENSG00000166016 | ABTB2 | 251.3992 | 1.732167 | 1.29E-21 | 6.67E-19 |
| ENSG00000073921 | PICALM | 5644.144 | 0.772974 | 1.45E-21 | 7.29E-19 |
| ENSG00000162367 | TAL1 | 126.4536 | 1.739432 | 4.63E-21 | 2.25E-18 |
| ENSG00000124762 | CDKN1A | 8582.052 | 1.087779 | 5.24E-21 | 2.47E-18 |
| ENSG00000080546 | SESN1 | 1296.666 | -1.38536 | 8.86E-21 | 4.06E-18 |
| ENSG00000147872 | PLIN2 | 721.8125 | -0.99551 | 4.63E-20 | 2.06E-17 |
| ENSG00000088992 | TESC | 181.531 | 1.297549 | 6.18E-20 | 2.67E-17 |
| ENSG00000074416 | MGLL | 2182.77 | 1.432533 | 1.20E-19 | 5.06E-17 |
| ENSG00000170113 | NIPA1 | 1256.95 | 1.053112 | 1.50E-19 | 6.13E-17 |

| | | | | | |
|---|---|---|---|---|---|
| ENSG00000136689 | IL1RN | 4634.596 | 1.375503 | 3.74E-19 | 1.49E-16 |
| ENSG00000104267 | CA2 | 1050.405 | -0.98201 | 8.68E-19 | 3.38E-16 |
| ENSG00000178175 | ZNF366 | 547.7235 | 1.236073 | 9.06E-19 | 3.44E-16 |
| ENSG00000101236 | RNF24 | 1033.406 | 0.926184 | 3.44E-18 | 1.28E-15 |
| ENSG00000141458 | NPC1 | 1276.431 | 0.896887 | 5.04E-18 | 1.82E-15 |
| ENSG00000113749 | HRH2 | 946.7547 | 1.188868 | 9.56E-18 | 3.38E-15 |
| ENSG00000124151 | NCOA3 | 2233.064 | 0.842963 | 1.62E-17 | 5.60E-15 |
| ENSG00000122986 | HVCN1 | 1287.694 | 0.892052 | 1.89E-17 | 6.39E-15 |
| ENSG00000107338 | SHB | 84.33651 | 1.548335 | 2.33E-17 | 7.72E-15 |
| ENSG00000167642 | SPINT2 | 3307.18 | 1.222544 | 5.71E-17 | 1.81E-14 |
| ENSG00000206073 | SERPINB4 | 34.26284 | 1.604529 | 5.65E-17 | 1.81E-14 |
| ENSG00000155846 | PPARGC1B | 211.8981 | 1.174958 | 8.47E-17 | 2.63E-14 |
| ENSG00000163293 | NIPAL1 | 47.77979 | 1.590327 | 9.51E-17 | 2.90E-14 |
| ENSG00000170345 | FOS | 757.6026 | -1.16745 | 2.10E-16 | 6.29E-14 |
| ENSG00000164442 | CITED2 | 10922.75 | 1.209772 | 3.24E-16 | 9.51E-14 |
| ENSG00000147036 | LANCL3 | 170.3177 | -1.20194 | 3.43E-16 | 9.89E-14 |
| ENSG00000186431 | FCAR | 229.0304 | -1.17752 | 3.90E-16 | 1.10E-13 |
| ENSG00000105219 | CNTD2 | 66.18752 | 1.565225 | 6.18E-16 | 1.72E-13 |
| ENSG00000165757 | KIAA1462 | 46.28499 | 1.553878 | 7.47E-16 | 2.04E-13 |
| ENSG00000142920 | AZIN2 | 468.8866 | 1.30965 | 8.20E-16 | 2.20E-13 |
| ENSG00000029153 | ARNTL2 | 861.6077 | 0.897781 | 9.03E-16 | 2.38E-13 |
| ENSG00000141506 | PIK3R5 | 1243.435 | 1.135195 | 1.89E-15 | 4.91E-13 |
| ENSG00000176597 | B3GNT5 | 3089.376 | 1.453613 | 2.31E-15 | 5.89E-13 |
| ENSG00000111424 | VDR | 836.9933 | 0.918978 | 7.22E-15 | 1.81E-12 |
| ENSG00000131370 | SH3BP5 | 278.1929 | -0.98835 | 1.55E-14 | 3.84E-12 |
| ENSG00000107816 | LZTS2 | 2654.924 | 0.715372 | 1.60E-14 | 3.89E-12 |
| ENSG00000213846 | - | 102.4978 | 1.267156 | 3.75E-14 | 8.98E-12 |
| ENSG00000188211 | NCR3LG1 | 403.0744 | 0.847529 | 7.35E-14 | 1.73E-11 |
| ENSG00000259330 | INAFM2 | 212.5775 | 1.088691 | 7.56E-14 | 1.75E-11 |
| ENSG00000099337 | KCNK6 | 1165.709 | 1.015814 | 1.36E-13 | 3.11E-11 |
| ENSG00000134243 | SORT1 | 3452.443 | 0.802506 | 2.39E-13 | 5.38E-11 |
| ENSG00000111647 | UHRF1BP1L | 932.9837 | 0.782525 | 3.19E-13 | 7.09E-11 |
| ENSG00000123685 | BATF3 | 50.38248 | 1.378251 | 3.56E-13 | 7.69E-11 |
| ENSG00000143374 | TARS2 | 1145.915 | 0.886095 | 3.53E-13 | 7.69E-11 |
| ENSG00000077684 | JADE1 | 782.4118 | 1.0268 | 5.23E-13 | 1.11E-10 |
| ENSG00000052126 | PLEKHA5 | 602.4493 | 0.944383 | 8.78E-13 | 1.84E-10 |
| ENSG00000111087 | GLI1 | 51.37189 | 1.323733 | 3.38E-12 | 7.01E-10 |
| ENSG00000003989 | SLC7A2 | 391.3409 | 1.139213 | 5.80E-12 | 1.17E-09 |
| ENSG00000168334 | XIRP1 | 4820.539 | 0.983219 | 5.75E-12 | 1.17E-09 |
| ENSG00000138135 | CH25H | 36.48181 | 1.334798 | 7.17E-12 | 1.41E-09 |
| ENSG00000142512 | SIGLEC10 | 189.1629 | 1.263986 | 7.10E-12 | 1.41E-09 |
| ENSG00000261269 | - | 406.2419 | 1.073565 | 8.84E-12 | 1.72E-09 |

| | | | | | |
|---|---|---|---|---|---|
| ENSG00000143226 | FCGR2A | 939.1041 | 1.298794 | 1.08E-11 | 2.06E-09 |
| ENSG00000129422 | MTUS1 | 32.99127 | 1.31333 | 1.52E-11 | 2.86E-09 |
| ENSG00000276600 | RAB7B | 388.6502 | -1.06864 | 1.52E-11 | 2.86E-09 |
| ENSG00000165685 | TMEM52B | 1547.246 | 1.262776 | 1.63E-11 | 3.01E-09 |
| ENSG00000143507 | DUSP10 | 882.518 | -0.97376 | 1.68E-11 | 3.06E-09 |
| ENSG00000164849 | GPR146 | 46.32859 | 1.276426 | 1.69E-11 | 3.06E-09 |
| ENSG00000169252 | ADRB2 | 106.1043 | -1.20943 | 1.83E-11 | 3.28E-09 |
| ENSG00000139269 | INHBE | 285.2457 | 1.305128 | 2.23E-11 | 3.94E-09 |
| ENSG00000115594 | IL1R1 | 92.81784 | 1.287445 | 2.72E-11 | 4.75E-09 |
| ENSG00000038427 | VCAN | 34.9529 | 1.29267 | 2.79E-11 | 4.82E-09 |
| ENSG00000185262 | UBALD2 | 1849.434 | 0.683257 | 3.84E-11 | 6.57E-09 |
| ENSG00000133789 | SWAP70 | 1151.556 | -0.73489 | 4.90E-11 | 8.28E-09 |
| ENSG00000275342 | - | 1334.906 | 0.879369 | 4.99E-11 | 8.34E-09 |
| ENSG00000064225 | ST3GAL6 | 666.464 | -0.78007 | 6.16E-11 | 1.02E-08 |
| ENSG00000169991 | IFFO2 | 228.5582 | 0.958873 | 8.85E-11 | 1.45E-08 |
| ENSG00000169554 | ZEB2 | 1715.302 | -0.80314 | 1.36E-10 | 2.21E-08 |
| ENSG00000155099 | TMEM55A | 291.603 | 0.992665 | 1.89E-10 | 3.04E-08 |
| ENSG00000150347 | ARID5B | 112.2024 | -1.13056 | 2.47E-10 | 3.92E-08 |
| ENSG00000178199 | ZC3H12D | 398.2125 | 0.894508 | 2.53E-10 | 3.97E-08 |
| ENSG00000001084 | GCLC | 2364.152 | -0.99652 | 3.14E-10 | 4.89E-08 |
| ENSG00000115159 | GPD2 | 642.3814 | 0.710495 | 3.59E-10 | 5.52E-08 |
| ENSG00000198959 | TGM2 | 6520.889 | 1.171972 | 3.81E-10 | 5.81E-08 |
| ENSG00000139668 | WDFY2 | 1463.709 | 0.66439 | 4.58E-10 | 6.92E-08 |
| ENSG00000163590 | PPM1L | 735.7008 | 0.757074 | 5.57E-10 | 8.34E-08 |
| ENSG00000116260 | QSOX1 | 4608.475 | 0.508829 | 7.79E-10 | 1.15E-07 |
| ENSG00000072694 | FCGR2B | 48.56863 | 1.193049 | 8.46E-10 | 1.24E-07 |
| ENSG00000197852 | FAM212B | 227.8589 | 0.840064 | 1.11E-09 | 1.62E-07 |
| ENSG00000004455 | AK2 | 2646.706 | 0.690954 | 2.25E-09 | 3.21E-07 |
| ENSG00000172840 | PDP2 | 613.6187 | 0.907624 | 2.25E-09 | 3.21E-07 |
| ENSG00000112195 | TREML2 | 382.0724 | 1.048714 | 2.51E-09 | 3.55E-07 |
| ENSG00000110237 | ARHGEF17 | 666.4797 | 1.062293 | 2.55E-09 | 3.58E-07 |
| ENSG00000103064 | SLC7A6 | 1192.874 | 0.532875 | 3.25E-09 | 4.52E-07 |
| ENSG00000186432 | KPNA4 | 3059.926 | 0.496001 | 3.57E-09 | 4.92E-07 |
| ENSG00000114738 | MAPKAPK3 | 2304.204 | 0.613574 | 4.04E-09 | 5.51E-07 |
| ENSG00000124782 | RREB1 | 1965.334 | -0.57984 | 5.97E-09 | 8.08E-07 |
| ENSG00000150764 | DIXDC1 | 2932.13 | 0.488435 | 6.72E-09 | 9.01E-07 |
| ENSG00000268734 | - | 85.90904 | -1.02828 | 8.20E-09 | 1.09E-06 |
| ENSG00000070759 | TESK2 | 217.3383 | -0.80365 | 8.66E-09 | 1.14E-06 |
| ENSG00000175782 | SLC35E3 | 211.4377 | 0.762285 | 1.03E-08 | 1.35E-06 |
| ENSG00000169508 | GPR183 | 2325.644 | 0.651902 | 1.10E-08 | 1.42E-06 |
| ENSG00000126561 | STAT5A | 1493.342 | 0.661141 | 1.27E-08 | 1.63E-06 |
| ENSG00000133069 | TMCC2 | 400.757 | 0.867637 | 1.30E-08 | 1.66E-06 |

| | | | | | |
|---|---|---|---|---|---|
| ENSG00000124831 | LRRFIP1 | 2214.364 | 0.50988 | 1.91E-08 | 2.42E-06 |
| ENSG00000136869 | TLR4 | 411.6405 | -0.78182 | 2.21E-08 | 2.77E-06 |
| ENSG00000235316 | DUSP8P5 | 304.9913 | 1.026187 | 2.25E-08 | 2.80E-06 |
| ENSG00000169255 | B3GALNT1 | 285.1716 | 0.782244 | 3.53E-08 | 4.35E-06 |
| ENSG00000095951 | HIVEP1 | 1654.032 | -0.8238 | 3.73E-08 | 4.57E-06 |
| ENSG00000106948 | AKNA | 1122.255 | -0.47602 | 4.01E-08 | 4.87E-06 |
| ENSG00000109861 | CTSC | 4155.305 | 0.685763 | 4.20E-08 | 5.06E-06 |
| ENSG00000157927 | RADIL | 83.055 | 0.97398 | 4.31E-08 | 5.15E-06 |
| ENSG00000176845 | METRNL | 3248.152 | 0.675684 | 4.38E-08 | 5.20E-06 |
| ENSG00000115604 | IL18R1 | 896.2331 | 0.990273 | 4.69E-08 | 5.53E-06 |
| ENSG00000169902 | TPST1 | 562.2538 | -0.66042 | 5.33E-08 | 6.23E-06 |
| ENSG00000127951 | FGL2 | 667.5615 | 1.029419 | 5.49E-08 | 6.37E-06 |
| ENSG00000106799 | TGFBR1 | 2089.923 | -0.63011 | 5.70E-08 | 6.57E-06 |
| ENSG00000168916 | ZNF608 | 129.7483 | -1.05168 | 6.83E-08 | 7.82E-06 |
| ENSG00000163171 | CDC42EP3 | 1536.344 | 0.716628 | 7.12E-08 | 8.08E-06 |
| ENSG00000171522 | PTGER4 | 475.9697 | -0.68064 | 7.35E-08 | 8.28E-06 |
| ENSG00000165030 | NFIL3 | 748.8318 | 0.766216 | 7.62E-08 | 8.52E-06 |
| ENSG00000162772 | ATF3 | 1248.246 | 0.882608 | 7.86E-08 | 8.73E-06 |
| ENSG00000184557 | SOCS3 | 206.3934 | 0.901082 | 8.93E-08 | 9.85E-06 |
| ENSG00000116473 | RAP1A | 3461.442 | 0.624492 | 9.05E-08 | 9.92E-06 |
| ENSG00000100030 | MAPK1 | 3163.772 | 0.465214 | 9.55E-08 | 1.04E-05 |
| ENSG00000169439 | SDC2 | 1967.369 | 0.721021 | 1.25E-07 | 1.35E-05 |
| ENSG00000133805 | AMPD3 | 1905.519 | -0.56764 | 1.33E-07 | 1.43E-05 |
| ENSG00000138670 | RASGEF1B | 212.1545 | -0.78295 | 1.36E-07 | 1.45E-05 |
| ENSG00000111269 | CREBL2 | 882.1999 | 0.554581 | 1.47E-07 | 1.56E-05 |
| ENSG00000120217 | CD274 | 46.389 | 1.006084 | 1.54E-07 | 1.62E-05 |
| ENSG00000171608 | PIK3CD | 1708.935 | 0.823228 | 1.69E-07 | 1.77E-05 |
| ENSG00000174485 | DENND4A | 674.6546 | 0.853317 | 1.99E-07 | 2.06E-05 |
| ENSG00000119042 | SATB2 | 2084.868 | -0.55401 | 2.36E-07 | 2.43E-05 |
| ENSG00000109320 | NFKB1 | 2451.117 | 0.444418 | 2.40E-07 | 2.46E-05 |
| ENSG00000049759 | NEDD4L | 90.91801 | 1.001975 | 2.60E-07 | 2.64E-05 |
| ENSG00000148204 | CRB2 | 59.17201 | 0.996714 | 3.01E-07 | 3.04E-05 |
| ENSG00000264230 | ANXA8L1 | 38.98752 | 0.996402 | 3.28E-07 | 3.30E-05 |
| ENSG00000113532 | ST8SIA4 | 618.2459 | -0.59798 | 3.67E-07 | 3.66E-05 |
| ENSG00000115525 | ST3GAL5 | 459.9653 | 0.688596 | 4.03E-07 | 3.99E-05 |
| ENSG00000128016 | ZFP36 | 1702.387 | 0.578963 | 4.12E-07 | 4.05E-05 |
| ENSG00000064763 | FAR2 | 561.754 | 0.559067 | 4.44E-07 | 4.28E-05 |
| ENSG00000121957 | GPSM2 | 309.5776 | -0.78354 | 4.42E-07 | 4.28E-05 |
| ENSG00000174718 | KIAA1551 | 919.861 | -0.54099 | 4.42E-07 | 4.28E-05 |
| ENSG00000118689 | FOXO3 | 1418.326 | -0.7823 | 4.73E-07 | 4.54E-05 |
| ENSG00000265190 | ANXA8 | 25.15105 | 0.965076 | 7.25E-07 | 6.91E-05 |
| ENSG00000139112 | GABARAPL1 | 3223.99 | 0.909548 | 8.14E-07 | 7.72E-05 |

| | | | | | |
|---|---|---|---|---|---|
| ENSG00000169105 | CHST14 | 361.1277 | 0.608291 | 9.35E-07 | 8.82E-05 |
| ENSG00000104951 | IL4I1 | 6094.1 | 0.797357 | 9.48E-07 | 8.84E-05 |
| ENSG00000125726 | CD70 | 398.1323 | -0.72443 | 9.50E-07 | 8.84E-05 |
| ENSG00000245848 | CEBPA | 3680.061 | 0.810165 | 1.18E-06 | 0.000109 |
| ENSG00000129521 | EGLN3 | 99.6711 | 0.932721 | 1.20E-06 | 0.000111 |
| ENSG00000172349 | IL16 | 114.1468 | -0.81675 | 1.26E-06 | 0.000116 |
| ENSG00000174456 | C12orf76 | 234.2047 | 0.757312 | 1.53E-06 | 0.000139 |
| ENSG00000112701 | SENP6 | 3378.391 | 0.46534 | 1.62E-06 | 0.000147 |
| ENSG00000167850 | CD300C | 259.8554 | 0.670135 | 1.68E-06 | 0.000151 |
| ENSG00000067082 | KLF6 | 827.8277 | -0.76892 | 1.75E-06 | 0.000156 |
| ENSG00000143847 | PPFIA4 | 334.221 | 0.696444 | 2.12E-06 | 0.000189 |
| ENSG00000057149 | SERPINB3 | 10.84501 | 0.77287 | 2.14E-06 | 0.000189 |
| ENSG00000166783 | KIAA0430 | 1849.935 | -0.43589 | 2.43E-06 | 0.000213 |
| ENSG00000235750 | KIAA0040 | 377.0716 | 0.744032 | 2.58E-06 | 0.000225 |
| ENSG00000160223 | ICOSLG | 161.6357 | -0.69955 | 2.64E-06 | 0.000229 |
| ENSG00000173110 | HSPA6 | 16.39353 | 0.876751 | 2.67E-06 | 0.000231 |
| ENSG00000162928 | PEX13 | 1232.881 | 0.491078 | 2.71E-06 | 0.000233 |
| ENSG00000110324 | IL10RA | 1795.68 | 0.864366 | 2.73E-06 | 0.000233 |
| ENSG00000116852 | KIF21B | 4339.989 | -0.34277 | 2.80E-06 | 0.000237 |
| ENSG00000132170 | PPARG | 268.1301 | 0.876056 | 2.81E-06 | 0.000237 |
| ENSG00000109906 | ZBTB16 | 60.3171 | 0.909692 | 3.09E-06 | 0.00026 |
| ENSG00000140455 | USP3 | 733.0875 | -0.44403 | 3.16E-06 | 0.000264 |
| ENSG00000092969 | TGFB2 | 28.22706 | -0.90885 | 3.19E-06 | 0.000266 |
| ENSG00000161929 | SCIMP | 18.36631 | 0.899258 | 3.34E-06 | 0.000276 |
| ENSG00000250959 | GLUD1P3 | 211.695 | 0.877816 | 3.39E-06 | 0.000279 |
| ENSG00000240583 | AQP1 | 230.489 | 0.875548 | 3.46E-06 | 0.000284 |
| ENSG00000015532 | XYLT2 | 668.8396 | 0.510232 | 3.51E-06 | 0.000286 |
| ENSG00000106415 | GLCCI1 | 810.19 | -0.43558 | 3.64E-06 | 0.000295 |
| ENSG00000170571 | EMB | 590.9698 | 0.577848 | 4.05E-06 | 0.000326 |
| ENSG00000164604 | GPR85 | 354.5411 | 0.671346 | 4.13E-06 | 0.000331 |
| ENSG00000103257 | SLC7A5 | 6368.374 | 0.705876 | 4.15E-06 | 0.000331 |
| ENSG00000155100 | OTUD6B | 373.0708 | 0.708333 | 4.48E-06 | 0.000355 |
| ENSG00000197405 | C5AR1 | 142.7651 | -0.81233 | 5.67E-06 | 0.000447 |
| ENSG00000198900 | TOP1 | 837.722 | 0.645096 | 5.75E-06 | 0.000452 |
| ENSG00000197208 | SLC22A4 | 92.69682 | 0.776005 | 6.05E-06 | 0.000473 |
| ENSG00000211891 | IGHE | 8.52667 | 0.745443 | 6.23E-06 | 0.000485 |
| ENSG00000140968 | IRF8 | 278.4263 | 0.879668 | 6.55E-06 | 0.000507 |
| ENSG00000104312 | RIPK2 | 322.0853 | 0.544189 | 6.66E-06 | 0.000513 |
| ENSG00000175874 | CREG2 | 40.33243 | 0.872368 | 7.63E-06 | 0.000584 |
| ENSG00000164951 | PDP1 | 93.03389 | -0.85558 | 7.72E-06 | 0.000588 |
| ENSG00000112679 | DUSP22 | 951.5611 | 0.51549 | 7.84E-06 | 0.000595 |
| ENSG00000118946 | PCDH17 | 37.46661 | 0.864057 | 8.01E-06 | 0.000602 |

| | | | | | |
|---|---|---|---|---|---|
| ENSG00000196396 | PTPN1 | 1661.609 | 0.452329 | 8.00E-06 | 0.000602 |
| ENSG00000099998 | GGT5 | 38.50769 | 0.853676 | 8.09E-06 | 0.000605 |
| ENSG00000204103 | MAFB | 747.2226 | -0.69801 | 8.13E-06 | 0.000605 |
| ENSG00000109099 | PMP22 | 26.67495 | 0.870324 | 8.20E-06 | 0.000607 |
| ENSG00000115170 | ACVR1 | 493.4952 | 0.706981 | 9.53E-06 | 0.000702 |
| ENSG00000026652 | AGPAT4 | 1457.301 | 0.660396 | 9.66E-06 | 0.000709 |
| ENSG00000116922 | C1orf109 | 340.199 | 0.500337 | 1.03E-05 | 0.000751 |
| ENSG00000118985 | ELL2 | 3910.032 | 0.712782 | 1.05E-05 | 0.000766 |
| ENSG00000130340 | SNX9 | 4231.246 | -0.64309 | 1.07E-05 | 0.000774 |
| ENSG00000168769 | TET2 | 1337.575 | -0.4636 | 1.11E-05 | 0.000801 |
| ENSG00000108700 | CCL8 | 15.71005 | 0.693292 | 1.14E-05 | 0.000818 |
| ENSG00000113083 | LOX | 20.51404 | 0.751686 | 1.19E-05 | 0.00085 |
| ENSG00000178860 | MSC | 153.7267 | -0.65624 | 1.25E-05 | 0.000886 |
| ENSG00000115602 | IL1RL1 | 37.45416 | 0.844144 | 1.25E-05 | 0.000887 |
| ENSG00000143816 | WNT9A | 78.01244 | 0.783338 | 1.30E-05 | 0.000916 |
| ENSG00000179630 | LACC1 | 445.4366 | -0.48448 | 1.36E-05 | 0.00095 |
| ENSG00000157778 | PSMG3 | 830.4351 | 0.414415 | 1.48E-05 | 0.001029 |
| ENSG00000169116 | PARM1 | 149.2785 | 0.761684 | 1.48E-05 | 0.001029 |
| ENSG00000140459 | CYP11A1 | 23.09314 | 0.821606 | 1.52E-05 | 0.001048 |
| ENSG00000197646 | PDCD1LG2 | 42.36119 | 0.785119 | 1.55E-05 | 0.001067 |
| ENSG00000131759 | RARA | 628.0948 | 0.513484 | 1.70E-05 | 0.001165 |
| ENSG00000221968 | FADS3 | 832.7096 | 0.452134 | 1.74E-05 | 0.001189 |
| ENSG00000103528 | SYT17 | 56.07252 | 0.818635 | 1.76E-05 | 0.001194 |
| ENSG00000117643 | MAN1C1 | 85.93535 | 0.726578 | 1.77E-05 | 0.0012 |
| ENSG00000185669 | SNAI3 | 417.9474 | 0.719183 | 1.82E-05 | 0.001226 |
| ENSG00000186806 | VSIG10L | 193.6593 | 0.785691 | 2.14E-05 | 0.001433 |
| ENSG00000102531 | FNDC3A | 4130.236 | 0.556905 | 2.20E-05 | 0.00147 |
| ENSG00000137747 | TMPRSS13 | 81.31468 | 0.787095 | 2.31E-05 | 0.001536 |
| ENSG00000132640 | BTBD3 | 1121.868 | -0.37305 | 2.35E-05 | 0.001555 |
| ENSG00000197380 | DACT3 | 152.5781 | -0.6236 | 2.41E-05 | 0.001591 |
| ENSG00000143786 | CNIH3 | 787.9272 | -0.72989 | 2.68E-05 | 0.001761 |
| ENSG00000141655 | TNFRSF11A | 34.7183 | 0.802025 | 3.05E-05 | 0.001994 |
| ENSG00000123200 | ZC3H13 | 4078.413 | -0.35917 | 3.11E-05 | 0.002022 |
| ENSG00000150556 | LYPD6B | 16.18693 | 0.740846 | 3.17E-05 | 0.002052 |
| ENSG00000188549 | C15orf52 | 73.11012 | 0.716269 | 3.30E-05 | 0.002128 |
| ENSG00000144749 | LRIG1 | 763.2591 | -0.53071 | 3.31E-05 | 0.002128 |
| ENSG00000118762 | PKD2 | 661.7218 | 0.562179 | 3.35E-05 | 0.002145 |
| ENSG00000126262 | FFAR2 | 307.8976 | -0.73405 | 3.41E-05 | 0.002174 |
| ENSG00000177614 | PGBD5 | 376.6934 | -0.54271 | 3.52E-05 | 0.002237 |
| ENSG00000078269 | SYNJ2 | 2353.419 | 0.777107 | 4.05E-05 | 0.002561 |
| ENSG00000116990 | MYCL | 92.49975 | -0.80034 | 4.11E-05 | 0.002586 |
| ENSG00000026103 | FAS | 71.37475 | 0.749916 | 4.19E-05 | 0.002625 |

| | | | | | |
|---|---|---|---|---|---|
| ENSG00000116016 | EPAS1 | 149.4652 | 0.648609 | 4.22E-05 | 0.002638 |
| ENSG00000135824 | RGS8 | 58.08433 | -0.73213 | 4.43E-05 | 0.002755 |
| ENSG00000004809 | SLC22A16 | 116.4075 | 0.708129 | 4.82E-05 | 0.002986 |
| ENSG00000170791 | CHCHD7 | 227.3156 | 0.694482 | 4.85E-05 | 0.002994 |
| ENSG00000196712 | NF1 | 2253.456 | 0.364168 | 5.02E-05 | 0.003086 |
| ENSG00000172197 | MBOAT1 | 222.2396 | -0.53683 | 5.20E-05 | 0.003185 |
| ENSG00000100644 | HIF1A | 2538.419 | 0.371309 | 5.65E-05 | 0.003448 |
| ENSG00000186832 | KRT16 | 6.645537 | 0.632169 | 6.08E-05 | 0.003695 |
| ENSG00000233680 | HNRNPA1P27 | 21.0097 | -0.7549 | 6.20E-05 | 0.003754 |
| ENSG00000119943 | PYROXD2 | 285.8461 | 0.582667 | 6.54E-05 | 0.003944 |
| ENSG00000158683 | PKD1L1 | 158.7098 | 0.763563 | 6.64E-05 | 0.003988 |
| ENSG00000186628 | FSD2 | 60.65878 | -0.70966 | 6.76E-05 | 0.004043 |
| ENSG00000140948 | ZCCHC14 | 2682.788 | 0.552817 | 6.80E-05 | 0.004053 |
| ENSG00000141540 | TTYH2 | 119.5425 | 0.651297 | 6.96E-05 | 0.004129 |
| ENSG00000163380 | LMOD3 | 10.70845 | 0.697408 | 7.00E-05 | 0.004141 |
| ENSG00000164506 | STXBP5 | 2501.576 | 0.502685 | 7.24E-05 | 0.004265 |
| ENSG00000072864 | NDE1 | 486.8586 | -0.44831 | 7.33E-05 | 0.004301 |
| ENSG00000152760 | TCTEX1D1 | 751.9751 | -0.46748 | 7.44E-05 | 0.004317 |
| ENSG00000163704 | PRRT3 | 182.4339 | 0.589889 | 7.42E-05 | 0.004317 |
| ENSG00000197471 | SPN | 4444.412 | 0.551504 | 7.42E-05 | 0.004317 |
| ENSG00000151012 | SLC7A11 | 617.4692 | 0.648736 | 8.00E-05 | 0.004624 |
| ENSG00000233621 | LINC01137 | 200.1323 | 0.605342 | 8.07E-05 | 0.00465 |
| ENSG00000189067 | LITAF | 1866.78 | 0.44916 | 8.44E-05 | 0.004846 |
| ENSG00000244405 | ETV5 | 885.423 | -0.42684 | 8.48E-05 | 0.00485 |
| ENSG00000165474 | GJB2 | 21.27204 | 0.713091 | 8.77E-05 | 0.004998 |
| ENSG00000118503 | TNFAIP3 | 935.5209 | -0.61355 | 9.19E-05 | 0.005215 |
| ENSG00000162692 | VCAM1 | 61.62872 | 0.736479 | 9.73E-05 | 0.005504 |
| ENSG00000163219 | ARHGAP25 | 1124.558 | 0.597343 | 9.91E-05 | 0.005584 |
| ENSG00000171115 | GIMAP8 | 212.8021 | -0.673 | 0.0001 | 0.005621 |
| ENSG00000064703 | DDX20 | 589.689 | 0.376355 | 0.000103 | 0.005764 |
| ENSG00000173930 | SLCO4C1 | 61.53298 | 0.757279 | 0.000103 | 0.005764 |
| ENSG00000174130 | TLR6 | 740.2438 | -0.53392 | 0.000104 | 0.005771 |
| ENSG00000163110 | PDLIM5 | 1033.309 | 0.413778 | 0.000105 | 0.005813 |
| ENSG00000122877 | EGR2 | 1444.219 | 0.430347 | 0.000109 | 0.005991 |
| ENSG00000134480 | CCNH | 368.6411 | 0.510622 | 0.00011 | 0.006028 |
| ENSG00000166128 | RAB8B | 415.0182 | -0.48928 | 0.000113 | 0.006191 |
| ENSG00000236345 | - | 143.5093 | -0.55894 | 0.000117 | 0.006373 |
| ENSG00000161091 | MFSD12 | 4000.46 | 0.418901 | 0.000118 | 0.00641 |
| ENSG00000143924 | EML4 | 1470.002 | 0.456331 | 0.000123 | 0.006658 |
| ENSG00000118513 | MYB | 92.86539 | -0.68727 | 0.000124 | 0.00669 |
| ENSG00000157216 | SSBP3 | 1810.825 | -0.48596 | 0.000125 | 0.006734 |
| ENSG00000168386 | FILIP1L | 640.0254 | -0.53044 | 0.000126 | 0.006752 |

| | | | | | |
|---|---|---|---|---|---|
| ENSG00000132334 | PTPRE | 1258.21 | 0.682083 | 0.000132 | 0.007045 |
| ENSG00000237945 | LINC00649 | 550.8595 | 0.57387 | 0.000134 | 0.007127 |
| ENSG00000149177 | PTPRJ | 4010.972 | -0.47768 | 0.000138 | 0.007342 |
| ENSG00000073008 | PVR | 1465.018 | 0.693404 | 0.000141 | 0.007467 |
| ENSG00000175538 | KCNE3 | 650.7227 | -0.5107 | 0.000148 | 0.007785 |
| ENSG00000260196 | - | 88.73219 | 0.693331 | 0.000148 | 0.007785 |
| ENSG00000162496 | DHRS3 | 178.7466 | -0.66405 | 0.000154 | 0.00805 |
| ENSG00000147166 | ITGB1BP2 | 121.7593 | 0.674401 | 0.000155 | 0.008064 |
| ENSG00000172578 | KLHL6 | 896.4336 | -0.37853 | 0.000165 | 0.0086 |
| ENSG00000115652 | UXS1 | 795.3846 | -0.3756 | 0.000166 | 0.008628 |
| ENSG00000166483 | WEE1 | 407.2798 | -0.57047 | 0.000175 | 0.00903 |
| ENSG00000259959 | - | 38.55926 | 0.731292 | 0.000177 | 0.009102 |
| ENSG00000137872 | SEMA6D | 22.35044 | -0.70113 | 0.000179 | 0.009142 |
| ENSG00000151748 | SAV1 | 1215.128 | 0.333708 | 0.000179 | 0.009142 |
| ENSG00000223749 | MIR503HG | 506.6318 | 0.706056 | 0.000178 | 0.009142 |
| ENSG00000198355 | PIM3 | 663.2431 | 0.480039 | 0.000183 | 0.009297 |
| ENSG00000171729 | TMEM51 | 131.1425 | 0.60638 | 0.00019 | 0.009637 |
| ENSG00000253522 | - | 39.75196 | -0.72641 | 0.000192 | 0.009707 |
| ENSG00000140030 | GPR65 | 862.0919 | 0.505712 | 0.000212 | 0.010684 |
| ENSG00000003137 | CYP26B1 | 171.3159 | 0.721403 | 0.000214 | 0.010758 |
| ENSG00000054967 | RELT | 838.8751 | 0.389132 | 0.000215 | 0.01077 |
| ENSG00000171621 | SPSB1 | 529.99 | 0.510602 | 0.00022 | 0.010961 |
| ENSG00000105639 | JAK3 | 461.0134 | 0.52954 | 0.000231 | 0.011459 |
| ENSG00000121895 | TMEM156 | 384.7457 | -0.56156 | 0.000231 | 0.011459 |
| ENSG00000136040 | PLXNC1 | 419.4076 | -0.51504 | 0.00024 | 0.011795 |
| ENSG00000185361 | TNFAIP8L1 | 633.0093 | -0.50331 | 0.000239 | 0.011795 |
| ENSG00000033867 | SLC4A7 | 1440.339 | 0.676474 | 0.000242 | 0.011887 |
| ENSG00000081320 | STK17B | 1617.653 | -0.47143 | 0.000256 | 0.012536 |
| ENSG00000232653 | GOLGA8N | 91.7704 | 0.623917 | 0.000259 | 0.012612 |
| ENSG00000017427 | IGF1 | 5.818151 | 0.550862 | 0.000262 | 0.012752 |
| ENSG00000111859 | NEDD9 | 279.9565 | -0.50317 | 0.000263 | 0.012752 |
| ENSG00000172331 | BPGM | 384.206 | 0.451701 | 0.000289 | 0.013974 |
| ENSG00000132819 | RBM38 | 2150.598 | -0.32344 | 0.000294 | 0.014167 |
| ENSG00000109332 | UBE2D3 | 4335.01 | 0.262045 | 0.000298 | 0.014292 |
| ENSG00000126106 | TMEM53 | 112.6795 | -0.57389 | 0.000306 | 0.014663 |
| ENSG00000170837 | GPR27 | 276.4687 | 0.536552 | 0.000311 | 0.014828 |
| ENSG00000136826 | KLF4 | 79.43513 | -0.67196 | 0.000321 | 0.0152 |
| ENSG00000165434 | PGM2L1 | 241.3009 | -0.54332 | 0.00032 | 0.0152 |
| ENSG00000197860 | SGTB | 353.117 | -0.43546 | 0.000344 | 0.01625 |
| ENSG00000109501 | WFS1 | 166.8441 | 0.611422 | 0.000347 | 0.016335 |
| ENSG00000138172 | CALHM2 | 349.4478 | -0.49589 | 0.000349 | 0.01639 |
| ENSG00000100311 | PDGFB | 206.546 | 0.670374 | 0.000369 | 0.017287 |

| | | | | | |
|---|---|---|---|---|---|
| ENSG00000229921 | KIF25-AS1 | 213.0206 | 0.646341 | 0.000377 | 0.017607 |
| ENSG00000100784 | RPS6KA5 | 124.6048 | -0.57136 | 0.000383 | 0.017834 |
| ENSG00000197147 | LRRC8B | 816.3005 | 0.56732 | 0.000407 | 0.01889 |
| ENSG00000167207 | NOD2 | 161.1588 | 0.689072 | 0.00041 | 0.018963 |
| ENSG00000111181 | SLC6A12 | 127.8217 | -0.55586 | 0.000431 | 0.019845 |
| ENSG00000168036 | CTNNB1 | 9530.626 | 0.369216 | 0.000431 | 0.019845 |
| ENSG00000204577 | LILRB3 | 17.76637 | 0.672215 | 0.000445 | 0.020402 |
| ENSG00000197506 | SLC28A3 | 41.06837 | 0.680047 | 0.000455 | 0.020812 |
| ENSG00000164691 | TAGAP | 780.4593 | 0.677828 | 0.00051 | 0.023271 |
| ENSG00000166825 | ANPEP | 13339.53 | 0.31135 | 0.00052 | 0.023662 |
| ENSG00000028277 | POU2F2 | 610.8517 | -0.4936 | 0.00053 | 0.024022 |
| ENSG00000100100 | PIK3IP1 | 415.9234 | -0.62054 | 0.000543 | 0.024388 |
| ENSG00000109089 | CDR2L | 316.8352 | 0.50859 | 0.000542 | 0.024388 |
| ENSG00000117155 | SSX2IP | 595.683 | 0.401974 | 0.00054 | 0.024388 |
| ENSG00000177189 | RPS6KA3 | 6631.778 | -0.27919 | 0.000558 | 0.024991 |
| ENSG00000173221 | GLRX | 373.674 | 0.502154 | 0.00056 | 0.025048 |
| ENSG00000163874 | ZC3H12A | 601.9757 | 0.649311 | 0.000573 | 0.025526 |
| ENSG00000163694 | RBM47 | 1037.52 | 0.451968 | 0.000583 | 0.025893 |
| ENSG00000148175 | STOM | 980.0816 | 0.309532 | 0.000611 | 0.027087 |
| ENSG00000140320 | BAHD1 | 688.6419 | 0.41415 | 0.000622 | 0.027465 |
| ENSG00000102471 | NDFIP2 | 2068.376 | 0.373772 | 0.000626 | 0.027582 |
| ENSG00000164830 | OXR1 | 525.9321 | -0.35966 | 0.000631 | 0.027737 |
| ENSG00000186810 | CXCR3 | 256.0337 | 0.428943 | 0.000636 | 0.027875 |
| ENSG00000134574 | DDB2 | 136.1752 | 0.584611 | 0.000646 | 0.028222 |
| ENSG00000152229 | PSTPIP2 | 176.1753 | 0.662806 | 0.000656 | 0.02858 |
| ENSG00000274139 | - | 7.150934 | 0.563516 | 0.000677 | 0.029432 |
| ENSG00000024422 | EHD2 | 1089.913 | 0.55483 | 0.000681 | 0.029487 |
| ENSG00000082898 | XPO1 | 3795.729 | -0.41555 | 0.000692 | 0.029918 |
| ENSG00000198488 | B3GNT6 | 59.94821 | 0.660347 | 0.000697 | 0.030045 |
| ENSG00000185070 | FLRT2 | 168.9563 | -0.56968 | 0.000702 | 0.030168 |
| ENSG00000090659 | CD209 | 50.31922 | 0.646622 | 0.000713 | 0.030465 |
| ENSG00000173404 | INSM1 | 10.26559 | 0.583165 | 0.000713 | 0.030465 |
| ENSG00000213024 | NUP62 | 3151.108 | 0.37533 | 0.000735 | 0.031336 |
| ENSG00000147526 | TACC1 | 1649.209 | -0.30423 | 0.000773 | 0.03286 |
| ENSG00000124225 | PMEPA1 | 401.1782 | -0.51474 | 0.000778 | 0.032973 |
| ENSG00000138434 | SSFA2 | 2101.322 | -0.34713 | 0.000787 | 0.033243 |
| ENSG00000109062 | SLC9A3R1 | 322.1701 | 0.456861 | 0.000798 | 0.033655 |
| ENSG00000113645 | WWC1 | 260.7832 | -0.57251 | 0.000801 | 0.033657 |
| ENSG00000181467 | RAP2B | 1796.046 | -0.35067 | 0.000819 | 0.034326 |
| ENSG00000082397 | EPB41L3 | 976.2207 | 0.544671 | 0.000829 | 0.034447 |
| ENSG00000124813 | RUNX2 | 138.7394 | 0.549349 | 0.000831 | 0.034447 |
| ENSG00000164823 | OSGIN2 | 586.1669 | 0.333512 | 0.000828 | 0.034447 |

| | | | | | |
|---|---|---|---|---|---|
| ENSG00000187796 | CARD9 | 488.2089 | 0.569715 | 0.000827 | 0.034447 |
| ENSG00000124145 | SDC4 | 830.9358 | 0.445775 | 0.000848 | 0.035084 |
| ENSG00000095015 | MAP3K1 | 994.0146 | 0.534622 | 0.00086 | 0.035398 |
| ENSG00000203706 | SERTAD4-AS1 | 5.773145 | 0.500518 | 0.00086 | 0.035398 |
| ENSG00000198668 | CALM1 | 5173.718 | 0.297747 | 0.000906 | 0.0372 |
| ENSG00000113657 | DPYSL3 | 578.9211 | -0.47396 | 0.000923 | 0.037773 |
| ENSG00000122574 | WIPF3 | 1022.519 | -0.54647 | 0.000933 | 0.037996 |
| ENSG00000157404 | KIT | 37.85666 | -0.64216 | 0.000932 | 0.037996 |
| ENSG00000151474 | FRMD4A | 637.5974 | 0.642617 | 0.00094 | 0.038189 |
| ENSG00000214900 | LINC01588 | 266.5862 | 0.606371 | 0.000997 | 0.040404 |
| ENSG00000006576 | PHTF2 | 759.4396 | 0.349204 | 0.001005 | 0.040503 |
| ENSG00000166317 | SYNPO2L | 456.4873 | 0.584334 | 0.001003 | 0.040503 |
| ENSG00000107554 | DNMBP | 739.5847 | 0.518318 | 0.001044 | 0.041969 |
| ENSG00000185477 | GPRIN3 | 80.07894 | -0.63322 | 0.00105 | 0.042081 |
| ENSG00000099282 | TSPAN15 | 822.4829 | 0.352154 | 0.001058 | 0.042282 |
| ENSG00000123405 | NFE2 | 73.98367 | 0.552844 | 0.00106 | 0.042282 |
| ENSG00000167703 | SLC43A2 | 925.063 | -0.46719 | 0.001097 | 0.043625 |
| ENSG00000185989 | RASA3 | 4702.061 | -0.25208 | 0.001104 | 0.043794 |
| ENSG00000102760 | RGCC | 534.087 | -0.5474 | 0.001114 | 0.043952 |
| ENSG00000135090 | TAOK3 | 1722.974 | -0.2696 | 0.001116 | 0.043952 |
| ENSG00000155011 | DKK2 | 19.55881 | 0.615848 | 0.001114 | 0.043952 |
| ENSG00000153214 | TMEM87B | 1628.528 | -0.27783 | 0.001133 | 0.044499 |
| ENSG00000198825 | INPP5F | 111.1762 | -0.53893 | 0.001152 | 0.045125 |
| ENSG00000062716 | VMP1 | 1643.885 | 0.500977 | 0.001181 | 0.046105 |
| ENSG00000122223 | CD244 | 237.8641 | -0.52032 | 0.001183 | 0.046105 |
| ENSG00000170425 | ADORA2B | 28.63241 | -0.62451 | 0.001216 | 0.047286 |
| ENSG00000137312 | FLOT1 | 1776.26 | 0.293621 | 0.001219 | 0.047286 |
| ENSG00000082458 | DLG3 | 356.4044 | -0.53102 | 0.001263 | 0.048855 |
| ENSG00000114735 | HEMK1 | 224.2836 | 0.523387 | 0.001352 | 0.052197 |
| ENSG00000134250 | NOTCH2 | 2943.327 | -0.3293 | 0.001362 | 0.052376 |
| ENSG00000272767 | JMJD1C-AS1 | 170.5584 | 0.579415 | 0.001364 | 0.052376 |
| ENSG00000022567 | SLC45A4 | 385.8895 | 0.526671 | 0.001374 | 0.052621 |
| ENSG00000113369 | ARRDC3 | 675.0187 | -0.55364 | 0.00142 | 0.054278 |
| ENSG00000125772 | GPCPD1 | 691.748 | 0.575773 | 0.001432 | 0.054585 |
| ENSG00000157873 | TNFRSF14 | 378.4321 | 0.39287 | 0.001445 | 0.054955 |
| ENSG00000135932 | CAB39 | 3589.933 | -0.40199 | 0.001457 | 0.055269 |
| ENSG00000050405 | LIMA1 | 404.2639 | 0.519834 | 0.001497 | 0.056641 |
| ENSG00000125037 | EMC3 | 910.5567 | 0.331239 | 0.001516 | 0.057237 |
| ENSG00000177606 | JUN | 540.7926 | 0.552405 | 0.001582 | 0.059583 |
| ENSG00000134061 | CD180 | 318.2454 | 0.498225 | 0.001611 | 0.060365 |
| ENSG00000134324 | LPIN1 | 803.552 | -0.41486 | 0.001609 | 0.060365 |
| ENSG00000155760 | FZD7 | 605.5577 | -0.5588 | 0.001631 | 0.060996 |

| | | | | | |
|---|---|---|---|---|---|
| ENSG00000276043 | UHRF1 | 789.3237 | -0.32403 | 0.001642 | 0.061237 |
| ENSG00000168310 | IRF2 | 616.919 | -0.33407 | 0.001652 | 0.061465 |
| ENSG00000023171 | GRAMD1B | 366.1566 | -0.48397 | 0.001676 | 0.062228 |
| ENSG00000282608 | ADORA3 | 60.49573 | 0.598584 | 0.001683 | 0.062319 |
| ENSG00000166963 | MAP1A | 262.8713 | 0.542991 | 0.001727 | 0.06382 |
| ENSG00000023445 | BIRC3 | 509.2937 | -0.42113 | 0.001736 | 0.06383 |
| ENSG00000121743 | GJA3 | 107.7442 | -0.49022 | 0.001735 | 0.06383 |
| ENSG00000223573 | TINCR | 30.1149 | -0.60696 | 0.001749 | 0.064156 |
| ENSG00000088305 | DNMT3B | 399.6299 | -0.41268 | 0.001774 | 0.064783 |
| ENSG00000168906 | MAT2A | 4558.6 | 0.514796 | 0.001774 | 0.064783 |
| ENSG00000172575 | RASGRP1 | 25.49328 | 0.580151 | 0.001783 | 0.06496 |
| ENSG00000206560 | ANKRD28 | 2353.872 | -0.29653 | 0.001829 | 0.066456 |
| ENSG00000118242 | MREG | 153.7615 | 0.50004 | 0.001848 | 0.066841 |
| ENSG00000183160 | TMEM119 | 414.8108 | -0.46715 | 0.001844 | 0.066841 |
| ENSG00000169047 | IRS1 | 108.1308 | -0.55928 | 0.001853 | 0.066886 |
| ENSG00000135077 | HAVCR2 | 998.4496 | -0.53389 | 0.001864 | 0.067111 |
| ENSG00000165029 | ABCA1 | 329.8107 | -0.6056 | 0.001886 | 0.067758 |
| ENSG00000184988 | TMEM106A | 479.1252 | 0.411385 | 0.001892 | 0.067804 |
| ENSG00000126777 | KTN1 | 4030.624 | 0.291525 | 0.001904 | 0.068063 |
| ENSG00000175155 | YPEL2 | 406.3008 | -0.34114 | 0.001909 | 0.06811 |
| ENSG00000107485 | GATA3 | 20.79315 | -0.59483 | 0.001929 | 0.068653 |
| ENSG00000112182 | BACH2 | 67.76601 | -0.60441 | 0.001942 | 0.068977 |
| ENSG00000163683 | SMIM14 | 533.213 | -0.49081 | 0.001963 | 0.069551 |
| ENSG00000103056 | SMPD3 | 8.414308 | 0.505289 | 0.001973 | 0.069728 |
| ENSG00000160219 | GAB3 | 380.0924 | 0.364675 | 0.002008 | 0.070838 |
| ENSG00000128268 | MGAT3 | 263.614 | -0.46433 | 0.002027 | 0.071214 |
| ENSG00000153976 | HS3ST3A1 | 81.20444 | 0.601684 | 0.002033 | 0.071214 |
| ENSG00000224189 | HAGLR | 48.65755 | -0.59767 | 0.002032 | 0.071214 |
| ENSG00000173237 | C11orf86 | 56.8983 | -0.59896 | 0.002067 | 0.072257 |
| ENSG00000158715 | SLC45A3 | 1089.822 | 0.410543 | 0.002072 | 0.072273 |
| ENSG00000132623 | ANKEF1 | 66.1368 | 0.597909 | 0.002181 | 0.075898 |
| ENSG00000185947 | ZNF267 | 638.2464 | -0.32656 | 0.002204 | 0.076522 |
| ENSG00000131242 | RAB11FIP4 | 2112.781 | 0.463833 | 0.002241 | 0.077626 |
| ENSG00000169122 | FAM110B | 46.87798 | 0.594145 | 0.002262 | 0.078201 |
| ENSG00000180739 | S1PR5 | 91.73625 | 0.595209 | 0.002285 | 0.078819 |
| ENSG00000184588 | PDE4B | 101.2497 | -0.57726 | 0.00229 | 0.078819 |
| ENSG00000198719 | DLL1 | 485.9072 | -0.51542 | 0.002317 | 0.079555 |
| ENSG00000047346 | FAM214A | 224.4855 | -0.40028 | 0.0024 | 0.082218 |
| ENSG00000118515 | SGK1 | 391.004 | -0.36611 | 0.002437 | 0.083311 |
| ENSG00000159388 | BTG2 | 3478.304 | -0.24644 | 0.002464 | 0.083999 |
| ENSG00000170412 | GPRC5C | 782.6974 | 0.468299 | 0.002468 | 0.083999 |
| ENSG00000188827 | SLX4 | 279.0527 | 0.466754 | 0.002525 | 0.085751 |

| | | | | | |
|---|---|---|---|---|---|
| ENSG00000110047 | EHD1 | 1564.125 | -0.36025 | 0.002607 | 0.087985 |
| ENSG00000152076 | CCDC74B | 330.1354 | -0.35343 | 0.002608 | 0.087985 |
| ENSG00000197417 | SHPK | 46.43773 | 0.559964 | 0.002599 | 0.087985 |
| ENSG00000174945 | AMZ1 | 194.0296 | -0.50936 | 0.002653 | 0.089316 |
| ENSG00000129538 | RNASE1 | 83.84518 | 0.512032 | 0.002686 | 0.090051 |
| ENSG00000134602 | STK26 | 994.0729 | 0.437815 | 0.002685 | 0.090051 |
| ENSG00000112837 | TBX18 | 655.9278 | -0.30411 | 0.002698 | 0.090261 |
| ENSG00000149289 | ZC3H12C | 1711.947 | -0.44299 | 0.002736 | 0.091334 |
| ENSG00000135549 | PKIB | 1392.991 | 0.460056 | 0.002801 | 0.093082 |
| ENSG00000173852 | DPY19L1 | 1673.504 | 0.321274 | 0.002796 | 0.093082 |
| ENSG00000165527 | ARF6 | 3937.292 | 0.398772 | 0.002842 | 0.094241 |
| ENSG00000111912 | NCOA7 | 614.2882 | -0.5064 | 0.002932 | 0.097019 |
| ENSG00000166881 | NEMP1 | 773.6189 | -0.35578 | 0.002975 | 0.098241 |
| ENSG00000141456 | PELP1 | 690.1055 | 0.322613 | 0.003024 | 0.099012 |
| ENSG00000154822 | PLCL2 | 395.2802 | -0.4796 | 0.003022 | 0.099012 |
| ENSG00000176749 | CDK5R1 | 123.1312 | -0.53233 | 0.00302 | 0.099012 |
| ENSG00000231690 | LINC00574 | 7.011699 | 0.478149 | 0.003017 | 0.099012 |
| ENSG00000124491 | F13A1 | 733.8706 | 0.504682 | 0.003059 | 0.099965 |

# APPENDIX C

Table 6 The differential expressed genes comparing between unstimulation and IL-4 stimulated NIC1 overexpressing THP-1

| GENES | Symbol | Base mean | log2(FC) | P-value | P-adj |
|---|---|---|---|---|---|
| ENSG00000114737 | CISH | 744.3618 | 4.587051 | 8.07E-249 | 1.28E-244 |
| ENSG00000185338 | SOCS1 | 343.9671 | 3.729855 | 5.56E-121 | 4.39E-117 |
| ENSG00000106266 | SNX8 | 1870.911 | 2.126072 | 1.22E-109 | 6.43E-106 |
| ENSG00000103044 | HAS3 | 662.0742 | 2.895347 | 3.59E-84 | 1.42E-80 |
| ENSG00000166224 | SGPL1 | 2972.551 | 1.705733 | 6.83E-83 | 2.16E-79 |
| ENSG00000100592 | DAAM1 | 690.4554 | 2.025904 | 5.96E-78 | 1.57E-74 |
| ENSG00000198743 | SLC5A3 | 2715.817 | 2.080523 | 1.60E-64 | 3.62E-61 |
| ENSG00000138821 | SLC39A8 | 848.3681 | 1.663623 | 1.41E-53 | 2.79E-50 |
| ENSG00000127863 | TNFRSF19 | 224.3326 | 2.665763 | 1.37E-51 | 2.40E-48 |
| ENSG00000111729 | CLEC4A | 173.8792 | 2.686079 | 5.41E-51 | 8.55E-48 |
| ENSG00000171992 | SYNPO | 311.4789 | 1.940352 | 1.13E-46 | 1.62E-43 |
| ENSG00000040531 | CTNS | 761.0049 | 1.597723 | 5.39E-45 | 7.11E-42 |
| ENSG00000169136 | ATF5 | 3006.528 | 1.326569 | 7.78E-45 | 9.46E-42 |
| ENSG00000138134 | STAMBPL1 | 434.375 | 2.178214 | 2.04E-44 | 2.31E-41 |
| ENSG00000143226 | FCGR2A | 993.8921 | 1.995083 | 2.89E-42 | 3.05E-39 |
| ENSG00000168748 | CA7 | 315.0486 | 2.375322 | 9.13E-41 | 9.03E-38 |
| ENSG00000173198 | CYSLTR1 | 3079.118 | 1.254639 | 1.37E-40 | 1.27E-37 |
| ENSG00000074416 | MGLL | 1743.621 | 1.619969 | 1.36E-39 | 1.20E-36 |
| ENSG00000111424 | VDR | 891.3547 | 1.229986 | 7.16E-37 | 5.96E-34 |
| ENSG00000176597 | B3GNT5 | 2421.564 | 1.834511 | 6.41E-36 | 5.07E-33 |
| ENSG00000116514 | RNF19B | 2812.243 | 1.603578 | 7.88E-36 | 5.94E-33 |
| ENSG00000141506 | PIK3R5 | 1281.52 | 1.209055 | 3.83E-35 | 2.75E-32 |
| ENSG00000164442 | CITED2 | 10811.53 | 1.317757 | 3.51E-34 | 2.41E-31 |
| ENSG00000167642 | SPINT2 | 2787.966 | 1.418671 | 1.19E-32 | 7.83E-30 |
| ENSG00000162367 | TAL1 | 118.4882 | 1.914834 | 2.04E-32 | 1.29E-29 |
| ENSG00000142512 | SIGLEC10 | 216.8862 | 1.96488 | 8.83E-32 | 5.37E-29 |
| ENSG00000205730 | ITPRIPL2 | 2998.677 | 1.15761 | 4.15E-31 | 2.43E-28 |
| ENSG00000080546 | SESN1 | 1296.371 | -1.39194 | 4.43E-31 | 2.50E-28 |
| ENSG00000178175 | ZNF366 | 655.5775 | 1.424275 | 5.72E-30 | 3.12E-27 |
| ENSG00000107338 | SHB | 114.3856 | 1.922728 | 2.07E-29 | 1.09E-26 |
| ENSG00000161905 | ALOX15 | 82.16533 | 2.046652 | 5.60E-29 | 2.86E-26 |
| ENSG00000134243 | SORT1 | 3240.986 | 0.973206 | 8.35E-29 | 4.12E-26 |
| ENSG00000156127 | BATF | 261.2199 | 1.577761 | 2.90E-28 | 1.39E-25 |
| ENSG00000167641 | PPP1R14A | 44.51857 | 2.048155 | 1.48E-27 | 6.86E-25 |
| ENSG00000112773 | FAM46A | 1451.947 | -1.37524 | 1.91E-27 | 8.61E-25 |
| ENSG00000206073 | SERPINB4 | 40.7274 | 2.039863 | 2.26E-27 | 9.91E-25 |
| ENSG00000138135 | CH25H | 77.25351 | 1.943708 | 4.10E-27 | 1.75E-24 |

| | | | | | |
|---|---|---|---|---|---|
| ENSG00000108262 | GIT1 | 2738.506 | 1.039824 | 6.46E-27 | 2.69E-24 |
| ENSG00000113749 | HRH2 | 838.385 | 1.289823 | 7.38E-27 | 2.99E-24 |
| ENSG00000124762 | CDKN1A | 9075.77 | 1.0489 | 8.52E-27 | 3.37E-24 |
| ENSG00000115159 | GPD2 | 700.6871 | 1.07912 | 1.27E-26 | 4.89E-24 |
| ENSG00000029153 | ARNTL2 | 817.423 | 0.978236 | 2.17E-25 | 8.16E-23 |
| ENSG00000099337 | KCNK6 | 1051.951 | 1.169467 | 2.47E-25 | 9.10E-23 |
| ENSG00000052126 | PLEKHA5 | 576.6014 | 1.102839 | 1.24E-24 | 4.46E-22 |
| ENSG00000105219 | CNTD2 | 65.62054 | 1.905318 | 2.92E-24 | 1.03E-21 |
| ENSG00000168334 | XIRP1 | 4681.972 | 1.07459 | 3.97E-24 | 1.37E-21 |
| ENSG00000152217 | SETBP1 | 108.5711 | 1.785389 | 1.33E-23 | 4.46E-21 |
| ENSG00000198829 | SUCNR1 | 7106.157 | 0.988551 | 1.45E-23 | 4.77E-21 |
| ENSG00000170448 | NFXL1 | 309.2501 | 1.274254 | 8.80E-23 | 2.84E-20 |
| ENSG00000243927 | MRPS6 | 1054.149 | 1.286631 | 2.60E-22 | 8.22E-20 |
| ENSG00000139269 | INHBE | 243.4534 | 1.73033 | 5.71E-22 | 1.77E-19 |
| ENSG00000136689 | IL1RN | 5860.131 | 1.274021 | 6.26E-22 | 1.90E-19 |
| ENSG00000104267 | CA2 | 1244.41 | -0.97681 | 1.23E-21 | 3.66E-19 |
| ENSG00000171488 | LRRC8C | 4014.168 | 1.024056 | 1.75E-21 | 5.13E-19 |
| ENSG00000261269 | - | 480.0056 | 1.316612 | 3.76E-21 | 1.08E-18 |
| ENSG00000166016 | ABTB2 | 215.5369 | 1.527618 | 7.92E-21 | 2.24E-18 |
| ENSG00000188211 | NCR3LG1 | 421.4234 | 1.190657 | 1.26E-20 | 3.50E-18 |
| ENSG00000143374 | TARS2 | 1191.11 | 0.987597 | 2.09E-19 | 5.69E-17 |
| ENSG00000170113 | NIPA1 | 1291.889 | 1.090909 | 2.34E-19 | 6.27E-17 |
| ENSG00000152766 | ANKRD22 | 116.8626 | 1.666526 | 4.65E-19 | 1.22E-16 |
| ENSG00000163293 | NIPAL1 | 51.96699 | 1.645137 | 9.06E-19 | 2.35E-16 |
| ENSG00000049759 | NEDD4L | 110.0118 | 1.577667 | 9.60E-19 | 2.45E-16 |
| ENSG00000139668 | WDFY2 | 1494.063 | 0.770496 | 1.06E-18 | 2.67E-16 |
| ENSG00000162772 | ATF3 | 1409.39 | 0.940435 | 1.15E-18 | 2.83E-16 |
| ENSG00000115594 | IL1R1 | 171.7862 | 1.507884 | 1.86E-18 | 4.53E-16 |
| ENSG00000240583 | AQP1 | 206.1892 | 1.354626 | 6.04E-18 | 1.45E-15 |
| ENSG00000122986 | HVCN1 | 1437.191 | 0.808836 | 7.06E-18 | 1.67E-15 |
| ENSG00000067082 | KLF6 | 978.2754 | -0.79584 | 8.49E-18 | 1.97E-15 |
| ENSG00000115604 | IL18R1 | 1362.189 | 1.00706 | 2.68E-17 | 6.14E-15 |
| ENSG00000100311 | PDGFB | 482.8978 | 1.48732 | 3.90E-17 | 8.81E-15 |
| ENSG00000248187 | - | 277.2794 | 1.468559 | 5.40E-17 | 1.20E-14 |
| ENSG00000163590 | PPM1L | 970.9777 | 0.995755 | 6.01E-17 | 1.32E-14 |
| ENSG00000141458 | NPC1 | 1402.238 | 1.044574 | 6.52E-17 | 1.41E-14 |
| ENSG00000077684 | JADE1 | 656.7262 | 1.110816 | 9.36E-17 | 2.00E-14 |
| ENSG00000126561 | STAT5A | 1531.347 | 0.824373 | 1.69E-16 | 3.56E-14 |
| ENSG00000245848 | CEBPA | 3430.825 | 1.039913 | 1.72E-16 | 3.58E-14 |
| ENSG00000111647 | UHRF1BP1L | 844.2837 | 0.815462 | 3.08E-16 | 6.32E-14 |
| ENSG00000155846 | PPARGC1B | 212.0901 | 1.212112 | 3.21E-16 | 6.50E-14 |
| ENSG00000103257 | SLC7A5 | 6635.284 | 0.815582 | 4.49E-16 | 8.99E-14 |

| | | | | | |
|---|---|---|---|---|---|
| ENSG00000164506 | STXBP5 | 2256.938 | 0.655133 | 5.61E-16 | 1.11E-13 |
| ENSG00000073921 | PICALM | 5790.111 | 0.740311 | 2.25E-15 | 4.38E-13 |
| ENSG00000169508 | GPR183 | 2438.908 | 0.769744 | 3.32E-15 | 6.41E-13 |
| ENSG00000132170 | PPARG | 306.3725 | 1.250871 | 5.16E-15 | 9.83E-13 |
| ENSG00000133789 | SWAP70 | 1022.294 | -0.73845 | 5.67E-15 | 1.07E-12 |
| ENSG00000235750 | KIAA0040 | 337.4199 | 0.966746 | 6.56E-15 | 1.22E-12 |
| ENSG00000185262 | UBALD2 | 1910.286 | 0.671147 | 1.28E-14 | 2.36E-12 |
| ENSG00000003989 | SLC7A2 | 333.2896 | 1.105921 | 2.57E-14 | 4.68E-12 |
| ENSG00000125772 | GPCPD1 | 646.2297 | 0.956149 | 5.49E-14 | 9.87E-12 |
| ENSG00000101236 | RNF24 | 1017.407 | 0.961675 | 8.30E-14 | 1.47E-11 |
| ENSG00000143507 | DUSP10 | 1033.972 | -0.82954 | 1.12E-13 | 1.97E-11 |
| ENSG00000001084 | GCLC | 2600.75 | -1.08975 | 1.25E-13 | 2.16E-11 |
| ENSG00000164951 | PDP1 | 125.3099 | -1.15089 | 1.39E-13 | 2.40E-11 |
| ENSG00000151012 | SLC7A11 | 840.5974 | 0.87073 | 1.88E-13 | 3.20E-11 |
| ENSG00000110841 | PPFIBP1 | 2054.857 | 1.165234 | 2.88E-13 | 4.84E-11 |
| ENSG00000140968 | IRF8 | 297.5551 | 1.214578 | 3.05E-13 | 5.08E-11 |
| ENSG00000150347 | ARID5B | 140.5139 | -1.1364 | 4.98E-13 | 8.21E-11 |
| ENSG00000112195 | TREML2 | 554.6687 | 1.080724 | 5.10E-13 | 8.29E-11 |
| ENSG00000157927 | RADIL | 94.56231 | 1.230467 | 5.14E-13 | 8.29E-11 |
| ENSG00000131759 | RARA | 646.6284 | 0.72167 | 6.09E-13 | 9.63E-11 |
| ENSG00000165757 | KIAA1462 | 51.60718 | 1.329097 | 6.08E-13 | 9.63E-11 |
| ENSG00000155099 | TMEM55A | 327.0949 | 1.043914 | 6.18E-13 | 9.68E-11 |
| ENSG00000198959 | TGM2 | 8775.94 | 1.074301 | 6.85E-13 | 1.06E-10 |
| ENSG00000188001 | TPRG1 | 170.6834 | 1.144622 | 7.40E-13 | 1.14E-10 |
| ENSG00000129625 | REEP5 | 2414.011 | 0.700618 | 7.93E-13 | 1.21E-10 |
| ENSG00000038427 | VCAN | 53.41728 | 1.320301 | 1.07E-12 | 1.61E-10 |
| ENSG00000100030 | MAPK1 | 3228.116 | 0.585196 | 1.67E-12 | 2.49E-10 |
| ENSG00000198488 | B3GNT6 | 63.54097 | 1.273792 | 2.10E-12 | 3.11E-10 |
| ENSG00000109861 | CTSC | 4888.005 | 0.696237 | 2.33E-12 | 3.41E-10 |
| ENSG00000142920 | AZIN2 | 442.4391 | 1.10656 | 2.45E-12 | 3.56E-10 |
| ENSG00000164849 | GPR146 | 41.36263 | 1.307869 | 3.12E-12 | 4.48E-10 |
| ENSG00000169252 | ADRB2 | 130.42 | -1.11454 | 3.14E-12 | 4.48E-10 |
| ENSG00000143786 | CNIH3 | 857.8351 | -0.87162 | 3.52E-12 | 4.97E-10 |
| ENSG00000186806 | VSIG10L | 184.8672 | 1.090524 | 3.59E-12 | 5.03E-10 |
| ENSG00000124151 | NCOA3 | 2278.444 | 0.867817 | 4.16E-12 | 5.76E-10 |
| ENSG00000072694 | FCGR2B | 61.87979 | 1.261901 | 6.22E-12 | 8.55E-10 |
| ENSG00000169255 | B3GALNT1 | 276.6547 | 0.914144 | 6.45E-12 | 8.79E-10 |
| ENSG00000124491 | F13A1 | 656.9206 | 0.907387 | 9.75E-12 | 1.32E-09 |
| ENSG00000178199 | ZC3H12D | 371.6795 | 0.862849 | 1.23E-11 | 1.64E-09 |
| ENSG00000197646 | PDCD1LG2 | 30.58868 | 1.251727 | 1.46E-11 | 1.94E-09 |
| ENSG00000151474 | FRMD4A | 514.7618 | 1.102767 | 1.54E-11 | 2.03E-09 |
| ENSG00000275342 | - | 1482.421 | 0.841359 | 1.73E-11 | 2.26E-09 |

| | | | | | |
|---|---|---|---|---|---|
| ENSG00000033867 | SLC4A7 | 1495.405 | 0.928945 | 2.56E-11 | 3.32E-09 |
| ENSG00000171608 | PIK3CD | 1731.85 | 0.948972 | 2.72E-11 | 3.49E-09 |
| ENSG00000110237 | ARHGEF17 | 550.0125 | 1.117081 | 3.06E-11 | 3.91E-09 |
| ENSG00000250959 | GLUD1P3 | 220.0626 | 1.108585 | 3.34E-11 | 4.22E-09 |
| ENSG00000157933 | SKI | 1173.754 | 0.694999 | 3.88E-11 | 4.87E-09 |
| ENSG00000197852 | FAM212B | 218.1205 | 0.869951 | 4.42E-11 | 5.50E-09 |
| ENSG00000104951 | IL4I1 | 6363.761 | 0.830566 | 9.57E-11 | 1.18E-08 |
| ENSG00000171115 | GIMAP8 | 168.7843 | -0.94102 | 1.07E-10 | 1.31E-08 |
| ENSG00000073008 | PVR | 1913.913 | 0.974529 | 1.10E-10 | 1.34E-08 |
| ENSG00000175874 | CREG2 | 38.23428 | 1.20904 | 1.12E-10 | 1.35E-08 |
| ENSG00000174485 | DENND4A | 561.8347 | 0.894511 | 1.30E-10 | 1.55E-08 |
| ENSG00000088992 | TESC | 266.43 | 0.857864 | 1.32E-10 | 1.57E-08 |
| ENSG00000150764 | DIXDC1 | 2593.466 | 0.547909 | 2.71E-10 | 3.20E-08 |
| ENSG00000110324 | IL10RA | 1452.491 | 1.03815 | 3.43E-10 | 4.01E-08 |
| ENSG00000095951 | HIVEP1 | 1609.255 | -0.73423 | 4.68E-10 | 5.44E-08 |
| ENSG00000107554 | DNMBP | 727.7904 | 0.709574 | 5.94E-10 | 6.86E-08 |
| ENSG00000180739 | S1PR5 | 131.5626 | 1.107708 | 6.16E-10 | 7.06E-08 |
| ENSG00000117114 | ADGRL2 | 3763.079 | 0.505209 | 6.54E-10 | 7.44E-08 |
| ENSG00000147872 | PLIN2 | 681.052 | -0.81338 | 6.73E-10 | 7.61E-08 |
| ENSG00000131242 | RAB11FIP4 | 2235.101 | 0.596006 | 7.58E-10 | 8.50E-08 |
| ENSG00000115602 | IL1RL1 | 100.01 | 0.99155 | 7.73E-10 | 8.61E-08 |
| ENSG00000113645 | WWC1 | 339.5419 | -0.72153 | 9.67E-10 | 1.07E-07 |
| ENSG00000118503 | TNFAIP3 | 1097.543 | -0.62919 | 1.06E-09 | 1.17E-07 |
| ENSG00000147036 | LANCL3 | 210.8709 | -1.00953 | 1.23E-09 | 1.34E-07 |
| ENSG00000259330 | INAFM2 | 196.6425 | 0.909977 | 1.40E-09 | 1.51E-07 |
| ENSG00000123685 | BATF3 | 45.42124 | 1.131104 | 1.42E-09 | 1.52E-07 |
| ENSG00000154447 | SH3RF1 | 356.4745 | -0.90903 | 1.53E-09 | 1.63E-07 |
| ENSG00000078269 | SYNJ2 | 3114.78 | 1.023065 | 1.78E-09 | 1.87E-07 |
| ENSG00000115170 | ACVR1 | 451.4938 | 0.759024 | 1.77E-09 | 1.87E-07 |
| ENSG00000165030 | NFIL3 | 874.3118 | 0.693804 | 1.93E-09 | 2.03E-07 |
| ENSG00000095015 | MAP3K1 | 920.0473 | 0.65779 | 2.02E-09 | 2.10E-07 |
| ENSG00000129422 | MTUS1 | 40.42432 | 1.124963 | 2.33E-09 | 2.41E-07 |
| ENSG00000138670 | RASGEF1B | 363.7007 | -0.77221 | 2.64E-09 | 2.71E-07 |
| ENSG00000264230 | ANXA8L1 | 24.20766 | 1.09464 | 2.69E-09 | 2.75E-07 |
| ENSG00000116016 | EPAS1 | 133.4201 | 0.980566 | 3.78E-09 | 3.83E-07 |
| ENSG00000124831 | LRRFIP1 | 2285.185 | 0.518468 | 3.83E-09 | 3.86E-07 |
| ENSG00000123405 | NFE2 | 34.13373 | 1.102686 | 4.14E-09 | 4.14E-07 |
| ENSG00000196712 | NF1 | 2092.76 | 0.531219 | 4.29E-09 | 4.27E-07 |
| ENSG00000182489 | XKRX | 448.506 | -1.0893 | 4.73E-09 | 4.68E-07 |
| ENSG00000133805 | AMPD3 | 1832.513 | -0.64444 | 5.14E-09 | 5.05E-07 |
| ENSG00000004455 | AK2 | 2751.638 | 0.619049 | 6.00E-09 | 5.85E-07 |
| ENSG00000118946 | PCDH17 | 41.74013 | 1.094944 | 6.03E-09 | 5.85E-07 |

| | | | | | |
|---|---|---|---|---|---|
| ENSG00000155100 | OTUD6B | 345.8659 | 0.699776 | 6.09E-09 | 5.88E-07 |
| ENSG00000196396 | PTPN1 | 1623.583 | 0.497583 | 6.26E-09 | 6.00E-07 |
| ENSG00000111087 | GLI1 | 50.58743 | 1.081972 | 6.36E-09 | 6.06E-07 |
| ENSG00000140030 | GPR65 | 1019.905 | 0.59281 | 7.81E-09 | 7.40E-07 |
| ENSG00000121957 | GPSM2 | 317.1203 | -0.86168 | 9.09E-09 | 8.56E-07 |
| ENSG00000136826 | KLF4 | 103.0842 | -0.96019 | 9.53E-09 | 8.92E-07 |
| ENSG00000213846 | - | 79.0361 | 0.987608 | 1.01E-08 | 9.40E-07 |
| ENSG00000115525 | ST3GAL5 | 454.0882 | 0.71903 | 1.07E-08 | 9.93E-07 |
| ENSG00000235316 | DUSP8P5 | 316.2269 | 1.009952 | 1.17E-08 | 1.08E-06 |
| ENSG00000158683 | PKD1L1 | 196.4065 | 1.022902 | 1.24E-08 | 1.14E-06 |
| ENSG00000118689 | FOXO3 | 1163.438 | -0.6865 | 1.68E-08 | 1.52E-06 |
| ENSG00000172575 | RASGRP1 | 28.31752 | 1.054896 | 1.97E-08 | 1.78E-06 |
| ENSG00000130340 | SNX9 | 5123.577 | -0.67458 | 2.21E-08 | 1.98E-06 |
| ENSG00000168916 | ZNF608 | 87.85003 | -1.02604 | 2.27E-08 | 2.03E-06 |
| ENSG00000103064 | SLC7A6 | 1221.46 | 0.574027 | 2.37E-08 | 2.10E-06 |
| ENSG00000121895 | TMEM156 | 456.5483 | -0.67813 | 2.44E-08 | 2.16E-06 |
| ENSG00000176845 | METRNL | 3496.401 | 0.560738 | 2.51E-08 | 2.20E-06 |
| ENSG00000197147 | LRRC8B | 780.6588 | 0.753735 | 2.59E-08 | 2.26E-06 |
| ENSG00000166963 | MAP1A | 248.9069 | 0.89245 | 2.96E-08 | 2.58E-06 |
| ENSG00000198900 | TOP1 | 994.2713 | 0.673704 | 3.07E-08 | 2.65E-06 |
| ENSG00000133069 | TMCC2 | 337.2102 | 0.838652 | 3.23E-08 | 2.78E-06 |
| ENSG00000186431 | FCAR | 193.2714 | -0.87673 | 3.49E-08 | 2.98E-06 |
| ENSG00000003137 | CYP26B1 | 197.1846 | 0.985184 | 3.74E-08 | 3.18E-06 |
| ENSG00000119042 | SATB2 | 2066.623 | -0.51224 | 4.24E-08 | 3.59E-06 |
| ENSG00000103966 | EHD4 | 1083.327 | -0.75447 | 4.50E-08 | 3.77E-06 |
| ENSG00000169902 | TPST1 | 603.7922 | -0.60998 | 4.49E-08 | 3.77E-06 |
| ENSG00000155011 | DKK2 | 38.49465 | 1.022625 | 5.01E-08 | 4.17E-06 |
| ENSG00000077238 | IL4R | 2035.07 | 0.569882 | 5.10E-08 | 4.22E-06 |
| ENSG00000102531 | FNDC3A | 4340.221 | 0.655697 | 5.50E-08 | 4.53E-06 |
| ENSG00000173930 | SLCO4C1 | 68.31645 | 0.982773 | 6.00E-08 | 4.92E-06 |
| ENSG00000276600 | RAB7B | 373.4129 | -0.81835 | 6.74E-08 | 5.50E-06 |
| ENSG00000109906 | ZBTB16 | 35.27483 | 1.010072 | 7.92E-08 | 6.42E-06 |
| ENSG00000140459 | CYP11A1 | 22.52611 | 0.987523 | 8.20E-08 | 6.61E-06 |
| ENSG00000185669 | SNAI3 | 401.2881 | 0.84226 | 9.67E-08 | 7.77E-06 |
| ENSG00000178860 | MSC | 146.7513 | -0.78266 | 1.02E-07 | 8.11E-06 |
| ENSG00000015532 | XYLT2 | 646.2114 | 0.616605 | 1.10E-07 | 8.75E-06 |
| ENSG00000118985 | ELL2 | 4403.987 | 0.717953 | 1.13E-07 | 8.88E-06 |
| ENSG00000157483 | MYO1E | 4234.393 | 0.428928 | 1.13E-07 | 8.88E-06 |
| ENSG00000172840 | PDP2 | 647.4883 | 0.821401 | 1.18E-07 | 9.20E-06 |
| ENSG00000120217 | CD274 | 39.6977 | 0.988393 | 1.23E-07 | 9.58E-06 |
| ENSG00000114738 | MAPKAPK3 | 2763.6 | 0.582893 | 1.25E-07 | 9.70E-06 |
| ENSG00000139112 | GABARAPL1 | 2681.025 | 0.917666 | 1.32E-07 | 1.02E-05 |

| | | | | | |
|---|---|---|---|---|---|
| ENSG00000119943 | PYROXD2 | 345.2277 | 0.708713 | 1.53E-07 | 1.18E-05 |
| ENSG00000081320 | STK17B | 1843.844 | -0.52717 | 1.70E-07 | 1.29E-05 |
| ENSG00000155307 | SAMSN1 | 276.1182 | 0.977343 | 1.70E-07 | 1.29E-05 |
| ENSG00000186432 | KPNA4 | 3297.653 | 0.466582 | 1.70E-07 | 1.29E-05 |
| ENSG00000102760 | RGCC | 802.3139 | -0.66264 | 1.84E-07 | 1.39E-05 |
| ENSG00000024422 | EHD2 | 1183.415 | 0.748391 | 1.90E-07 | 1.42E-05 |
| ENSG00000116260 | QSOX1 | 4062.532 | 0.507362 | 2.01E-07 | 1.48E-05 |
| ENSG00000116473 | RAP1A | 3846.055 | 0.539271 | 2.01E-07 | 1.48E-05 |
| ENSG00000174456 | C12orf76 | 235.0012 | 0.683749 | 2.01E-07 | 1.48E-05 |
| ENSG00000141540 | TTYH2 | 114.7454 | 0.810887 | 2.71E-07 | 2.00E-05 |
| ENSG00000166483 | WEE1 | 371.4682 | -0.67407 | 2.96E-07 | 2.17E-05 |
| ENSG00000109320 | NFKB1 | 2562.984 | 0.420248 | 3.24E-07 | 2.36E-05 |
| ENSG00000176438 | SYNE3 | 577.0158 | 0.745322 | 4.00E-07 | 2.90E-05 |
| ENSG00000107816 | LZTS2 | 2303.967 | 0.63924 | 4.10E-07 | 2.96E-05 |
| ENSG00000104312 | RIPK2 | 312.1688 | 0.637446 | 4.40E-07 | 3.15E-05 |
| ENSG00000155760 | FZD7 | 550.2789 | -0.6885 | 4.40E-07 | 3.15E-05 |
| ENSG00000143924 | EML4 | 1419.497 | 0.475537 | 5.34E-07 | 3.81E-05 |
| ENSG00000170345 | FOS | 670.291 | -0.83376 | 5.42E-07 | 3.85E-05 |
| ENSG00000064225 | ST3GAL6 | 635.8583 | -0.66148 | 5.67E-07 | 4.00E-05 |
| ENSG00000152760 | TCTEX1D1 | 619.5246 | -0.56019 | 5.72E-07 | 4.02E-05 |
| ENSG00000072310 | SREBF1 | 1274.378 | 0.584238 | 7.12E-07 | 4.96E-05 |
| ENSG00000237945 | LINC00649 | 493.583 | 0.640042 | 7.12E-07 | 4.96E-05 |
| ENSG00000122547 | EEPD1 | 968.1054 | 0.595697 | 7.66E-07 | 5.31E-05 |
| ENSG00000172197 | MBOAT1 | 193.6613 | -0.66073 | 8.16E-07 | 5.64E-05 |
| ENSG00000184557 | SOCS3 | 261.1999 | 0.81674 | 8.76E-07 | 6.02E-05 |
| ENSG00000135932 | CAB39 | 4092.707 | -0.47325 | 8.84E-07 | 6.05E-05 |
| ENSG00000104921 | FCER2 | 15.06139 | 0.863598 | 9.03E-07 | 6.16E-05 |
| ENSG00000111052 | LIN7A | 721.5113 | 0.469216 | 9.18E-07 | 6.21E-05 |
| ENSG00000211891 | IGHE | 11.09068 | 0.776293 | 9.19E-07 | 6.21E-05 |
| ENSG00000111879 | FAM184A | 35.42724 | 0.920742 | 9.71E-07 | 6.53E-05 |
| ENSG00000165029 | ABCA1 | 387.0301 | -0.73447 | 9.82E-07 | 6.58E-05 |
| ENSG00000170571 | EMB | 609.6663 | 0.658155 | 1.01E-06 | 6.72E-05 |
| ENSG00000182831 | C16orf72 | 2238.522 | -0.40248 | 1.12E-06 | 7.44E-05 |
| ENSG00000186810 | CXCR3 | 226.6135 | 0.671423 | 1.31E-06 | 8.66E-05 |
| ENSG00000070759 | TESK2 | 212.8811 | -0.63799 | 1.33E-06 | 8.76E-05 |
| ENSG00000106799 | TGFBR1 | 1854.849 | -0.56045 | 1.40E-06 | 9.16E-05 |
| ENSG00000140948 | ZCCHC14 | 2463.597 | 0.68806 | 1.54E-06 | 0.0001 |
| ENSG00000187796 | CARD9 | 418.5927 | 0.57319 | 1.89E-06 | 0.000123 |
| ENSG00000131370 | SH3BP5 | 252.8068 | -0.77125 | 1.93E-06 | 0.000125 |
| ENSG00000183688 | FAM101B | 831.073 | 0.748043 | 1.97E-06 | 0.000127 |
| ENSG00000124788 | ATXN1 | 1905.531 | 0.713646 | 2.00E-06 | 0.000128 |
| ENSG00000154822 | PLCL2 | 388.1033 | -0.59061 | 1.99E-06 | 0.000128 |

| | | | | | |
|---|---|---|---|---|---|
| ENSG00000197471 | SPN | 4608.204 | 0.554204 | 2.00E-06 | 0.000128 |
| ENSG00000125726 | CD70 | 324.0685 | -0.6642 | 2.15E-06 | 0.000137 |
| ENSG00000113369 | ARRDC3 | 662.5947 | -0.62081 | 2.24E-06 | 0.000141 |
| ENSG00000127951 | FGL2 | 863.3133 | 0.831357 | 2.24E-06 | 0.000141 |
| ENSG00000108700 | CCL8 | 14.57505 | 0.776071 | 2.30E-06 | 0.000144 |
| ENSG00000119686 | FLVCR2 | 129.5051 | 0.849475 | 2.71E-06 | 0.000169 |
| ENSG00000134686 | PHC2 | 3915.967 | -0.57799 | 2.80E-06 | 0.000174 |
| ENSG00000169554 | ZEB2 | 1556.68 | -0.54887 | 2.92E-06 | 0.000181 |
| ENSG00000167703 | SLC43A2 | 764.5243 | -0.5407 | 3.05E-06 | 0.000189 |
| ENSG00000152818 | UTRN | 2542.277 | 0.495217 | 3.32E-06 | 0.000204 |
| ENSG00000213024 | NUP62 | 2922.755 | 0.455995 | 3.60E-06 | 0.000221 |
| ENSG00000116990 | MYCL | 180.0781 | -0.80776 | 3.65E-06 | 0.000223 |
| ENSG00000174718 | KIAA1551 | 988.4956 | -0.52393 | 3.77E-06 | 0.000229 |
| ENSG00000057149 | SERPINB3 | 9.943866 | 0.712303 | 3.81E-06 | 0.000231 |
| ENSG00000110987 | BCL7A | 487.3633 | 0.506361 | 4.16E-06 | 0.000251 |
| ENSG00000169116 | PARM1 | 198.8353 | 0.72332 | 4.33E-06 | 0.00026 |
| ENSG00000110047 | EHD1 | 1797.51 | -0.42302 | 4.43E-06 | 0.000265 |
| ENSG00000164061 | BSN | 205.0458 | 0.727157 | 4.46E-06 | 0.000266 |
| ENSG00000141655 | TNFRSF11A | 30.30503 | 0.855391 | 4.56E-06 | 0.00027 |
| ENSG00000143816 | WNT9A | 70.12112 | 0.82198 | 4.54E-06 | 0.00027 |
| ENSG00000168036 | CTNNB1 | 9736.998 | 0.420286 | 4.59E-06 | 0.000271 |
| ENSG00000133794 | ARNTL | 609.4428 | 0.667275 | 5.01E-06 | 0.000295 |
| ENSG00000156011 | PSD3 | 690.3117 | 0.623747 | 5.10E-06 | 0.000299 |
| ENSG00000118762 | PKD2 | 653.9506 | 0.612702 | 5.22E-06 | 0.000305 |
| ENSG00000163694 | RBM47 | 941.7245 | 0.500914 | 5.47E-06 | 0.000318 |
| ENSG00000169991 | IFFO2 | 251.4648 | 0.694505 | 5.48E-06 | 0.000318 |
| ENSG00000109501 | WFS1 | 175.2438 | 0.692354 | 5.65E-06 | 0.000326 |
| ENSG00000050405 | LIMA1 | 353.5545 | 0.555103 | 5.78E-06 | 0.000332 |
| ENSG00000052795 | FNIP2 | 791.4402 | 0.528482 | 5.87E-06 | 0.000336 |
| ENSG00000136869 | TLR4 | 369.2135 | -0.68258 | 5.90E-06 | 0.000336 |
| ENSG00000211455 | STK38L | 5641.537 | -0.43882 | 5.88E-06 | 0.000336 |
| ENSG00000144749 | LRIG1 | 713.073 | -0.5699 | 6.00E-06 | 0.00034 |
| ENSG00000178996 | SNX18 | 470.9346 | 0.495531 | 6.44E-06 | 0.000363 |
| ENSG00000237513 | - | 116.438 | 0.726965 | 6.43E-06 | 0.000363 |
| ENSG00000265190 | ANXA8 | 12.66426 | 0.757167 | 7.08E-06 | 0.000397 |
| ENSG00000150556 | LYPD6B | 17.9687 | 0.822388 | 7.25E-06 | 0.000405 |
| ENSG00000197405 | C5AR1 | 162.9529 | -0.75895 | 7.33E-06 | 0.000408 |
| ENSG00000139117 | CPNE8 | 577.4749 | 0.539063 | 7.75E-06 | 0.00043 |
| ENSG00000023909 | GCLM | 2794.424 | -0.42493 | 7.85E-06 | 0.000433 |
| ENSG00000082898 | XPO1 | 3912.929 | -0.49047 | 7.86E-06 | 0.000433 |
| ENSG00000103528 | SYT17 | 62.85469 | 0.807205 | 8.03E-06 | 0.000441 |
| ENSG00000164171 | ITGA2 | 42.81586 | 0.826406 | 8.14E-06 | 0.000446 |

| | | | | | |
|---|---|---|---|---|---|
| ENSG00000166387 | PPFIBP2 | 512.9562 | 0.580787 | 8.27E-06 | 0.000451 |
| ENSG00000172349 | IL16 | 179.7896 | -0.6628 | 8.39E-06 | 0.000456 |
| ENSG00000169439 | SDC2 | 2730.5 | 0.547743 | 8.43E-06 | 0.000457 |
| ENSG00000137747 | TMPRSS13 | 70.24061 | 0.774297 | 8.53E-06 | 0.00046 |
| ENSG00000167207 | NOD2 | 130.1749 | 0.774037 | 8.89E-06 | 0.000478 |
| ENSG00000174944 | P2RY14 | 192.871 | -0.70839 | 8.91E-06 | 0.000478 |
| ENSG00000184588 | PDE4B | 102.4961 | -0.82388 | 8.96E-06 | 0.000479 |
| ENSG00000164604 | GPR85 | 294.3081 | 0.646815 | 9.06E-06 | 0.000483 |
| ENSG00000131446 | MGAT1 | 3011.452 | 0.414601 | 9.76E-06 | 0.000518 |
| ENSG00000166317 | SYNPO2L | 465.0672 | 0.721189 | 1.04E-05 | 0.000551 |
| ENSG00000170915 | PAQR8 | 487.7042 | -0.69851 | 1.08E-05 | 0.00057 |
| ENSG00000184988 | TMEM106A | 430.7346 | 0.484781 | 1.18E-05 | 0.000618 |
| ENSG00000153317 | ASAP1 | 1335.091 | 0.443478 | 1.20E-05 | 0.000627 |
| ENSG00000162928 | PEX13 | 1004.42 | 0.424138 | 1.23E-05 | 0.00064 |
| ENSG00000118513 | MYB | 132.385 | -0.78008 | 1.27E-05 | 0.00066 |
| ENSG00000229921 | KIF25-AS1 | 202.1023 | 0.715634 | 1.28E-05 | 0.000665 |
| ENSG00000111269 | CREBL2 | 856.2455 | 0.528301 | 1.29E-05 | 0.000665 |
| ENSG00000166128 | RAB8B | 443.7781 | -0.51866 | 1.33E-05 | 0.000683 |
| ENSG00000163110 | PDLIM5 | 1071.828 | 0.437561 | 1.37E-05 | 0.000705 |
| ENSG00000112182 | BACH2 | 87.58767 | -0.7655 | 1.41E-05 | 0.000724 |
| ENSG00000148175 | STOM | 899.0072 | 0.415187 | 1.46E-05 | 0.000745 |
| ENSG00000106571 | GLI3 | 32.22954 | 0.812963 | 1.52E-05 | 0.000773 |
| ENSG00000163874 | ZC3H12A | 686.42 | 0.758716 | 1.55E-05 | 0.000787 |
| ENSG00000165527 | ARF6 | 4149.208 | 0.416981 | 1.56E-05 | 0.000789 |
| ENSG00000113532 | ST8SIA4 | 566.4012 | -0.47575 | 1.61E-05 | 0.000813 |
| ENSG00000231027 | - | 64.03421 | 0.779228 | 1.96E-05 | 0.000986 |
| ENSG00000082458 | DLG3 | 455.5409 | -0.60833 | 1.99E-05 | 0.000994 |
| ENSG00000147324 | MFHAS1 | 433.753 | 0.551191 | 2.01E-05 | 0.000998 |
| ENSG00000189067 | LITAF | 1714.745 | 0.488787 | 2.00E-05 | 0.000998 |
| ENSG00000163219 | ARHGAP25 | 1406.42 | 0.557047 | 2.24E-05 | 0.001112 |
| ENSG00000101384 | JAG1 | 1317.417 | -0.58078 | 2.32E-05 | 0.001142 |
| ENSG00000113083 | LOX | 20.35267 | 0.774418 | 2.32E-05 | 0.001142 |
| ENSG00000167851 | CD300A | 755.4661 | 0.433639 | 2.33E-05 | 0.001142 |
| ENSG00000173110 | HSPA6 | 18.25227 | 0.765369 | 2.50E-05 | 0.001223 |
| ENSG00000106415 | GLCCI1 | 777.7337 | -0.4318 | 2.62E-05 | 0.001279 |
| ENSG00000197893 | NRAP | 229.6799 | -0.77095 | 2.63E-05 | 0.001279 |
| ENSG00000260196 | - | 91.95525 | 0.74927 | 2.64E-05 | 0.001281 |
| ENSG00000173221 | GLRX | 317.7285 | 0.587117 | 2.65E-05 | 0.001283 |
| ENSG00000198355 | PIM3 | 770.2008 | 0.462772 | 2.70E-05 | 0.001302 |
| ENSG00000112679 | DUSP22 | 945.5481 | 0.49269 | 2.76E-05 | 0.001328 |
| ENSG00000028277 | POU2F2 | 757.7047 | -0.56311 | 2.81E-05 | 0.001344 |
| ENSG00000168386 | FILIP1L | 649.3838 | -0.4685 | 2.81E-05 | 0.001344 |

| | | | | | |
|---|---|---|---|---|---|
| ENSG00000036672 | USP2 | 411.6159 | 0.503316 | 2.91E-05 | 0.001384 |
| ENSG00000115009 | CCL20 | 172.8037 | -0.77132 | 3.02E-05 | 0.001425 |
| ENSG00000147650 | LRP12 | 462.6691 | 0.571861 | 3.01E-05 | 0.001425 |
| ENSG00000174307 | PHLDA3 | 243.4771 | -0.64452 | 3.01E-05 | 0.001425 |
| ENSG00000100100 | PIK3IP1 | 350.4526 | -0.60484 | 3.15E-05 | 0.001482 |
| ENSG00000197208 | SLC22A4 | 95.54749 | 0.717628 | 3.78E-05 | 0.001776 |
| ENSG00000102699 | PARP4 | 3335.326 | 0.354694 | 3.97E-05 | 0.001857 |
| ENSG00000136273 | HUS1 | 674.7805 | 0.477425 | 4.00E-05 | 0.001866 |
| ENSG00000122591 | FAM126A | 507.9751 | 0.474056 | 4.47E-05 | 0.002078 |
| ENSG00000144230 | GPR17 | 30.49591 | 0.764373 | 4.56E-05 | 0.002113 |
| ENSG00000136193 | SCRN1 | 2114.506 | 0.351742 | 4.62E-05 | 0.002138 |
| ENSG00000275302 | CCL4 | 154.9838 | 0.6575 | 4.73E-05 | 0.00218 |
| ENSG00000134602 | STK26 | 1081.779 | 0.427366 | 4.79E-05 | 0.002203 |
| ENSG00000183160 | TMEM119 | 276.2653 | -0.5263 | 4.87E-05 | 0.002235 |
| ENSG00000164691 | TAGAP | 576.2697 | 0.702109 | 4.99E-05 | 0.00228 |
| ENSG00000111912 | NCOA7 | 727.8316 | -0.57741 | 5.11E-05 | 0.002323 |
| ENSG00000171492 | LRRC8D | 822.2009 | 0.404098 | 5.10E-05 | 0.002323 |
| ENSG00000223749 | MIR503HG | 484.5416 | 0.677799 | 5.40E-05 | 0.002449 |
| ENSG00000163171 | CDC42EP3 | 1576.028 | 0.520469 | 5.44E-05 | 0.002458 |
| ENSG00000092969 | TGFB2 | 16.07503 | -0.72419 | 5.84E-05 | 0.002626 |
| ENSG00000117155 | SSX2IP | 580.94 | 0.435403 | 5.84E-05 | 0.002626 |
| ENSG00000138316 | ADAMTS14 | 53.87131 | 0.740739 | 6.04E-05 | 0.0027 |
| ENSG00000185344 | ATP6V0A2 | 878.3476 | 0.40154 | 6.03E-05 | 0.0027 |
| ENSG00000116285 | ERRFI1 | 280.44 | 0.753388 | 6.26E-05 | 0.002791 |
| ENSG00000157216 | SSBP3 | 1981.948 | -0.47375 | 6.47E-05 | 0.002875 |
| ENSG00000023902 | PLEKHO1 | 4625.137 | -0.39963 | 6.81E-05 | 0.003018 |
| ENSG00000175782 | SLC35E3 | 186.1481 | 0.604163 | 6.91E-05 | 0.003054 |
| ENSG00000185432 | METTL7A | 982.0188 | -0.61768 | 7.45E-05 | 0.003282 |
| ENSG00000101670 | LIPG | 279.9393 | 0.580144 | 7.66E-05 | 0.003366 |
| ENSG00000173227 | SYT12 | 3489.561 | -0.44205 | 7.69E-05 | 0.003368 |
| ENSG00000102034 | ELF4 | 1275.468 | 0.427472 | 7.71E-05 | 0.003369 |
| ENSG00000169105 | CHST14 | 310.6083 | 0.506298 | 7.91E-05 | 0.003445 |
| ENSG00000090339 | ICAM1 | 8049.334 | 0.60006 | 8.06E-05 | 0.003501 |
| ENSG00000106948 | AKNA | 1258.862 | -0.39404 | 8.08E-05 | 0.003502 |
| ENSG00000152127 | MGAT5 | 2545.673 | 0.405903 | 8.34E-05 | 0.003604 |
| ENSG00000132819 | RBM38 | 2430.276 | -0.34217 | 8.40E-05 | 0.003618 |
| ENSG00000136997 | MYC | 570.1035 | -0.4925 | 8.57E-05 | 0.003684 |
| ENSG00000180044 | C3orf80 | 54.38944 | -0.73829 | 8.65E-05 | 0.003708 |
| ENSG00000107719 | PALD1 | 2574.093 | 0.447088 | 8.68E-05 | 0.003709 |
| ENSG00000112701 | SENP6 | 3427.989 | 0.342462 | 8.75E-05 | 0.003732 |
| ENSG00000124145 | SDC4 | 668.9416 | 0.439007 | 8.94E-05 | 0.003801 |
| ENSG00000102471 | NDFIP2 | 2419.105 | 0.411624 | 9.03E-05 | 0.003814 |

| | | | | | |
|---|---|---|---|---|---|
| ENSG00000166825 | ANPEP | 12653.05 | 0.435949 | 9.02E-05 | 0.003814 |
| ENSG00000197872 | FAM49A | 1051.542 | -0.38389 | 9.04E-05 | 0.003814 |
| ENSG00000158715 | SLC45A3 | 1048.11 | 0.452829 | 9.47E-05 | 0.003984 |
| ENSG00000124225 | PMEPA1 | 382.0081 | -0.55127 | 9.50E-05 | 0.003986 |
| ENSG00000083312 | TNPO1 | 3261.882 | 0.339245 | 9.53E-05 | 0.003989 |
| ENSG00000113368 | LMNB1 | 1332.693 | -0.38576 | 0.0001 | 0.004186 |
| ENSG00000053254 | FOXN3 | 2282.23 | 0.335731 | 0.000105 | 0.004362 |
| ENSG00000132334 | PTPRE | 1421.489 | 0.616954 | 0.000105 | 0.004362 |
| ENSG00000164211 | STARD4 | 544.6043 | -0.51749 | 0.000109 | 0.004519 |
| ENSG00000176170 | SPHK1 | 2111.179 | 0.564081 | 0.000116 | 0.004774 |
| ENSG00000148204 | CRB2 | 81.39142 | 0.723401 | 0.000118 | 0.004845 |
| ENSG00000082397 | EPB41L3 | 691.7835 | 0.54231 | 0.00012 | 0.004909 |
| ENSG00000054983 | GALC | 2489.642 | 0.336863 | 0.000121 | 0.004939 |
| ENSG00000181467 | RAP2B | 1672.254 | -0.33114 | 0.000122 | 0.004966 |
| ENSG00000140455 | USP3 | 694.8598 | -0.3949 | 0.000123 | 0.005033 |
| ENSG00000165685 | TMEM52B | 1454.275 | 0.682558 | 0.000127 | 0.00518 |
| ENSG00000112137 | PHACTR1 | 284.0218 | -0.56409 | 0.000131 | 0.005329 |
| ENSG00000165617 | DACT1 | 182.0413 | -0.6494 | 0.000132 | 0.00534 |
| ENSG00000140320 | BAHD1 | 693.8898 | 0.445954 | 0.000135 | 0.005439 |
| ENSG00000186174 | BCL9L | 495.2506 | 0.458036 | 0.000141 | 0.005658 |
| ENSG00000088305 | DNMT3B | 485.183 | -0.39912 | 0.000147 | 0.005908 |
| ENSG00000153250 | RBMS1 | 1388.912 | 0.42355 | 0.00015 | 0.006012 |
| ENSG00000173559 | NABP1 | 409.291 | -0.55105 | 0.000151 | 0.006012 |
| ENSG00000135549 | PKIB | 1222.024 | 0.489314 | 0.000151 | 0.006015 |
| ENSG00000088179 | PTPN4 | 252.8044 | 0.491846 | 0.000152 | 0.00603 |
| ENSG00000214900 | LINC01588 | 276.3776 | 0.585252 | 0.000153 | 0.006056 |
| ENSG00000010818 | HIVEP2 | 706.6 | 0.404684 | 0.000154 | 0.006098 |
| ENSG00000198668 | CALM1 | 5854.192 | 0.341381 | 0.000155 | 0.006098 |
| ENSG00000166002 | SMCO4 | 265.7626 | -0.51066 | 0.000155 | 0.006103 |
| ENSG00000123200 | ZC3H13 | 3822.302 | -0.28446 | 0.00016 | 0.006284 |
| ENSG00000022567 | SLC45A4 | 343.0179 | 0.55131 | 0.000173 | 0.006765 |
| ENSG00000143382 | ADAMTSL4 | 232.2381 | 0.574043 | 0.000173 | 0.006765 |
| ENSG00000134480 | CCNH | 347.4683 | 0.518004 | 0.000176 | 0.00686 |
| ENSG00000139354 | GAS2L3 | 63.95633 | 0.691439 | 0.00018 | 0.007 |
| ENSG00000166783 | KIAA0430 | 1730.472 | -0.34584 | 0.000183 | 0.007095 |
| ENSG00000109654 | TRIM2 | 538.0893 | -0.44273 | 0.000185 | 0.007155 |
| ENSG00000135077 | HAVCR2 | 1042.416 | -0.59883 | 0.000192 | 0.007398 |
| ENSG00000186832 | KRT16 | 6.752919 | 0.53472 | 0.000199 | 0.007644 |
| ENSG00000164683 | HEY1 | 89.59692 | 0.675038 | 0.0002 | 0.007695 |
| ENSG00000026103 | FAS | 79.89513 | 0.624778 | 0.000202 | 0.007745 |
| ENSG00000160223 | ICOSLG | 185.3496 | -0.5104 | 0.000205 | 0.00782 |
| ENSG00000173852 | DPY19L1 | 1478.615 | 0.359817 | 0.000216 | 0.00823 |

| | | | | | |
|---|---|---|---|---|---|
| ENSG00000109099 | PMP22 | 30.71107 | 0.686738 | 0.000225 | 0.008544 |
| ENSG00000090659 | CD209 | 53.54842 | 0.687268 | 0.000228 | 0.008645 |
| ENSG00000141456 | PELP1 | 703.6206 | 0.4084 | 0.000228 | 0.008645 |
| ENSG00000072864 | NDE1 | 536.0933 | -0.40684 | 0.00023 | 0.008695 |
| ENSG00000162496 | DHRS3 | 219.4743 | -0.60184 | 0.000244 | 0.009179 |
| ENSG00000153531 | ADPRHL1 | 586.2268 | -0.54995 | 0.000247 | 0.009297 |
| ENSG00000143847 | PPFIA4 | 345.7993 | 0.629708 | 0.000251 | 0.009392 |
| ENSG00000171522 | PTGER4 | 466.565 | -0.48157 | 0.000255 | 0.009536 |
| ENSG00000099998 | GGT5 | 27.14592 | 0.682858 | 0.000264 | 0.009797 |
| ENSG00000136040 | PLXNC1 | 644.6426 | -0.47933 | 0.000264 | 0.009797 |
| ENSG00000152270 | PDE3B | 431.2987 | 0.521255 | 0.000264 | 0.009797 |
| ENSG00000230487 | PSMG3-AS1 | 146.3033 | 0.549116 | 0.000263 | 0.009797 |
| ENSG00000119408 | NEK6 | 2296.7 | 0.310896 | 0.000272 | 0.010034 |
| ENSG00000154237 | LRRK1 | 1087.498 | 0.487828 | 0.000273 | 0.010034 |
| ENSG00000175538 | KCNE3 | 534.963 | -0.44266 | 0.000273 | 0.010034 |
| ENSG00000136630 | HLX | 3089.442 | 0.486291 | 0.000275 | 0.010081 |
| ENSG00000106829 | TLE4 | 349.3835 | -0.46001 | 0.000276 | 0.010107 |
| ENSG00000268734 | - | 76.68935 | -0.68088 | 0.000278 | 0.010172 |
| ENSG00000168769 | TET2 | 1168.827 | -0.38354 | 0.00028 | 0.010189 |
| ENSG00000122574 | WIPF3 | 1076.155 | -0.55203 | 0.000286 | 0.010411 |
| ENSG00000162692 | VCAM1 | 48.37948 | 0.681106 | 0.000288 | 0.010432 |
| ENSG00000174130 | TLR6 | 683.0438 | -0.35212 | 0.000297 | 0.010734 |
| ENSG00000169047 | IRS1 | 108.7863 | -0.62568 | 0.00032 | 0.011546 |
| ENSG00000111885 | MAN1A1 | 583.9222 | 0.618344 | 0.00033 | 0.011879 |
| ENSG00000185818 | NAT8L | 139.9597 | 0.535047 | 0.000336 | 0.012066 |
| ENSG00000280088 | - | 78.58377 | 0.633643 | 0.000339 | 0.012151 |
| ENSG00000140470 | ADAMTS17 | 155.0693 | 0.503309 | 0.000359 | 0.012833 |
| ENSG00000173237 | C11orf86 | 61.77915 | -0.66982 | 0.000372 | 0.013297 |
| ENSG00000114735 | HEMK1 | 183.3927 | 0.517984 | 0.000384 | 0.013685 |
| ENSG00000186350 | RXRA | 2387.573 | -0.2804 | 0.000394 | 0.014011 |
| ENSG00000141480 | ARRB2 | 683.7444 | 0.365585 | 0.000401 | 0.014203 |
| ENSG00000149177 | PTPRJ | 3256.15 | -0.40538 | 0.000403 | 0.014242 |
| ENSG00000100784 | RPS6KA5 | 127.478 | -0.56046 | 0.000415 | 0.014667 |
| ENSG00000221968 | FADS3 | 773.2097 | 0.451405 | 0.000424 | 0.014923 |
| ENSG00000170412 | GPRC5C | 718.3133 | 0.477028 | 0.000429 | 0.015079 |
| ENSG00000177606 | JUN | 501.7733 | 0.553794 | 0.000432 | 0.015139 |
| ENSG00000169122 | FAM110B | 32.76264 | 0.661072 | 0.000435 | 0.015206 |
| ENSG00000109062 | SLC9A3R1 | 339.9023 | 0.468954 | 0.000437 | 0.015259 |
| ENSG00000026652 | AGPAT4 | 1601.958 | 0.52615 | 0.00044 | 0.015341 |
| ENSG00000122042 | UBL3 | 2299.658 | 0.297051 | 0.000442 | 0.01535 |
| ENSG00000113657 | DPYSL3 | 621.1739 | -0.40657 | 0.000446 | 0.015469 |
| ENSG00000133639 | BTG1 | 4604.78 | -0.31038 | 0.000451 | 0.015615 |

| | | | | | |
|---|---|---|---|---|---|
| ENSG00000126262 | FFAR2 | 168.9345 | -0.5772 | 0.000456 | 0.015739 |
| ENSG00000030419 | IKZF2 | 229.988 | 0.51634 | 0.000457 | 0.015755 |
| ENSG00000138172 | CALHM2 | 343.819 | -0.43529 | 0.000459 | 0.015781 |
| ENSG00000133874 | RNF122 | 163.9116 | -0.5157 | 0.000501 | 0.017182 |
| ENSG00000128016 | ZFP36 | 2188.367 | 0.456371 | 0.000507 | 0.017363 |
| ENSG00000026508 | CD44 | 17063.12 | 0.514181 | 0.000509 | 0.017399 |
| ENSG00000049449 | RCN1 | 574.4045 | 0.357041 | 0.000517 | 0.017633 |
| ENSG00000253522 | - | 42.86692 | -0.65316 | 0.000525 | 0.01786 |
| ENSG00000184838 | PRR16 | 74.70573 | 0.598858 | 0.000546 | 0.01852 |
| ENSG00000138434 | SSFA2 | 2254.136 | -0.3099 | 0.000555 | 0.018759 |
| ENSG00000160219 | GAB3 | 379.7343 | 0.412081 | 0.000554 | 0.018759 |
| ENSG00000274253 | - | 127.3605 | 0.52559 | 0.000563 | 0.018971 |
| ENSG00000105656 | ELL | 941.8757 | 0.347171 | 0.000576 | 0.019368 |
| ENSG00000103569 | AQP9 | 26.22615 | 0.604051 | 0.000588 | 0.019754 |
| ENSG00000171621 | SPSB1 | 579.7208 | 0.541891 | 0.000596 | 0.019961 |
| ENSG00000203706 | SERTAD4-AS1 | 5.671565 | 0.476491 | 0.000597 | 0.019975 |
| ENSG00000187486 | KCNJ11 | 102.1721 | 0.544415 | 0.000622 | 0.020763 |
| ENSG00000133056 | PIK3C2B | 143.6172 | 0.55669 | 0.00071 | 0.023656 |
| ENSG00000004809 | SLC22A16 | 98.84685 | 0.581128 | 0.000721 | 0.023943 |
| ENSG00000023445 | BIRC3 | 584.2493 | -0.36122 | 0.000726 | 0.024058 |
| ENSG00000009790 | TRAF3IP3 | 426.6129 | -0.46204 | 0.000767 | 0.025326 |
| ENSG00000180354 | MTURN | 430.5563 | -0.41397 | 0.000767 | 0.025326 |
| ENSG00000144040 | SFXN5 | 147.2004 | 0.493552 | 0.000783 | 0.025787 |
| ENSG00000233621 | LINC01137 | 200.1568 | 0.468762 | 0.000789 | 0.025934 |
| ENSG00000151748 | SAV1 | 1140.797 | 0.322394 | 0.000796 | 0.026125 |
| ENSG00000109787 | KLF3 | 472.4647 | -0.43743 | 0.0008 | 0.026209 |
| ENSG00000169896 | ITGAM | 3137.176 | 0.354742 | 0.000806 | 0.026299 |
| ENSG00000171659 | GPR34 | 35.3306 | -0.62724 | 0.000806 | 0.026299 |
| ENSG00000110042 | DTX4 | 96.74223 | 0.630669 | 0.000813 | 0.026466 |
| ENSG00000169926 | KLF13 | 3670.981 | 0.416224 | 0.000827 | 0.026813 |
| ENSG00000204103 | MAFB | 611.5519 | -0.51976 | 0.000827 | 0.026813 |
| ENSG00000103056 | SMPD3 | 8.44723 | 0.509434 | 0.000829 | 0.026821 |
| ENSG00000165795 | NDRG2 | 3275.813 | -0.31041 | 0.000831 | 0.026823 |
| ENSG00000115419 | GLS | 4267.961 | -0.4206 | 0.000839 | 0.027028 |
| ENSG00000122779 | TRIM24 | 1086.934 | -0.29668 | 0.000845 | 0.027103 |
| ENSG00000164024 | METAP1 | 4645.048 | -0.31473 | 0.000844 | 0.027103 |
| ENSG00000096696 | DSP | 65.29469 | -0.60994 | 0.000875 | 0.028009 |
| ENSG00000198719 | DLL1 | 472.0001 | -0.56817 | 0.000887 | 0.028336 |
| ENSG00000035403 | VCL | 4322.975 | 0.46631 | 0.000929 | 0.029614 |
| ENSG00000198019 | FCGR1B | 46.18606 | 0.60675 | 0.000943 | 0.030021 |
| ENSG00000109321 | AREG | 125.8094 | -0.62066 | 0.000951 | 0.030162 |
| ENSG00000116922 | C1orf109 | 316.783 | 0.419024 | 0.000954 | 0.030162 |

| | | | | | |
|---|---|---|---|---|---|
| ENSG00000142798 | HSPG2 | 4989.375 | 0.394972 | 0.000952 | 0.030162 |
| ENSG00000017427 | IGF1 | 5.253214 | 0.446948 | 0.000997 | 0.031425 |
| ENSG00000174236 | REP15 | 10.94943 | 0.555377 | 0.000996 | 0.031425 |
| ENSG00000131873 | CHSY1 | 4312.932 | 0.388089 | 0.001 | 0.03144 |
| ENSG00000164543 | STK17A | 606.2828 | -0.39286 | 0.001004 | 0.031514 |
| ENSG00000197860 | SGTB | 321.7714 | -0.42908 | 0.001011 | 0.031674 |
| ENSG00000181523 | SGSH | 701.3457 | 0.347786 | 0.001039 | 0.032463 |
| ENSG00000100644 | HIF1A | 2573.596 | 0.294706 | 0.001057 | 0.032972 |
| ENSG00000180758 | GPR157 | 266.3127 | -0.46889 | 0.001059 | 0.032975 |
| ENSG00000164400 | CSF2 | 19.81001 | 0.58063 | 0.001108 | 0.034429 |
| ENSG00000172216 | CEBPB | 971.0151 | 0.397361 | 0.001112 | 0.034488 |
| ENSG00000163704 | PRRT3 | 161.217 | 0.479479 | 0.001126 | 0.034864 |
| ENSG00000272767 | JMJD1C-AS1 | 132.8578 | 0.485774 | 0.001138 | 0.03515 |
| ENSG00000075391 | RASAL2 | 2211.552 | 0.34239 | 0.001146 | 0.035322 |
| ENSG00000176014 | TUBB6 | 943.6857 | 0.336061 | 0.001155 | 0.035531 |
| ENSG00000000003 | TSPAN6 | 362.4785 | -0.43777 | 0.001167 | 0.035843 |
| ENSG00000086758 | HUWE1 | 5060.648 | 0.311142 | 0.001177 | 0.035994 |
| ENSG00000123146 | ADGRE5 | 6260.828 | -0.34619 | 0.001176 | 0.035994 |
| ENSG00000153071 | DAB2 | 368.3132 | 0.454035 | 0.001186 | 0.036219 |
| ENSG00000088826 | SMOX | 1387.119 | 0.47615 | 0.001201 | 0.03659 |
| ENSG00000168906 | MAT2A | 4376.167 | 0.46311 | 0.00121 | 0.036792 |
| ENSG00000109089 | CDR2L | 330.852 | 0.433865 | 0.001219 | 0.037 |
| ENSG00000095383 | TBC1D2 | 91.93216 | 0.524543 | 0.001245 | 0.03772 |
| ENSG00000122223 | CD244 | 235.5717 | -0.4976 | 0.001251 | 0.037833 |
| ENSG00000047597 | XK | 556.3463 | -0.42852 | 0.001259 | 0.03799 |
| ENSG00000163380 | LMOD3 | 11.47142 | 0.530774 | 0.001273 | 0.038344 |
| ENSG00000166033 | HTRA1 | 1602.51 | -0.37658 | 0.001281 | 0.038506 |
| ENSG00000198053 | SIRPA | 4154.143 | 0.309013 | 0.001283 | 0.038519 |
| ENSG00000133816 | MICAL2 | 1793.155 | 0.471961 | 0.001333 | 0.039922 |
| ENSG00000047662 | FAM184B | 49.04207 | 0.587922 | 0.001338 | 0.039998 |
| ENSG00000264522 | OTUD7B | 584.8342 | -0.35386 | 0.001433 | 0.042757 |
| ENSG00000105374 | NKG7 | 111.4416 | 0.528434 | 0.001463 | 0.043585 |
| ENSG00000184785 | SMIM10 | 77.7041 | 0.584507 | 0.001486 | 0.044166 |
| ENSG00000064763 | FAR2 | 509.7162 | 0.384815 | 0.0015 | 0.0445 |
| ENSG00000175215 | CTDSP2 | 4950.098 | -0.31323 | 0.001532 | 0.045365 |
| ENSG00000276231 | PIK3R6 | 220.7459 | 0.505834 | 0.001566 | 0.046307 |
| ENSG00000196581 | AJAP1 | 26.30605 | -0.59452 | 0.001569 | 0.046311 |
| ENSG00000011523 | CEP68 | 664.6501 | 0.400631 | 0.00159 | 0.046839 |
| ENSG00000154127 | UBASH3B | 50.02924 | -0.5841 | 0.001593 | 0.046845 |
| ENSG00000198825 | INPP5F | 104.7739 | -0.51049 | 0.00162 | 0.047528 |
| ENSG00000168564 | CDKN2AIP | 720.9362 | -0.37376 | 0.00166 | 0.048613 |
| ENSG00000170425 | ADORA2B | 34.87526 | -0.59073 | 0.001693 | 0.049486 |

| | | | | | |
|---|---|---|---|---|---|
| ENSG00000100628 | ASB2 | 78.92346 | -0.55979 | 0.00172 | 0.050187 |
| ENSG00000177426 | TGIF1 | 441.7455 | -0.36375 | 0.001825 | 0.053148 |
| ENSG00000143702 | CEP170 | 3679.133 | 0.300641 | 0.001836 | 0.05337 |
| ENSG00000232653 | GOLGA8N | 112.0825 | 0.542085 | 0.001839 | 0.05337 |
| ENSG00000211456 | SACM1L | 1397.733 | 0.279501 | 0.001911 | 0.055349 |
| ENSG00000126500 | FLRT1 | 52.32639 | 0.581512 | 0.001926 | 0.055702 |
| ENSG00000231528 | FAM225A | 47.68984 | -0.57484 | 0.001934 | 0.055704 |
| ENSG00000253738 | OTUD6B-AS1 | 401.3238 | 0.352986 | 0.001933 | 0.055704 |
| ENSG00000122641 | INHBA | 1639.379 | -0.42096 | 0.001991 | 0.057208 |
| ENSG00000161091 | MFSD12 | 4102.427 | 0.278826 | 0.001993 | 0.057208 |
| ENSG00000110031 | LPXN | 1577.047 | -0.43908 | 0.002015 | 0.057747 |
| ENSG00000139725 | RHOF | 576.2351 | 0.336482 | 0.002027 | 0.057968 |
| ENSG00000112893 | MAN2A1 | 824.3719 | 0.322598 | 0.002043 | 0.058315 |
| ENSG00000110422 | HIPK3 | 1612.107 | 0.286374 | 0.002057 | 0.058616 |
| ENSG00000124782 | RREB1 | 1824.159 | -0.32151 | 0.002182 | 0.062069 |
| ENSG00000048545 | GUCA1A | 4.468338 | 0.376769 | 0.002201 | 0.06239 |
| ENSG00000167850 | CD300C | 255.5215 | 0.467559 | 0.002199 | 0.06239 |
| ENSG00000168310 | IRF2 | 621.5304 | -0.31788 | 0.002206 | 0.062414 |
| ENSG00000112561 | TFEB | 1290.242 | -0.28307 | 0.002239 | 0.063124 |
| ENSG00000180357 | ZNF609 | 910.5907 | 0.371892 | 0.002237 | 0.063124 |
| ENSG00000029534 | ANK1 | 12.10054 | 0.52916 | 0.002307 | 0.064915 |
| ENSG00000126777 | KTN1 | 3988.14 | 0.267519 | 0.002318 | 0.06513 |
| ENSG00000179630 | LACC1 | 379.5306 | -0.37773 | 0.002337 | 0.065535 |
| ENSG00000169908 | TM4SF1 | 24.89846 | -0.54908 | 0.002381 | 0.066652 |
| ENSG00000111860 | CEP85L | 368.4622 | 0.537889 | 0.002394 | 0.066909 |
| ENSG00000148680 | HTR7 | 73.52075 | -0.53424 | 0.002399 | 0.066921 |
| ENSG00000051382 | PIK3CB | 1084.262 | -0.35312 | 0.002412 | 0.067087 |
| ENSG00000119326 | CTNNAL1 | 184.9625 | 0.42636 | 0.002414 | 0.067087 |
| ENSG00000117394 | SLC2A1 | 416.9967 | 0.348642 | 0.002434 | 0.06744 |
| ENSG00000197380 | DACT3 | 167.0034 | -0.43297 | 0.002435 | 0.06744 |
| ENSG00000183087 | GAS6 | 60.81831 | 0.547607 | 0.002459 | 0.068002 |
| ENSG00000124813 | RUNX2 | 167.3959 | 0.436838 | 0.002464 | 0.06801 |
| ENSG00000164823 | OSGIN2 | 603.3351 | 0.348949 | 0.002473 | 0.068131 |
| ENSG00000104081 | BMF | 3593.891 | 0.367124 | 0.002477 | 0.068138 |
| ENSG00000065989 | PDE4A | 2738.444 | 0.36548 | 0.002536 | 0.069623 |
| ENSG00000244682 | FCGR2C | 16.23445 | 0.541962 | 0.002585 | 0.070861 |
| ENSG00000142599 | RERE | 2146.32 | 0.424061 | 0.002597 | 0.071008 |
| ENSG00000153976 | HS3ST3A1 | 99.22234 | 0.55495 | 0.002599 | 0.071008 |
| ENSG00000096060 | FKBP5 | 1571.491 | 0.339292 | 0.002608 | 0.071115 |
| ENSG00000204577 | LILRB3 | 15.79305 | 0.5455 | 0.002615 | 0.071177 |
| ENSG00000233680 | HNRNPA1P27 | 29.09817 | -0.55178 | 0.00264 | 0.07174 |
| ENSG00000181631 | P2RY13 | 13.8882 | -0.53412 | 0.002647 | 0.071815 |

| | | | | | |
|---|---|---|---|---|---|
| ENSG00000104549 | SQLE | 4710.893 | -0.35843 | 0.002687 | 0.07252 |
| ENSG00000118242 | MREG | 140.9959 | 0.504268 | 0.002687 | 0.07252 |
| ENSG00000230630 | DNM3OS | 136.6853 | -0.51618 | 0.002683 | 0.07252 |
| ENSG00000146192 | FGD2 | 104.0113 | 0.555016 | 0.002714 | 0.073122 |
| ENSG00000107968 | MAP3K8 | 108.1845 | 0.480579 | 0.002724 | 0.073257 |
| ENSG00000101412 | E2F1 | 470.1466 | -0.43396 | 0.002756 | 0.073992 |
| ENSG00000157778 | PSMG3 | 857.2408 | 0.309097 | 0.002763 | 0.074075 |
| ENSG00000085185 | BCORL1 | 356.8286 | 0.42993 | 0.002772 | 0.074186 |
| ENSG00000188549 | C15orf52 | 47.98835 | 0.562918 | 0.002803 | 0.074897 |
| ENSG00000161929 | SCIMP | 22.58371 | 0.559539 | 0.002834 | 0.075579 |
| ENSG00000088832 | FKBP1A | 2293.125 | 0.26488 | 0.002862 | 0.076088 |
| ENSG00000166501 | PRKCB | 1372.528 | 0.261264 | 0.00286 | 0.076088 |
| ENSG00000163607 | GTPBP8 | 309.4823 | -0.38437 | 0.002876 | 0.076333 |
| ENSG00000105851 | PIK3CG | 1386.811 | 0.271148 | 0.002942 | 0.077948 |
| ENSG00000148154 | UGCG | 518.205 | -0.33682 | 0.002958 | 0.078243 |
| ENSG00000170791 | CHCHD7 | 211.5413 | 0.412261 | 0.002979 | 0.078631 |
| ENSG00000174437 | ATP2A2 | 6237.893 | 0.232896 | 0.002983 | 0.078631 |
| ENSG00000135363 | LMO2 | 1538.52 | 0.283231 | 0.003021 | 0.079513 |
| ENSG00000147526 | TACC1 | 1908.537 | -0.28713 | 0.003053 | 0.080205 |
| ENSG00000110080 | ST3GAL4 | 214.7343 | 0.410819 | 0.003104 | 0.081424 |
| ENSG00000039068 | CDH1 | 23.62704 | 0.554241 | 0.003111 | 0.081467 |
| ENSG00000006459 | KDM7A | 440.0807 | 0.355137 | 0.00312 | 0.08157 |
| ENSG00000267414 | - | 5.611019 | 0.414269 | 0.00314 | 0.081943 |
| ENSG00000236345 | - | 131.8114 | -0.43553 | 0.00316 | 0.082342 |
| ENSG00000147852 | VLDLR | 149.3384 | -0.43201 | 0.003191 | 0.083011 |
| ENSG00000265798 | - | 114.3562 | 0.489199 | 0.003251 | 0.084417 |
| ENSG00000138678 | AGPAT9 | 132.8608 | -0.50346 | 0.003311 | 0.085844 |
| ENSG00000066084 | DIP2B | 1777.242 | 0.260046 | 0.003356 | 0.086722 |
| ENSG00000171729 | TMEM51 | 159.6993 | 0.519219 | 0.003354 | 0.086722 |
| ENSG00000162517 | PEF1 | 689.3018 | 0.313607 | 0.003371 | 0.086987 |
| ENSG00000139083 | ETV6 | 1013.366 | 0.28903 | 0.003428 | 0.088025 |
| ENSG00000177542 | SLC25A22 | 238.6054 | 0.411062 | 0.003428 | 0.088025 |
| ENSG00000224413 | - | 11.52255 | 0.473269 | 0.00342 | 0.088025 |
| ENSG00000095637 | SORBS1 | 85.82979 | -0.51547 | 0.003485 | 0.089184 |
| ENSG00000259959 | - | 33.37629 | 0.54883 | 0.003483 | 0.089184 |
| ENSG00000033327 | GAB2 | 705.2357 | 0.351158 | 0.003509 | 0.089663 |
| ENSG00000198885 | ITPRIPL1 | 92.00624 | 0.4967 | 0.003568 | 0.091014 |
| ENSG00000165434 | PGM2L1 | 192.4526 | -0.4018 | 0.003624 | 0.092288 |
| ENSG00000188827 | SLX4 | 263.2656 | 0.389981 | 0.003651 | 0.092843 |
| ENSG00000143869 | GDF7 | 13.79832 | -0.51365 | 0.003688 | 0.093626 |
| ENSG00000104447 | TRPS1 | 91.25119 | -0.48677 | 0.003709 | 0.094013 |
| ENSG00000115165 | CYTIP | 1002.252 | -0.32255 | 0.00376 | 0.094991 |

| | | | | | |
|---|---|---|---|---|---|
| ENSG00000168389 | MFSD2A | 271.2973 | -0.5341 | 0.00376 | 0.094991 |
| ENSG00000081307 | UBA5 | 2539.181 | -0.3017 | 0.003789 | 0.0955 |
| ENSG00000225953 | SATB2-AS1 | 53.65276 | -0.53479 | 0.003792 | 0.0955 |
| ENSG00000181788 | SIAH2 | 635.3928 | -0.29385 | 0.003816 | 0.095962 |
| ENSG00000103489 | XYLT1 | 3419.444 | 0.327832 | 0.003824 | 0.096 |
| ENSG00000140406 | MESDC1 | 1131.217 | -0.3209 | 0.003914 | 0.098111 |
| ENSG00000129450 | SIGLEC9 | 470.679 | -0.33753 | 0.003952 | 0.098629 |
| ENSG00000185046 | ANKS1B | 6.932938 | 0.419996 | 0.003952 | 0.098629 |
| ENSG00000198682 | PAPSS2 | 182.571 | 0.435897 | 0.003954 | 0.098629 |
| ENSG00000196776 | CD47 | 2644.293 | 0.322254 | 0.003967 | 0.098817 |
| ENSG00000256235 | SMIM3 | 279.8409 | -0.40178 | 0.003983 | 0.099045 |
| ENSG00000120833 | SOCS2 | 73.75519 | -0.50134 | 0.004022 | 0.099865 |
| ENSG00000162222 | TTC9C | 264.8736 | 0.367508 | 0.004031 | 0.099865 |
| ENSG00000198742 | SMURF1 | 1563.879 | -0.25591 | 0.004035 | 0.099865 |

# VITA

I graduated from the Faculty of Allied Health Science, Chulalongkorn University with a Bachelor's degree in 2008. I received a certificate in Medical Technology and worked as medical technologist in Lab Plus One for 1 year.

In 2009-2011, I enrolled in a Graduate Program in Biotechnology, Faculty of Science, Chulalongkorn University.

In 2012-present, I enrolled in a Inter-disciplinary Graduate Program in Medical Microbiology, Faculty of Science, Chulalongkorn University.

Publications

1. Arayachukiat S., Seemork J., Pan-In P., Amornwachirabodee K., Sangphech N., Sansureerungsikul N., Sathornsantikun K., Vilaivan C., Shigyou K., PienpinijthamP., Vilaivan T., Palaga T., Banlunara W., Hamada T., Wanichwecharungruang S., Bringing macromolecules into cells and evading endosomes by oxidized carbon nanoparticles., Nano Lett., 15 (5), 3370–3376, 2015

2. Tree-Udom T., Seemork J., Shigyou K., Hamada T., Sangphech N., Palaga T., Insin N., Pan-In P., Wanichwecharungruang S., Shape Effect on Particle-Lipid Bilayer Membrane Association, Cellular Uptake and Cytotoxicity, ACS Appl. Mater. Interfaces, 7 (43), 23993–24000 (2015)

3. Sangphech, N, Osborne, B, Palaga, T. Notch signaling regulates the phosphorylation of Akt and survival of lipopolysaccharide-activated macrophages via regulator of G protein signaling 19 (RGS19). Immunobiology, 219, 653-660 (2014)

4. Sangthong, S, Sangphech, N, Palaga, T, Ngamrojanavanich, N, Puthong, S, Vilaivan, T, Muangsin, N. Anthracene-9, 10-dione derivatives induced apoptosis in human cervical cancer cell line (Ca Ski) by interfering with HPV E6 expression. Eur. J. Med. Chem. 77, 334-342 (2014)

5. Palaga, T, Ratanabunyong, S, Pattarakankul, T, Sangphech, N, Wongchana, W, Hadae, Y, Kuenjinda, P. Notch signaling regulates expression of Mcl-1 and apoptosis in PPD-treated macrophages. Cell. Mol. Immunol. 10, 444-52 (2013)

6. Boonyatecha, N, Sangphech, N, Wongchana, W, Kueanjinda, P, Palaga, T. Involvement of Notch signaling pathway in regulating IL-12 expression via c-Rel in activated macrophages. Mol. Immunol. 51, 255-62. (2012)

7. Kuncharin, Y, Sangphech, N, Kueanjinda, P, Bhattarakosol, P, Palaga, T. MAML1 regulates cell viability via the NF-kB pathway in cervical cancer cell lines. Exp. Cell Res. 317, 1830-1840. (2011)

Experiences

In 2011, got the third prize for oral presentation in the topic of "Phosphoproteome in lipopolysaccharide-stimulated macrophage treated with inhibitor Notch signaling." from the 16th Biological Sciences Graduate Congress (BSGC), National University of Singapore, Singapore, 12th-14th December

In 2012, got the excellent oral presentation award from the 1st ASEAN Plus Three Graduate Research Congress (AGRC). Chiang Mai University, Thailand, 1st-2nd March

In 2013, participated and presented poster in the topic of "Negative impact of Notch signaling pathway on activation of a nuclear hormone receptor, PPARg in human macrophages: Implications for M1/M2 Polarization in Macrophages" in the 12th FIMSA Advanced Training Course, Chiang Mai, Thailand, 15th-18 th October

In 2015, oral and poster presentation in the topic of "Interaction Between Notch Signaling and Hormone Receptor, Nur77, in Human Macrophages: Implications for Macrophages Polarization" in The 4th NIF (Network of Immunology Frontiers) Winter School on Advanced Immunology 2015, 18th-23rd January